THE BATCH AND CONTINUOUS BACTERIAL LEACHING KINETICS OF A REFRACTORY GOLD-BEARING PYRITE CONCENTRATE

by

J.T. CHAPMAN
B.Sc. Eng (UNIVERSITY OF PRETORIA) 1984

Submitted to the University of Cape Town in fulfillment of the requirements for the degree of Masters of Science in Engineering

May 1989

ACKNOWLEDGEMENTS

I would like to express my thanks to:

The COUNCIL FOR MINERAL TECHNOLOGY (MINTEK) for their finacial support and invaluable technical assistance.

Professor G.S. Hansford of the Department of Chemical Engineering, University of Cape Town, for his supervision and encouragement.

Dr. W.A.M. Te Riele and Dr. A. Pinches for their invaluable assistance and interest in this work.

The staff of the Department of Chemical Engineering at U.C.T. for their help and patience.

The staff of Ore Dressing Division at MINTEK for their assistance and encouragement throughout the duration of this work.

ABSTRACT

The recent focus on bacterial leaching as a pre-oxidation step in the treatment of refractory gold bearing sulphide ores and concentrates, has created the need for kinetic models to adequately describe bacterial leaching reactor performance.

This work is a kinetic study of the bacterial leaching of a refractory gold bearing, pyrite concentrate. The study includes the presentation of two mechanistically based, the shrinking particle and propagating pore (Hansford and Drossou, 1986), batch reactor kinetic models. These models are derived for single stage continuous reactor description. In addition, the empirical logistic growth model (Pinches *et al.*, 1987) is presented for both batch and continuous reactor description. The models are correlated with the experimental data.

Three narrow size fractions of the pyrite concentrate were subjected to batch and continuous bacterial oxidation, using a *Thiobacillus ferrooxidans* culture. Time profile data of the pyrite oxidation were obtained for the batch reactor study. Similarly, retention time profile data of pyrite oxidation was obtained for the single stage continuous reactor. The gold extraction as a function of sulphide oxidation as well as fraction arsenic leached, was established.

Of the two mechanistically based models, the propagating pore model presented the better correlation with the batch reactor experimental data. Similar to the batch data, the shrinking particle model did not present a good

correlation with the continuous reactor experimental data. However, the empirically based model presented the best correlation with both the batch and continuous reactor experimental data.

The propagating pore mechanism was confirmed in the present study. Scanning electron microscopic observations of whole leached particles and reflective light microscopic observations of polished sections complimented each other in supporting the propagating pore mechanism. However, the shrinking particle leach mechanism could not be totally discounted.

The surface oxidation leach rate proved to be a useful leach parameter. However, care should be taken in selecting the method to predict the surface area available for leaching, since neither the B.E.T. nor the geometric surface area determinations proved to be completely accurate.

Gold extraction was observed to be directly proportional to the fraction arsenic leached.

From this work it can be concluded that the propagating pore mechanism is dominant in the bacterial leaching of the pyrite concentrate. Of the models presented, the empirical logistic model provided the best correlation with the experimental data.

TABLE OF CONTENTS

Acknowledgements
Abstract
Nomenclature

CHAPTER 1
INTRODUCTION

CHAPTER 2
APPLICATION OF BACTERIA IN THE LEACHING OF MINERALS

2.1 Introduction 5
2.2 Iron and Sulphur Oxidizing Bacteria 5
2.3 Baterial Leaching Mechanisms 8
2.4 Bacterial Oxidation of Metal Sulphides 10
2.4.1 Oxidation of Pyrite and Arsenopyrite 10
2.4.2 Oxidation of Other Sulphide Minerals 13
2.5 Industrial Scale Bacterial Leaching Techniques 14
2.6 Factors Affecting Bacterial Activity 15
2.7 Bacterial Leaching of Auriferous Sulphide Minerals 17
2.7.1 Mineralogy of Auriferous Sulphide Minerals 17
2.7.2 Leaching Studies of Auriferous Sulphide Minerals 19

CHAPTER 3
MODELING DEVELOPMENTS IN BACTERIAL LEACHING

3.1 Introduction 23
3.2 The Implication of Bacterial Attachment to Solid Substrates 23
3.3 The Effect of Particle Size, Solids Concentration and Surface Area Concentration on Leach Rates 27
3.4 Kinetic Models for Bacterial Leaching 31

CHAPTER 4
THEORY : MODEL PRESENTATION

4.1 Introduction 41
4.2 The Shrinking Particle Model 41
4.2.1 Batch Operation
4.2.2 Continuous Reactor Operation 42
4.3 The Propagating Pore Model 45
4.3.1 Batch Operation 45
4.3.2 Continuous Reactor Operation 47
4.4 The Logistic Growth Model 52
4.4.1 Batch Operation 52
4.4.2 Continuous Reactor Operation 54

CHAPTER 5
MATERIALS, APPARATUS AND METHODS

5.1 Materials 57
5.1.1 Pyrite Concentrate : Description and Preparation 57
5.1.2 Bacteria 58
5.2 Apparatus 58
5.3 Experimental Procedures 61

5.3.1 Culture Maintenance and Growth Evaluation 61
5.3.2 Leaching Techniques 63
5.3.3 Analytical Procedures 65
5.3.4 Miscellaneous Measurements 66

CHAPTER 6
RESULTS AND DISCUSSION

6.1 Introduction 67
6.2 Batch Test Results 67
6.2.1 Experimental Results 70
6.2.2 Comparison of the Propagating Pore and Shrinking Particle Models 79
6.2.3 The Logistic Growth Model - Discussion, and Fitting the Model to the Experimental Data 95
6.3 Continuous Reactor Test Results 100
6.3.1 Experimental Results 100
6.3.2 Fitting the Models to the Experimental Data 108
6.4 Gold Extraction 116

CHAPTER 7
CONCLUSIONS AND RECOMMENDATIONS

7.1 Conclusions 121
7.2 Recommendations 124

REFERENCES 125

APPENDICES

A Unreacted solid residue analyses and mass balance calculations for the batch reactor tests

B Unreacted solid residue analyses and mass balance calculations for the continuous reactor tests

C B.E.T. Specific Surface Area Determinations

D Batch and Continuous Reactor Parameters : Redox Potentials and Dissolved Oxygen

NOMENCLATURE

r_v	volumetric oxidation rate, (kg m^{-3} day^{-1})
r_{vo}	initial volumetric oxidation rate, (kg m^{-3} day^{-1})
r_a	surface oxidation rate, (kg m^{-2} day^{-1})
r_{ao}	initial surface oxidation rate, (kg m^{-2} day^{-1})
n	number of particles per unit volume of solution, (m^{-3})
a_p	particle surface area, (m^2)
ρ	density, (kg m^{-3})
ρ_p	pyrite density, (kg m^{-3})
ρ_s	sulphur density in the pyrite concentrate (kg m^{-3})
d	particle diameter, (m)
d_o	initial particle diameter, (m)
c_t	solids concentration at time t, (kg m^{-3})
c_o	initial solids concentration, (kg m^{-3})
n_q	number of active pores per unit surface area, (m^{-2})
n_{qo}	initial number of active pores per unit surface area (m^{-2})
b	area of pore base, (m^2)
r_p	oxidation rate at pore base, (kg m^{-2} day^{-1})
v_p	rate of pore propagation, (m day^{-1})
L	pore length, (m)
L_1	minimum pore length (m)
L_e	maximum pore length (m)
t	time, (day)
T_1	time at which pore deactivation starts, (day)
T_e	time at which all pores have become inactive, (day)
F_m	maximum fraction of substrate oxidizable
F_o	fraction substrate oxidized at time zero
k_m	rate constant, (day^{-1})

CHAPTER 1

INTRODUCTION

Bacterial leaching, as a commercial metallurgical process, has gained increasing popularity in recent years. Traditionally bacterial leaching has been practiced in dump and heap leaching processes. About 10 to 15% of all the copper produced in the U.S.A. is obtained by means of bacterial leaching of low grade ores or waste dump material (Lundgren and Malouf, 1983). A variation on heap or dump leaching, is *in-situ* leaching, which has the economic advantage of eliminating the costs involved in bringing the ore above ground and subsequent crushing (Burton *et al.*, 1983). These methods are normally only applied to the recovery of base metals such as copper, nickel, zinc etc. from their sulphide minerals in low grade ores.

However, innovation in bacterial leaching has changed the emphasis from these low-cost, high-residence time processes to a more advanced high-cost, low-residence time process, involving the recovery of refractory precious metals. These refractory precious metals, such as gold and silver, often occur finely disseminated in sulphide minerals which do not respond well to conventional cyanidation processes. These refractory ores therefore require an additional oxidation step prior to cyanidation to 'liberate' the 'trapped' precious metals.

In the face of escalating mining and operating costs, it has become particularly important for the mining industry to recover the maximum possible fraction of precious metal in a single process, thus optimizing process efficiency. Re-treating dumped material can result in reduced profit margins. The commencement of backfilling

practices has placed an additional emphasis on obtaining maximum recoveries prior to returning waste material underground.

The pre-oxidation of sulphide minerals in order to recover refractory precious metals can be procured by means of roasting (Chant, 1975; Penman, 1985), pressure oxidation (Derry, 1972; Chant, 1975), or bacterial leaching (Chant, 1975; Livesey-Goldblatt *et al.*, 1983).

Roasting is a well-established and well-defined process. Although controls can be put on roasters to prevent the escape of large amounts of sulphur dioxide and arsenic gases generated, it has become very expensive, as environmental requirements for cleaner emission gases are continuously increasing. Another disadvantage of roasting is that the precious metal particles might be fused in the roast product and thus cannot be recovered. Bacterial leaching generates essentially no gases, and toxic elements such as arsenic and antimony can be converted into inert substances that can safely be deposited in tailing dumps.

Even though pressure oxidation has the advantage of low residence times, the process parameters of high oxygen partial pressures and high temperatures, generally make it an expensive procedure (Yen and Wyslozil, 1985). Bacterial leaching, on the other hand, is conducted at ambient pressure and temperature.

In cost-comparison studies of bacterial leaching with alternative processes, several investigators claim that bacterial leaching is an economically viable process. This has been reported by Livesey-Goldblatt *et al.* (1983), Renner *et al.* (1984), Lawrence and Gunn (1984), Bruynesteyn *et al.* (1985) and Haines (1986). However, these studies relied on bench scale evaluations. Even though a pilot scale study

with a working volume of 500 litre was reported by Bruynesteyn *et al.* (1986), scale-up appears to be empirical and not based on a quantitative kinetic model.

It would appear that some apprehension towards bacterial leaching as a whole exists due to a lack of sound modelling concepts to define the process. A need has therefore been established to obtain a kinetic model to characterize the leaching process, predict reactor performance, and process economics.

Several investigators have applied classical bacterial growth models to bacterial leaching in an attempt to fill this void. These models appeared to hold for ferrous oxidation in the liquid phase, but failed in the description of leach kinetics once a solid phase was introduced into the system.

The importance of physical parameters such as particle surface area and solids concentration in the leach slurry was recognized and led to the derivation and application of mechanistically based models such as the shrinking particle model proposed by Blancarte-Zurita *et al.* (1985), for the batch leaching of a metal sulphide concentrate.

Similarly, Hansford and Drossou (1986) derived a mathematical model to describe the kinetics of a batch bacterial leaching system in terms of the fraction sulphide oxidized. This mechanistic model, termed the propagating pore model, was based on the observation of pore formation in bacterial leach residues (Southwood and Southwood, 1985).

Subsequently, Pinches *et al.* (1987), proposed an empirical mathematical model that adequately describes both batch and continuous bacterial leach kinetics in terms of

fraction sulphide oxidized.

The main objective of the present study therefore is to evaluate the models proposed by Drossou and Hansford (1986), and Pinches *et al.* (1987). This was achieved by:

- obtaining pyrite oxidation versus time data for the batch and continuous leaching of a refractory gold-bearing pyrite concentrate for three narrow size fractions.
- extending the shrinking particle and propagating pore models for the continuous case
- examining the model parameters generated for the logistic model, as proposed by Pinches *et al.*(1987)

This thesis therefore contains:

- a survey of the literature giving some background information on bacterial leaching and its application
- a review on the modeling developments in bacterial leaching
- a theoretical presentation where the shrinking particle, propagating pore and the logistic models are presented for both the batch and continuous cases.
- a presentation and discussion of the batch and continuous leaching data generated for the refractory gold-bearing pyrite concentrate.
- and, in conclusion the findings of this study are summarized and the recommendations for future work are presented.

CHAPTER 2

APPLICATION OF BACTERIA IN THE LEACHING OF MINERALS

2.1 Introduction.

In this chapter some general background information on the bacteria used in bacterial leaching is provided. Also included are the basic principles of the bacterial leaching of sulphide minerals. Pertinent information is given on previous studies related to gold recovery and the bio-oxidation of pyrite. The influence of various parameters such as surface area, attachment of bacteria to solids, pulp density, pH and temperature on bacterial leaching is discussed.

2.2 Iron and Sulphur Oxidizing Bacteria.

In a period of forty years the variety of bacteria known to be involved directly or indirectly in the leaching of sulphide minerals has mushroomed from one, *Thiobacillus ferrooxidans*, isolated by Colmer and Hinkle (1947), to a diverse collection of mesophiles, thermophiles, heterotrophs, autotrophs and mixotrophs showing complex ecological relationships.

There are three basic metabolic types:

- *Thiobacillus ferrooxidans* (iron and sulphur oxidizing)
- *Ferrobacillus ferrooxidans* (iron oxidizing)
- *Thiobacillus thiooxidans* (sulphur oxidizing)

Other bacteria that have been isolated and fall into this category, but exhibit specific characteristics (Kelly, 1987) are:

- *Thiobacillus sulfolobus*	thermophilic
- *Thiobacillus acidophilus*	sulphur oxidizing
- *Thiobacillus albertis*	acidophillic
- *Leptospirillum ferrooxidans*	iron oxidizing mesophile

In recent studies (Helle and Onken, 1987), the importance of mixed cultures, especially in continuous operated systems, has been noted : a leach rate increase of approximately four times for pyrite was observed for a *Thiobacillus ferrooxidans* culture in the presence of *Leptospirillum* bacteria. Similarly, Brierley (1982) observed that certain minerals are leached more effectively with mixed cultures as opposed to pure cultures. Of these bacterial cultures, *Thiobacillus ferrooxidans* will be discussed in greater detail as it the main bacterium utilized in the present study.

Thiobacillus ferrooxidans. A number of comprehensive reviews and studies on the morphology, physiology and metabolism of the bacterium *Thiobacillus ferrooxidans* are in existence and have been presented by Silverman and Ehlrich (1964), Tuovien and Kelly (1972), Karavaiko *et al.* (1977), Torma (1977), Brierley (1978) and Kelly *et al.* (1979). A summary of the characteristics of *Thiobacillus ferrooxidans* was obtained from these reviews.

The morphological characteristics are: it is a motile, flagellated, non-spore forming, gram-negative bacterium with an approximate diameter of 0,1 μm and a length of 1,5 μm. It usually occurs singly, but occasionally in

pairs, duplicating by binary fission. The growing cell goes through lag, log, stationary and death phases.

The cell structure of *Thiobacillus ferrooxidans* has been found to be similar to that of other gram-negative bacteria, and the following approximate cell composition has been reported:

- protein 44%
- lipid 26%
- carbohydrate 15%
- ash 10%

and at least two B-group vitamins (riboflavin and thiamine).

The ability of the bacterium to utilize energy released from the metabolic oxidation of inorganic substrates, such as reduced-valence inorganic sulphur, classifies it as a chemolithotroph. The organism is able to oxidize:

- ferrous ion to ferric ion and,
- sulphur in various reduced states to sulphate (SO_4^{2-})

The organism is further classified as an autotroph since it requires only inorganic nutrients for cell growth. These are:

- carbon dioxide as a carbon source
- ammonium sulphate and dipotassium hydrogen phosphate as nitrogen and phosphorus sources
- potassium chloride, magnesium sulphate and calcium nitrate as growth factors.

2.3 Bacterial Leaching Mechanisms.

Essentially two proposed mechanisms are presented in the literature:

- the direct mechanism and,
- the indirect mechanism.

The direct mechanism usually considers the bacterium in direct contact with the sulphide mineral substrate. The attached bacterium then oxidises the sulphide component of the mineral to sulphate, simultaneously dissolving the metal component. Tributsch and Bennet (1981) describe a direct mechanism which utilizes negatively charged sulphur ions in the form of $-SH^-$ groups, which are introduced into the bacteria by means of a carrier molecule. This carrier molecule group is then absorbed into the cell where the sulphide ion is oxidized to sulphate. Lundgren and Tano (1978) felt that the cell envelope, which forms the exterior of the bacteria, contained the necessary enzymes for sulphide oxidation, thus requiring direct contact for oxidation to occur. Southwood and Southwood (1986) observed pore formation in pyritic bacterial leach residues, and suggested that this was partly due to the direct action of bacteria. The latter authors concluded that bacteria attach preferentially to irregularities and crystal structure defects of the sulphide mineral.

Ferric ions are known to be good oxidizing agents of metal sulphides. The indirect mechanism proposes, therefore, that ferric ions oxidize the sulphide ions in the mineral to elemental sulphur, thus dissolving the metal moiety. Simultaneously, the ferric ions are reduced to the ferrous state. The ferrous ions subsequently serve as energy substrate for the bacteria and are oxidized to the ferric

state. A cycle is established where the bacteria only serve to re-oxidise the oxidant.

The relative importance of these two mechanisms is still uncertain. Duncan *et al.* (1967), studying the bacterial leaching of pyrite and chalcopyrite, used selective sulphide and ferrous oxidation inhibitors and found that iron and sulphide oxidation depended on the bacterial culture used. Beck and Brown (1973), also working on pyrite and chalcopyrite, found that the indirect mechanism dominated. Pore formation similar to that observed by Southwood and Southwood (1986), has been observed to occur in pressure leach residues, as well as in naturally oxidized pyrite (Keller and Murr, 1982; De Nooy, 1987). This suggests a purely chemical action indicating an indirect mechanism. Tributsch and Bennet (1981), suggested that in the presence of suitable oxidizing agents (e.g. ferric ions), electrons may be extracted from the valence bond of the mineral, thus more broken bonds are formed in the sulphide lattice. This leads to enhanced leaching, and it is suggested that the direct and indirect mechanisms might interact. The creation of broken bonds by the oxidant could facilitate the direct attack of bacteria on the mineral, however, it is not known if this combined effect would be equal to the sum of the two individual mechanisms.

There is still uncertainty in the literature as to the relative importance of the direct and indirect mechanisms. However, it is realised that various factors, such as the type of mineral and culture, the extent to which adaptation to the mineral has taken place, as well as certain physical conditions (e.g. pH, temperature, metal ion concentrations), might dictate the dominant mechanism.

2.4 Bacterial Oxidation of Metal Sulphides.

The basic reactions involved in the bacterial leaching of metal sulphides have been summarized by Torma (1977) and Karavaiko *et al.* (1977). As precious metals are often associated with pyrite and arsenopyrite, the oxidation of these sulphides has special interest and will be discussed in greater detail.

2.4.1 Oxidation of Pyrite and Arsenopyrite.

In the presence of bacteria, the oxidation of pyrite can be accelerated by a factor of 10^3, whilst the oxidation of ferrous ion to ferric ion can be accelerated by a factor of 10^6 (Karavaiko *et al.*, 1977; Lacey and Lawson, 1970)

Irrespective of the mechanism applied, the oxidation of pyrite is given by the following overall reaction:

$$FeS_2 + 15O_2 + 2H_2O \rightarrow 2Fe_2(SO_4)_3 + 2H_2SO_4 \qquad 2.1$$

This is obtained from a combination of intermediary reactions, where ferrous sulphate ($FeSO_4$) and elemental sulphur (S^0) are intermediary products. These intermediary products formed from the initial oxidation reactions are then further oxidized to ferric sulphate and sulphuric acid, as described by the following reactions (Karavaiko *et al.*, 1977; Kandemir, 1983):

$$2FeS_2 + 7O_2 + 2H_2O \rightarrow 2FeSO_4 + 2H_2SO_4 \qquad 2.2$$

$$4FeSO_4 + O_2 + 2H_2SO_4 \rightarrow 2Fe_2(SO_4)_3 + 2H_2O \qquad 2.3$$

$$FeS_2 + Fe_2(SO_4)_3 \rightarrow 3FeSO_4 + 2S^0 \qquad 2.4$$

$$2S^0 + 2H_2O + 3O_2 \rightarrow 2H_2SO_4 \qquad 2.5$$

Further secondary reactions can take place, depending on the pH of the pulp. These are mainly hydrolysis reactions and the possible insoluble products are:

- basic ferric sulphate

$$Fe_2(SO_4)_3 + 2H_2O \rightarrow 2Fe(OH)SO_4 + H_2SO_4 \qquad 2.6$$

- ferric hydroxide

$$Fe_2(SO_4)_3 + 6H_2O \rightarrow 2Fe(OH)_3 + 3H_2SO_4 \qquad 2.7$$

- and the most commonly found inorganic by-product, jarosite

$$3Fe_2(SO_4)_3 + 12H_2O \rightarrow 2H[Fe(SO_4)_2.2Fe(OH)_3] + 5H_2SO_4 \qquad 2.8$$

The H^+ ion in the jarosite can be replaced by a NH_4^+, Na^+, or a K^+ ion to form ammonio-, natro- or potassio-jarosite respectively. Laserhoff, Sigal and Wasserman (1982), suggested that bacteria produce a soluble precursor consisting of a hydroxo-bridged polymer, which contains sulphate ions in the outer co-ordination, prior to actual jarosite precipitation.

The precipitation of jarosite might have an adverse effect on bacterial leaching, as these precipitates may cover sulphide surfaces, reducing the surface area available for leaching. Consequently, the reaction rates may become diffusion controlled, and excessive precipitation may lead to nutrient depletion in the solution.

The corresponding overall reaction for the leaching

of arsenopyrite is given by Pinches (1975), and Torma (1977) as:

$$2FeAsS + 7O_2 + 2H_2O \rightarrow 2FeAsO_4 + 2H_2SO_4 \qquad 2.9$$

Initially the oxidation of arsenopyrite will give rise to the formation of arsenous acid and ferrous- and ferric sulphate:

$$4FeAsS + 11O_2 + 2H_2O \rightarrow 4HAsO_2 + 4FeSO_4 \qquad 2.10$$

$$4FeSO_4 + 2H_2SO_4 + O_2 \rightarrow 2Fe_2(SO_4)_3 + 2H_2O \qquad 2.11$$

Subsequently, arsenic acid is formed as described in the following reaction:

$$HAsO_2 + Fe_2(SO_4)_3 + H_2O \rightarrow H_3AsO_4 + 2FeSO_4 + H_2SO_4 \qquad 2.12$$

Arsenic acid may also be formed in an intermediary reaction, where ferric sulphate oxidises the arsenopyrite as follows:

$$2FeAsS + Fe_2(SO_4)_3 + 4H_2O + 6O_2 \rightarrow 2H_3AsO_4 + 4FeSO_4 + H_2SO_4 \qquad 2.13$$

The arsenic acid can react with ferric sulphate to precipitate as iron-arsenate:

$$2H_3AsO_4 + Fe_2(SO_4)_3 \rightarrow 2FeAsO_4 + 3H_2SO_4 \qquad 2.14$$

2.4.2 Oxidation of Other Sulphide Minerals.

Besides pyrite, *Thiobacillus ferrooxidans* also oxidises other iron sulphide minerals such as pyrrhotite (FeS) and marcasite (FeS_2) (Silverman *et al.* (1978)). Leaching of the following copper minerals has also been reported:

- chalcopyrite (CuFeS) (Bruynsteyn and Duncan, 1974; McElroy and Bruynsteyn, 1978)
- covelite (CuS) (Corrans *et al.*, 1972)
- chalcocite (Cu_2S) (Sakaguchi *et al.*, 1976).

The leaching of orpiment (As_2S_3) has been reported by Ehlrich (1963), whilst Gormely *et al.* (1975) reported the leaching of sphalerite (ZnS).

Other minerals that have been found to be oxidized by bacteria are, (Torma, 1977; Torma, 1978):

- molybdenite (MoS_2)
- antimonite (Sb_2S_3)
- energite (Cu_3AsS_4)
- pentlandite ($(Ni,Fe)_9S_8$)
- galena (PbS) etc.

A further application of bacteria in leaching is in the recovery of uranium. Iron oxidizing bacteria are used to oxidize ferrous ion to ferric ion. The ferric then serves as an oxidant in uranium leaching (Miller *et al.*, 1963; Guay *et al.*, 1976). Furthermore, iron and sulphur oxidizing bacteria are used in the de-sulphurization and ash removal of coal by leaching inorganic sulphur and sulphide minerals (Silverman *et al.*, 1961; Dugan and Apel, 1978; Pooley and Atkins, 1983; Beyer *et al.*, 1986).

2.5 Industrial Scale Bacterial Leaching Techniques.

Bacterial leaching techniques used on an industrial scale have been described by Corrans *et al.* (1972), Brierley (1978), Brierley (1982), and Lundgren and Malouf (1983). Currently the predominant commercial processes are heap and dump leaching.

Dump leaching is employed when treating low-grade (less than 0,4% metal content) run-of-mine ores or waste material dumps. These dumps are usually placed on trough shaped impermeable rock bases, and normally contain naturally occurring thiobacilli. The leach solution is introduced at the top of the dumps, usually by sprinkling or flooding, and is allowed to percolate through the dump. For copper leaching operations, these pregnant liquors typically contain 1 - 3 g l^{-1} copper in solution. Dump leaching is an uncontrolled process. Mass transfer limitations, localised high temperatures and metal concentrations can inhibit leach rates and even lead to premature termination of leaching. Furthermore, channeling and blockages due to precipitations (e.g. jarosite) can lead to reduced metal recoveries.

Ores with higher metal concentrations are normally subjected to heap leaching, which provides a more controlled process. The ore is usually crushed and placed on a specially prepared surface. Heaps are often provided with aeration systems for improved leach rates. Dump and heap leaching processes are currently employed in the leaching of low grade copper- and uranium ores in the U.S.A. (Brierley, 1978).

In-situ leaching is normally applied to low grade ores when conventional mining would be uneconomical, or, to abandoned, previously exploited ore bodies (Brierley, 1978;

Burton, 1983). Fracturing the ore body by means of an explosive charge allows the percolation of leach solutions. Pregnant leach solutions are recovered, stripped of the metal content and recycled. *In-situ* leaching has the advantage of reducing surface disturbance over the ore body, thus eliminating such problems as solid waste material disposal.

All the abovementioned methods have dealt with the leaching of low grade ores. However in the case of sulphide concentrates (e.g. obtained by flotation) with high precious metal grades, bacterial leaching can be performed in low-residence reactors (e.g. stirred tank or airlift type reactors). This involves the leaching of finely ground material under controlled conditions. To obtain high leach rates and metal dissolution, high oxygen transfer rates are normally required in these reactors. High leach rates result in high heat generation rates, therefore these reactors need to be equipped with adequate heat removal systems to facilitate temperature control. The performance of such full-scale reactors has, as yet, not been fully tested and modeled.

2.6 Factors Affecting Bacterial Activity.

The prospects of utilising the ability of bacteria to oxidize metal sulphides, have provoked studies into factors which influence bacterial activity and the subsequent practical implications.

In general, to avoid formation of insoluble ferric precipitates which may occur during bacterial leaching of sulphide iron, it is necessary to operate at low pH values (Vuorinen *et al.*, 1986). Inhibition of metal sulphide oxidation by *Thiobacillus ferrooxidans* has been observed by

Norris (1983) at a pH of 1,5. It has also been found that *Thiobacillus ferrooxidans* is unable to initiate growth on ferrous ion at a pH greater than 3,0 (Brierley, 1978). Optimum pH values of between 2,3 and 2,5 have been reported by Torma (1977).

Nitrogen, derived from ammonium sulphate, appears to be the most important nutrient (Brierley, 1978). It is noteworthy that nitrate salts do not seem to serve as a nitrogen source and might even have an inhibitory effect at high concentrations (Tuovinen *et al.*, 1971). A study of the effects of various nutrients on the bacterial leaching of a zinc sulphide concentrate, reported by Torma *et al.* (1970), showed that the ammonium sulphate concentration determines the final metal extraction, while di-hydrogen phosphate determines the leach rate.

The critical oxygen concentration, below which growth inhibition has been observed for *Thiobacillus ferrooxidans*, has been reported as 0,2 mg l^{-1} (Pinches *et al.*, 1987). Furthermore, the critical oxygen concentration below which dissolved oxygen becomes rate limiting in metal oxidation, has been found to be 0,29 mg l^{-1} (Lui *et al.*, 1987). Oxygen solubility in 9K basal salt at 35°C is approximately 6,5 mg l^{-1} (Lui *et al.*, 1973; Pinches *et al.*, 1987). The low solubility of oxygen and the apparent major effect it has on bacterial growth and metal oxidation, makes the transfer of oxygen from air to the liquid phase an important consideration in the design of bacterial leach reactors.

Goodman *et al.* (1984), have investigated the bacterial leaching of a natural zinc-iron sulphide under conditions where oxygen was excluded and carbon dioxide enhanced above atmospheric concentration. Under inoculated aerobic conditions, the maximum concentration of iron in

solution was found to be 48% of the total iron present, while 100% zinc extraction was achieved. The total fraction of iron leached from the ore by re-dissolving the precipitates was not determined. Under inoculated anaerobic conditions 63% zinc and 86% iron extraction was achieved in a similar time-span. Both the ferrous and ferric ions remained in solution. Additionally, no acid generation was observed under anaerobic conditions. Torma *et al.* (1972), studying the bacterial leaching of a zinc sulphide concentrate, found an increase in leach rates with an increase in the carbon dioxide content of the air used for aeration. Therefore, carbon dioxide enriching of air for bacterial leaching appears to be essential, especially at high solids concentrations.

The optimum temperature range for bacterial leaching of metal sulphides has been found to be limited, depending on the strain of bacterial culture and its' specific characteristics. The optimum temperature has been found to be in the range of 25°C to 45°C for different strains of *Thiobacillus ferrooxidans* (Torma, 1977).

2.7 Bacterial Leaching of Auriferous Sulphide Minerals.

2.7.1 Mineralogy of Auriferous Sulphide Minerals.

Gold is frequently associated with sulphide minerals that occur in various gold ore deposits. In a survey that included 115 deposits in the U.S.A., it was found that in 48 of these, gold was associated with pyrite. In a further 45 cases, gold was associated with arsenopyrite (Schwartz, 1944). It is important to note that the nature of gold association with sulphide minerals can vary considerably from one deposit to another. Haines (1986) compared the gold association with different sulphide minerals in the Sao

Bento (Brazil) and Fairview (South Africa) concentrates. In the case of the Sao Bento concentrate, the gold association with the sulphide minerals occurred as included (52%), attached (13%) and interstitial grains (33%). The included gold was mainly associated with the arsenopyrite, while the attached and interstitial gold appeared to have an affinity for the pyrrhotite. The gold appeared to have the least affinity for the pyrite. In the case of the Fairview concentrate, the investigation revealed that 95% of the gold occurs as inclusions in the pyrite (predominantly submicroscopic) while only 2% is associated with the arsenopyrite.

Southwood and Southwood (1986) suggest that gold which cannot be detected in a statistically sufficient number of polished sections using vertically reflected light microscopy (i.e. grain dimensions < 1 μm in diameter) and using scanning electron microscopy (i.e. grain dimensions < 0,01 μm in diameter) is considered to be submicroscopic. Submicroscopic gold can either occur in solid solution , or particulate and finely disseminated. In either case, under conditions of high temperatures and pressures (e.g. during metamorphism), gold can be remobilized to form discreet inclusions in the sulphide mineral. The resulting particulate inclusions cause disruptions and areas of high stress in the crystal structure of the sulphide mineral. It has been suggested that these structural imperfections are sites for accelerated leaching. This would result in the preferential leaching of sulphide minerals to give high gold recoveries for a relatively small fraction of sulphide oxidized. This phenomenon was observed by Drossou (1986), for an auriferous pyrite concentrate.

On the other hand, if the gold occurred in solid solution, an equivalent fraction of sulphide breakdown would be required for an equivalent fraction of refractory gold recovery.

2.7.2 Leaching Studies of Refractory Auriferous Sulphide Minerals.

Previously reported work has mainly been concerned with comparing the economical viability of bacterial leaching to existing methods of pre-oxidation and the amenability of different deposits to the process (usually on a bench scale). It is furthermore observed that few or no attempts have been made in this specific field of investigation to establish a procedure or model to enable scale-up and reactor performance prediction of bacterial leaching systems.

Recognizing the possibility of applying bacterial leaching as a pre-oxidation step in refractory gold recovery, Livesey-Goldblatt *et al.* (1983) looked at the cost implications for gold recovery from a pyrite-arsenopyrite run-of-mine ore and a flotation concentrate. A high overall gold recovery of 89,8% was reported for the flotation concentrate. Leaching was performed in five 20-litre vessels and it would appear to have been an in-series configuration. An overall residence time of 12 days was reported at a pulp density of 13,3% solids to achieve maximum gold recovery, but the equivalent fraction sulphide breakdown and leach rates were not reported. (Oxidation appears to near completion if calculated from data available). It is important to note that the investigators found it necessary to mill the flotation concentrate to 88% less than 75μm to obtain maximum gold recovery. Furthermore the necessity to develop equipment that requires a small energy input to achieve maximum oxygen solubilization is recognized. They concluded that the bacterial leaching of the flotation concentrate would be economically viable.

In an amenability study of gold and silver bearing ores, Bruynesteyn (1984) reported marked improvements in precious metal recoveries after bacterial leaching. However, leach kinetics for these ores were not reported. An important characteristic of bacterially leached residues observed in this study is a non-linear precious metal recovery vs. sulphide breakdown relationship, i.e. high recoveries for relatively low fractions of sulphide oxidation.

A similar phenomenon for gold recovery was observed by Marchant (1985) in the bacterial leaching of a gold and silver bearing flotation tailing. The gold recovery (65 to 75%) appeared to be independent of the pyrite oxidation (6 to 65% iron extraction). However, the silver recovery was highly dependent on the fraction iron extraction. This might indicate preferential oxidation of the precious metal bearing minerals. No attempt was made to model or predict the reactor performance, for either the bench-scale or the pilot-scale studies, and a four-in-parallel into a four-in-series reactor configuration was suggested.

In contrast to the configuration used by Marchant, Lawrence and Gunn (1985) used a two stage equal volume reactor system. The authors presented their leach data in the form of volumetric leach rates. These leach rates were calculated based on the overall volume of the reactor system and the residence time. However, the authors did not attempt to model or differentiate between the two leach vessels. They investigated the bacterial leaching of a refractory gold bearing flotation concentrate and reported an optimum solids concentration of 16% but do not provide any data on how this was established. They observed high fractions of sulphide oxidation in the two stage system, due to regrinding and recycling leached residues. In addition, the feed material was milled to 80% less than 17μm. The paper

presented confirmed the viability of increasing the refractory precious metal recovery by bacterial leaching.

Bruynesteyn *et al.* (1986) using a three-in-series, 5-litre air-sparged reactor system observed improvements in leach rates from the the rapid leaching phase in batch test results, to continuous testing. A sulphide oxidation of about 70% resulted in 97% gold recovery. Additional oxidation resulted in only a marginal increase in gold recovery. From the bench scale system the authors proceeded to a three-in-series, 167-litre mechanically agitated reactor pilot system. Volumetric oxidation rates obtained from the pilot plant were reported as 0,660 $gl^{-1}h^{-1}$ for iron, and as 0,280 $gl^{-1}h^{-1}$ for arsenic at a pulp density of 17,5% solids (90% less than 38μm). The iron oxidation rate agrees favourably with that reported by Lawrence and Gunn (1985). No apparent attempt was made at scaling up from the 15-litre to the 500-litre system other than maintaining the same configuration. A proposed full-scale plant design was based on the pilot plant data. Once again scale-up appears to be empirical. The full scale design proposed a reactor system of four reactors in parallel in the first stage, followed by a second and third stage of two reactors in parallel. The design residence time in the first stage is given as 48 hours. This is a similar residence time obtained for optimum conditions in the first reactor during pilot scale testwork. The second and third stages have a residence time of 24 hours. However, provision has been made in the design to run the system as four reactors in parallel into four reactors in series which would result in a configuration similar to that suggested by Marchant (1985). This provision is perhaps due to empirical scale-up, and the consequent uncertainty in design criteria.

In spite of the fact that the majority of studies have mainly been concerned with the improvements in gold

recoveries to be gained by pre-oxidation, it has generally been projected that commercial scale bacterial leaching of refractory auriferous sulphide minerals should prove economically viable and should hold certain advantages over conventional pre-oxidation procedures. Only tentative suggestions for full scale design and operation have been made, and no fundamental model has been suggested on which to base or project full scale leach reactor performance. However, it has become evident that the realisation of a full scale bacterial leaching plant is imminent, and therefore it is of paramount importance to obtain a design procedure to predict leach reactor performance.

CHAPTER 3

MODELING DEVELOPMENTS IN BACTERIAL LEACHING

3.1 Introduction.

Considering the objectives of this work, i.e. obtaining a mathematical model that adequately describes the bacterial leaching of a sulphide mineral, various aspects need to be taken into consideration. This chapter will give an overview of bacterial attachment to sulphide minerals and other surfaces, and the relevance of this to leaching mechanisms. Secondly, the effects of particle size and surface area on the kinetics of bacterial leaching will be presented from the available literature. Finally, models for bacterial leaching will be considered.

3.2 The Implication of Bacterial Attachment to Solid Substrates.

If bacterial attachment to solid substrates is a prerequisite for leaching to occur, this may reveal an important aspect of the leaching mechanism, and therefore should be an integral part of a fundamental model. This aspect may be revealed in such observations as selective bacterial attachment to particles recognized as oxidizable substrates. Even more revealing, would be if bacterial attachment sites coincided with corrosion sites or pits observed in leached particles.

Several comprehensive investigations of bacterial attachment to minerals and other surfaces have been published (McGoran *et al.*, 1969; Weis, 1973; Duncan and

Drummond, 1973; Murr and Berry, 1974; Berry and Murr, 1975; Berry and Murr, 1978; Bennet and Tributsch, 1978). However there does not appear to be consensus on the significance of cell attachment as an important parameter in leaching mechanisms.

This is illustrated by the diverse conclusions of various investigators. McGoran *et al.* (1969), studying the growth of *Thiobacillus ferrooxidans* on various substrates, found that 96% of the bacterial population was associated with the sulphide particles when grown on chalcopyrite. When using sulphur as a substrate, 77% of the cells were attached to sulphur surfaces. The difference in the fraction of the population attached to the different substrates does not signify much in itself, however, it does suggest that, because the majority of the bacteria are attached, attachment to solid surfaces could be an important parameter to consider.

Examining leached pyrite grains, Duncan and Drummond (1973) observed that bacterially leached surfaces were rough and etched. This, the authors suggested, is evidence of direct bacterial attack, as it was not observed for chemically leached surfaces.

In addition, Berry and Murr (1975) observed strain contrast features associated with pit formation at bacterial attachment sites. They suggested that these features indicated attachment prior to solid substrate removal. They also found that bacterial attachment was not specifically associated with the emergence of crystal dislocation lines. In a later study, Berry and Murr (1978) observed the attachment of *Thiobacillus ferrooxidans* and *Sulfolobus* cells to thin sections of a low grade chalcopyrite ore to be preferential to sulphide rich regions. They suggested that bacteria have the ability to distinguish between, and attach

to, optimum sites such as sulphide rich areas, i.e. abundant oxidizable substrate.

Similarly, Bennet and Tributch (1978) observed attached bacteria and chained corrosion pits that intersected each other at right angles on single pyrite crystals. Because pyrite crystal dislocations are often parallel to the crystallographic axes, thus perpendicular to each other, these corrosion chains appear to coincide with imperfections in the crystal lattice. Assuming that the corrosion pits and bacterial attachment sites coincide, the authors suggested that the micro-organisms are able to preferentially attach to optimum oxidation sites (optimum oxidation sites defined as sites where crystal dislocations occur, i.e. sites where more readily oxidizable substrate is available).

The evidence presented would suggest that only attached bacteria are able to oxidize solid substrate, thus that bacterial attachment is a prerequisite for leaching to occur. This would also suggest that only attached cells are able to reproduce, and that cells are able to select their attachment sites.

Unlike Duncan and Drummond (1973), Keller and Murr (1982) did observe pyrite particles to be etched after chemical leaching. In addition, even though Keller and Murr (1982) observed more complex etching patterns for bacterial leaching than those produced during ferric sulfate leaching of pyrite, they did not attribute this to bacterial contact.

Furthermore, Dispirito *et al.* (1983) studying the sorption kinetics of *Thiobacillus ferrooxidans* to both inert and oxidizable solids, found the steady state sorption to quartz and flowers of sulphur to be comparable. Similarly, comparable fractions of cell sorption was observed for pyrite, glass beads and fluorapetite. It would thus appear

that cell attachment is a function of the total number concentration and the surface area available, and not preferential to oxidizable solids, eg. pyrite. Similarly, Meyerson and Kline (1983) observed rapid irreversible adsorption of bacteria to coal and glass particles. Only a finite concentration of bacteria was observed to remain in solution.

Wakao *et al.* (1987) moved one step further away from the concept that attachment is a prerequisite to leaching of a solid substrate. Studying the bacterial oxidation of pyrite, they found that the cells of *Thiobacillus ferro-oxidans* were rapidly adsorped (more than 99%) onto the solid surfaces of an agitated flask, containing 1% w/v particles. However, significantly fewer cells were adsorped to pyrite particles than to the glass walls of the flask. The authors found the cells adsorped aggregatively on restricted areas of the pyrite particles, suggesting selective attachment as observed by other investigators, however no significant cell adsorption was observed in the extensively eroded areas and polyhedral pits of the leached pyrite particles. The authors also observed that, after cell adsorption onto solid surfaces had taken place, the iron oxidizing activity of the bacteria was inhibited. Furthermore, adsorped cells did not proliferate. The authors ascribed the enhancement of pyrite oxidation to the iron oxidizing activity of the freely dispersed *Thiobacillus ferrooxidans* cells in the aqueous phase, rather than to the bacterial population on the pyrite particles.

If leaching can be ascribed to the activity of the freely suspended cells, it means that leaching occurs through ferric oxidation of the insoluble substrate. This implies chemical leaching as opposed to direct bacterial leaching. The question now arises as to whether chemical leach rates are comparable to those in the presence of

bacteria. Huberts (1987) successfully illustrated that the chemical leach rate of synthetic Heazlewood (Ni_3S_2) under sterile but similar redox potential conditions, was equal to or better than that observed in the presence of bacteria.

It is clear that some controversy exists on the subject of bacterial attachment and the role it plays in the oxidation of solid substrates. In general, it would appear from these studies that the majority of bacteria in a *Thiobacillus ferrooxidans* leaching system are attached to solid surfaces. In view of evidence that *Thiobacillus ferrooxidans* adsorps irreversibly to inert surfaces, some doubt is placed on selective attachment of bacteria, even though some investigators have published evidence to substantiate this phenomenon. As yet, no conclusive evidence has been presented to prove or disprove the direct mechanism, i.e. bacterial attachment is required for leaching to occur. However, in the light of present thinking, it would appear that bacterial attachment to solid surfaces will not play an important part in establishing a fundamental model to describe or predict bacterial leaching performance.

3.3 The Effect of Particle Size, Solids Concentration and Surface Area Concentration on Leach Rates.

Several of the early studies in bacterial leaching were concerned with the effect of particle size and concentration on the observed leach rate. Malouf and Prater (1961) obtained the highest leach rate for pyrite with the finest size fraction. Silverman *et al.* (1961) observed very little leach activity at a particle size greater than 230 μm (65 mesh) for four different sulphuritic materials. A size reduction resulted in a marked improvement in leach performance for all four materials. Similarly, Duncan *et al.*

(1966) observed increased leach rates for copper from chalcopyrite for a decrease in particle size. Thus, in general, a particle size reduction resulted in an increased leach rate.

In addition to particle size, pulp density appears to be an important parameter to consider, because in many studies it has been found that high pulp densities adversely affects leach rates. A first order relationship of the leach rate with solids concentration over a range of values has in general been observed (Torma *et al.*, 1970; Torma *et al.*, 1971; Pinches, 1972; Torma and Subramanian, 1974; Pinches *et al.*, 1976).

Torma *et al.* (1970) observed a linear increase in leach rate with an increase in pulp density, for zinc extraction from a zinc sulphide concentrate, up to approximately 13% solids. Only a further marginal increase was observed up to 16% solids, after which the leach rate decreased. However, in a subsequent publication (Torma *et al.*, 1972) it was established that the linear relationship was disrupted due to carbon dioxide inhibition. The linear relationship was observed to hold up to 24% solids when carbon dioxide enriched air was used during experimentation.

The fact that the authors observed a linear relationship between the leach rate and the solids concentration, confirms the importance of this modeling parameter. In addition to this, an inhibitory effect was observed at higher solids concentrations, which can possibly be attributed to mass transfer limitations, or, perhaps mechanical trauma.

Even though solids concentration in itself is an important consideration, both particle size and solids concentration can be contained in a single parameter -

surface area concentration. The specific surface area (expressed as $m^2\ kg^{-1}$) is dependent on the size distribution of the concentrate, so that this together with the solids concentration in the slurry (expressed as $kg\ m^{-3}$) would determine the surface area concentration (expressed as $m^2\ m^{-3}$ slurry).

Torma *et al.* (1970, 1972) increased surface area concentration by increasing solids concentration at a constant size distribution, and, by decreasing the mean particle size at a constant solids concentration. In both cases a linear relationship was observed between the leach rate and the surface area concentration. Similarly, Pinches (1975) observed a linear relationship between the surface area concentration and the leach rate for pyrite in a pyrite-arsenopyrite concentrate. Surface areas were calculated from the mean Stokes diameter for the size ranges employed. Investigating the effect of pulp density, the author found the iron leach rate to be proportional to pulp density, for a range up to 10% solids. This relationship, however, became increasingly independent at higher pulp densities. The arsenic leach rate was proportional to the pulp density only at very low solids concentrations. In addition to this, Gormely *et al.* (1975) studying the bacterial leaching of a zinc sulphide concentrate in a continuous reactor, found a first order relationship between surface area concentration and the zinc leach rate.

This suggests that it would be possible to predict the overall leach rate from a constant surface oxidation rate and the total surface area concentration present. The surface area concentration can be obtained from the specific surface area of the mineral and the solids concentration of the mineral in the suspended slurry. Thus, both the particle size distribution and the solids concentration will be contained in a single parameter, i.e. the surface area

concentration of the slurry.

The surface area oxidation rate will therefore depend on the method used to measure the specific surface area of the mineral. There are various methods of obtaining specific surface area estimations. The following have been reported in the literature:

Firstly, there are methods that are based on the geometrical characteristics and the density of the particles, of which the simplest is to assume the particles to be uniform spheres, based on the mean particle diameter. This method is used later in the study and is referred to as the geometrical surface area.

Secondly, there are methods that are based based on gas adsortion onto the particle surface, such as the B.E.T. method. This method gives a measure of both the external as well as the internal (due to pores, cracks and fissures) surface area.

In the third instance, there are methods that give a measure of the external surface area and are based on a permeability cell (Lawrence, 1974; Pinches *et al.*, 1976; Sanmugasunderam, 1981).

Since the different methods provide different estimates of the surface area, different leaching mechanisms will dictate the procedure to be used. For instance, if chemical leaching (i.e. ferric leaching as in the indirect mechanism) is predominant, and no leach site selectivity is observed, the external surface area will most likely provide the better estimate of the surface area available for leaching (assuming that leaching at the internal surfaces are rate controlled by diffusion and is insignificant in

relation to the external leach rate). However, if the leach rate at the internal surface areas is not diffusion limited, then the B.E.T. method would provide the better estimate of the surface area available for oxidation.

Therefore, the appropriate surface area on which to base the surface oxidation rate should be carefully chosen, since it is linked to the mechanism by which oxidation takes place.

3.4 Kinetic Models For Bacterial Leaching.

As is apparent from the literature survey bacterial leaching is very difficult to model because very little is understood of the mechanism by which leaching takes place. In addition to this, besides the interaction of solids, liquids and gases, living matter is introduced to the system. However most models that have been reported, have assumed ideal conditions, ignoring such factors as mass transfer limitations, and related only growth or oxidation rate descriptions.

The bacterial models that have been developed to describe bacterial leaching systems, can be divided into two main categories, defined as:

- growth models, which predict bacterial growth in the system and relate oxidation rates to growth by a yield relationship (Gormely 1973; Chang and Meyerson, 1982) and,

- leach models, which directly predict the rate of oxidation of the metal sulphide substrate used (Blancarte-Zurita, 1985; Hansford and Drossou, 1986; Pinches *et al.*, 1987).

In a bacterial leaching system, both soluble (ferrous iron) and insoluble (metal sulphide, sulphur) substrates for bacterial growth occur. It is therefore a logical assumption that a model based on bacterial growth should account for growth on the soluble substrate as well as the insoluble substrate.

The growth of bacterial cultures on a soluble substrate has classically been described in several text books (Pirt, 1975 etc.) and it is not the purpose of the present study to deal with any of these fundamental studies in any depth.

However, several studies of the growth of Thiobacillus ferrooxidans on a soluble substrate are available in the literature. Lacey and Lawson (1970) observed that the batch wise liquid phase oxidation of ferrous sulphate by *Thiobacillus ferrooxidans* was accurately described by Monod kinetics. Similarly Mehta and Le Roux (1974) observed that the rate expression proposed by Herbert *et al.* (1956) for continuous culture was applicable for *Thiobacillus ferrooxidans* grown on ferrous sulphate.

In addition to this Jones and Kelley (1983) also observed that Monod kinetics are valid for ferrous sulphate oxidation by *Thiobacillus ferrooxidans* in the liquid phase. However, both product (ferric) and substrate (ferrous) inhibition was observed for various conditions, which resulted in unique anomalous wash-out curves. The authors derived mathematical models, which were modifications of the Monod model, to adequately describe competitive and non-competitive product inhibition.

It would, therefore, appear that classical model descriptions for bacterial growth on a soluble substrate *does hold true for ferrous sulphate oxidation by*

Thiobacillus ferrooxidans in the liquid phase. However, in the case where an insoluble substrate is introduced, kinetic and yield relationships may change. This means that, unlike for Monod kinetics, the specific growth rate of the bacteria might not necessarily be a unique function of the substrate concentration.

A useful basis for the introduction of a second, insoluble phase, appears to be the work of Erickson *et al.* (1970) who developed a model for bacterial growth on a hydrocarbon substrate, dispersed in a continuous liquid phase. This model accounts for drop size distribution, coalescence and redispersion, growth in the continuous phase and at the interface, and, adsorption and desorption of bacteria onto the interface. Gormely *et al.* (1975) recognized that the model of Erickson *et al.* offered the most promise since it considered the adsorption and desorption of bacteria at the surface of a dispersed phase. Gormely assumed that attachment to the solid surfaces is a prerequisite for zinc release and bacterial growth. Furthermore, he suggested that the attached bacteria should grow at their maximum specific growth rate, which is assumed to be constant. In addition he assumed that the free bacteria do not have access to substrate and therefore do not grow. A dynamic interaction was assumed to exist between the free and the attached bacteria, and that it followed first order kinetics. The following equation was derived to predict the steady state cell concentration as a function of the dilution rate and surface area concentration:

$$X = \frac{K}{a\left[\frac{D}{\mu_m} - 1\right]} + \frac{\mu_m S}{D\ a} \qquad 3.1$$

In general the predictions of the model were verified when tested against the experimental data. The model is able to predict wash-out at a dilution rate equal to the maximum specific growth rate. Unlike Monod kinetics, it was found that when a solid substrate is used, the specific growth rate of the bacteria is not a unique function of the substrate or surface area concentration. However, deviations were observed between experimental results and predicted values for the model parameters. The authors attributed this to non-ideal mixing, as well as to the method used for surface area estimation (B.E.T.), which usually overestimates the oxidizable surface area. However, they omitted to consider the effect of the iron present in the concentrate (4.8% iron) which provides a soluble growth substrate for the bacteria in solution and also influences the zinc release rate by the chemical leaching mechanism (Huberts 1986). This puts a major constraint on the model and eliminates it from being used for an iron containing sulphide. The authors did, however, recognize the fact that when the limiting substrate is a sulphide mineral, solid surface area is an important variable.

Also recognizing the importance of the surface area concentration, Torma and Sakaguchi (1978) used Monod's model, and replaced the substrate concentration with the initial total surface area concentration. Furthermore, they assumed the rate of product formation equal to the rate of bacterial growth. The B.E.T. method was used to determine

the surface areas of the solids. In general, a good correlation for the linearised form of the model was obtained, but the authors presented no conclusive evidence for the validity of their assumptions.

Returning to the model proposed by Gormely *et al.* (1975), Chang and Meyerson (1982) recognized its limitation : it neglected the role of the free bacteria. This model was extended to account for the growth of both free and attached bacteria. They assumed Monod kinetics to apply to the freely suspended cells, and that Langmuir-type adsorption kinetics existed between free and attached cells. Their model was derived to describe steady state conditions with two dilution rates, one for the solid phase and another for the liquid phase, which can be varied independently.

Whereas Gormely *et al.* (1975) assumed a constant growth rate for the attached bacteria, Chang and Meyerson (1982) proposed that the growth rate of the attached bacteria is a function of the surface area concentration and the solids dilution rate. They furthermore assumed bacterial leaching is a function of only the attached cells. The qualitative predictions of the model were verified experimentally, i.e. the pyrite leach rate increases with surface area concentration and the growth rate of the attached cells increases with solids dilution rate. This confirms the importance of surface area concentration as a parameter in the description of oxidation rates when a solid substrate is used.

Sanmugasunderam *et al.* (1985), extended the model proposed by Gormely *et al.* to apply to two CSTRs in series, with and without solids recycle. The same assumptions made in Gormelys' work were applied. However, the authors used an air permeability technique to measure the specific surface area of the concentrate used, and verified ideal mixing in

their reactors. The predicted values show good agreement with experimental results. The values for the model parameters, specific growth rates and area occupied by single cells differed from values given elsewhere in the literature (Chang and Meyerson, 1982; Meyerson and Klein, 1984). The authors suggested that the parameters are not universal constants, but depend on the nature of the mineral and the environmental conditions that are applied during leaching. However, once again the possible effect of the iron in the concentrate (2,4% iron) was neglected.

Moving away from a bacterial growth orientated modeling concept, Blancarte-Zurita *et al.* (1985) made use of a shrinking particle model to describe the bacterial batch leaching of a sulphide metal concentrate. The shrinking particle model is a special case of the shrinking core model proposed by Levenspiel (1972). An expression, utilising a metal leach rate and describing the time dependence of the mean particle size, was derived. The metal leach rate depends on the particle size and leach time.

The authors tested the model against the batch leach data of a chalcopyrite and a sphalerite concentrate. For the sphalerite concentrate, the linear sections observed in the batch extraction curves were assumed to represent a constant metal extraction rate. A relationship between these constant extraction rates and particle diameters was found and used in the mathematical model. The resulting particle diameter prediction as a function of leach time was found to agree well with experimental data.

In the case of the chalcopyrite, the model showed poor agreement with the experimental data. This was attributed to the low extent of metal extraction of this concentrate (29% copper solubilised) which would result in a small change in diameter, and be inadequate to test the

model. In addition, jarosite precipitation was observed on the particles, which would mask the size reducing effect a shrinking particle mechanism would have. However, scanning electron microscopic observations did reveal pit formation, which most likely eliminates a shrinking particle mechanism and would explain the poor correlation. The differences observed between the leaching characteristics of the sphalerite and the chalcopyrite provides confirmation that different leach mechanisms exist for different minerals.

Pitting or pore formation leads to a totally different leaching mechanism. The closest approximation is probably a shrinking core concept, where particles contain a large fraction of inert material which maintains the basic particle size and structure, whilst the mineral is leached out. However, in the case of a sulphide particle this concept will change to selective leaching, restricted to certain areas or crystal faces of the particle.

Southwood and Southwood (1985) observed pore formation in bacterially leached pyrite concentrates. Similar observations were made by Keller and Murr (1982). The authors observed a mean pore diameter of 4,5μm for pyrite and 8,0μm for arsenopyrite. Furthermore, pore diameter was essentially constant along the pore length and independent of the pore depth. The authors suggested that leaching was limited to the leading face of the pore, whilst the pore walls remained inactive.

Following the work done by Southwood and Southwood (1985), Hansford and Drossou (1987) derived a model based on pore formations observed in the bacterially leached pyrite, termed the propagating pore model. In parallel to modeling the batch-wise leaching of pyrite according to the propagating pore mechanism, a model was presented according to the shrinking particle mechanism. These mechanistic

models describe fraction metal leached, or fraction sulphide breakdown, as a function of time. The authors found that the model derived for the shrinking particle mechanism did correlate well with the experimental data. However, it was found that the propagating pore model correlated well with the experimental data. The propagating pore model in essence predicts individually the three different phases observed for a batch leach curve. These are:

- the linear "growth" section where the leach rate is constant and it is assumed that all the pores are active,

- the section where the leach rate starts to decrease at a rate equivalent to the rate of pore de-activation, and,

- a stationary phase where all leaching activity has ceased.

The authors utilized a surface area oxidation rate : $kg.m^{-2}.day^{-1}$, as opposed to the more often used volumetric oxidation rate: $kg.m^{-3}.day^{-1}$. The proposed model was not developed to describe a continuously operated system.

Pinches *et al.* (1987) proposed an empirical logistic model to describe the fraction of metal extraction as a function of time. This model is based on the logistic growth model as proposed by La Motta (1976). The model proposed by La Motta gives the following equation to describe the bacterial growth rate as a function of time in a batch situation:

$$\frac{dX}{dt} = nX\left(1 - \frac{X}{X_m}\right) \qquad 3.2$$

where n and X_m are model parameters.

The authors modified the model by proposing that the bacterial concentration (X) in the model be substituted by the fraction of substrate oxidized. The model was extended to include the description of a continuous system, which describes the steady state fraction metal extraction as a function of the residence time (τ). The model for the continuous case was developed to describe both single stage as well as multistage CSTR's. Not only was it found that the model adequately described metal extraction as a function of leach time in a batch system, but it correlated well with experimental data obtained for a continuous system.

It is the latter two models that will be tested in the present work, and will therefore be described more completely in the next chapter.

In conclusion, the literature survey has revealed that bacterial leaching has great potential in the recovery *of refractory gold from sulphide ores. Furthermore, Ferrobacillus ferrooxidans,* as the principal micro-organism involved, has been extensively studied and the optimum growth conditions well defined. Even though the attachment of bacterial cells to various solid substrates have been studied extensively, it is still unknown whether attachment is a prerequisite for leaching to occur. At present, very little is understood of the leaching mechanism involved in the oxidation of sulphide minerals in the presence of bacteria.

A large number of studies on bacterial leaching of various ores and sulphide concentrates have been presented in the literature. Amongst these are refractory precious

metal bearing ores and concentrates. However, the majority of these studies have been in the format where the effect of different physical parameters on oxidation rates have been established. Often no attempt was made to relate the effect on the leach rate with the observed parameter, such as particle size, solids and surface area concentration.

Only a few models have been described in the literature based on bacterial growth models (Gormely, 1973; Torma and Sakaguchi, 1978; Chang and Meyerson, 1982; Sanmugasunderam *et al.*, 1985). However, the emphasis in modeling has moved from the bacterial growth concept to a mechanistic concept obtained from physical observation of leach residues (Blancarte-Zurita *et al.*, 1985; Hansford and Drossou, 1987) and an empirical relationship (Pinches *et al.*, 1987) which affords a more practical easily applied result, which is preferable in the industry. There is, therefore, considerable scope for model development and confirmation of existing bacterial leaching models in experimental studies.

CHAPTER 4

THEORY : MODEL PRESENTATION

4.1 Introduction.

To optimally design any process, rate expressions and mass balance equations that adequately describe the process are required.

In this chapter three models will be presented that have been developed to describe bacterial leaching. Two of these models have been developed from mechanistic observations, while the third is an empirical relationship that has been extended to apply to bacterial leaching. These are:

- the shrinking particle model (Hansford and Drossou, 1986; Blancarte-Zurita *et al.*, 1985)
- the propagating pore model (Hansford and Drossou, 1986)
- the logistic model (Pinches *et al.*, 1987)

All of these models describe the fraction of mineral leached, or alternatively, the fraction sulphide breakdown, as a function of time (under batch operated conditions), or as a function of residence time (under continuous conditions).

4.2 The Shrinking Particle Model.

4.2.1 Batch Operation.

The following third order polynomial equation was

derived by Drossou (1986) to describe the fraction of pyrite oxidized in time:

$$F(t) = 6Rt - 12\ R^2t^2 + 8\ R^3t^3 \qquad 4.1$$

where $R = \frac{r_a}{\rho_p\ d_o}$

The following assumptions are made:

1. The mineral particles are considered to be spheres.
2. The particles consist of a single mineral.
3. Bacterial saturation on the solids takes place rapidly.
4. The rate of mineral dissolution per unit solid surface area, r_a, is constant throughout the leaching process.
5. The number of particles per unit volume of solution, n, does not change during the course of leaching.
6. Mass transfer of nutrients, oxygen and carbon dioxide to the bacteria and the solids surfaces and of reaction products away from the solid surface is not rate limiting.
7. The reaction products do not inhibit the growth of bacteria nor the rate of mineral leaching.
8. None of the soluble nutrients become rate limiting.

This model is discussed comprehensively by Drossou (1986) and will not be discussed in this chapter.

4.2.2 Continuous Reactor Operation.

If the abovementioned assumptions are applied, the performance equation for a continuous operated stirred tank reactor can be derived as follows:

Consider a single stage reactor and apply the shrinking particle mechanism. Also assume that the residence time in the reactor is greater than that of wash-out.

The volumetric oxidation rate can be expressed in terms of the surface oxidation rate as follows:

r_v = (oxidation per unit surface area)x(surface area per particle)x(number of particles per unit volume solution)

$$= r_a \pi d^2 n \qquad 4.2$$

where d is the particle diameter.

The number of particles per unit volume solution can be calculated from the initial solids concentration, C_o, and the particle density, ρ:

$$n = \frac{\text{(mass of solids per unit volume solution)}}{\text{(mass per particle)}}$$

$$= \frac{\text{(mass of solids per unit volume solution)}}{\text{(particle density)x(particle volume)}}$$

$$= \frac{6\ C_o}{\rho\ \pi\ d_o^3} \qquad 4.3$$

it thus follows that:

$$r_v = -\frac{dC}{dt} = \frac{6\ C_o\ r_v\ d^2}{\rho\ d_o^3} \qquad 4.4$$

Assuming a volumetric solution flow rate Q (m^3/unit time) entering a single stirred tank reactor at an initial solids concentration, C_o, a component balance over the

reactor gives:

input = output + disappearance by reaction + accumulation

4.5

(at steady state the accumulation term is equal to zero.)

The solids concentration after any contact time τ, can be given as:

C = (mass of single particle)x(total number of particles)

$$= \left[\frac{d}{d_o}\right]^3 C_o \qquad 4.6$$

The rate of disappearance by reaction is given by:

$$V\,(r_v) = \frac{6\,V\,r_a\,C_o}{\rho\,d_o^{\,3}}\,d^2 \qquad 4.7$$

thus from Equation 4.4 it follows that:

$$Q\,C_o = \frac{Q\,C_o}{d_o^{\,3}}\,d^3 + \frac{6\,r_a\,C_o}{\rho\,d_o^{\,3}}\,V\,d^2 \qquad 4.8$$

Re-arranging Equation 4.8 gives the residence time in terms of the outlet particle diameter:

$$\tau = \frac{\rho}{6\,r_a}\left(\frac{d_o^{\,3}}{d^2} - d\right) \qquad 4.9$$

where r_a = the surface leach rate ($kg/m^2/day$)

τ = the residence time in the reactor (days)

= V / Q

The fraction of mineral leached (F), can now be given in terms of the outlet particle diameter as follows:

$$F = \frac{\text{mass in - mass out}}{\text{mass in}}$$

$$= 1 - \frac{d^3}{d_o^3} \qquad 4.10$$

Re-arranging, and substitution of Equation 4.10 in 4.9, gives the residence time in terms of the fraction mineral leached:

$$\tau = \frac{\rho\ d_0}{6\ r_a}\left[\frac{1}{(1-F)^{2/3}} - (1-F)^{1/3}\right] \qquad 4.11(a)$$

If washout should occur, (i.e the fraction of oxidation is observed to be zero before the retention time reaches zero) then Equation 4.11(a) can easily be corrected for this as follows :

$$\tau - \tau_w = \frac{\rho\ d_0}{6\ r_a}\left[\frac{1}{(1-F)^{2/3}} - (1-F)^{1/3}\right] \qquad 4.11(b)$$

4.3 The Propagating-Pore Model.

4.3.1 Batch Operation.

The following set of equations were derived by Drossou (1986) to describe the fraction of sulphide oxidized as a function of the leach time in a batch reactor, when the propagating pore mechanism is applied:

$$F(t) = \frac{6\ r_a}{\rho_p\ d_o}\ t \qquad \text{for } t \leq T_i$$

$$F(t) = \frac{6\ r_a}{\rho_p\ d_o}\left[t - \frac{(t - T_i)^2}{2\ (T_e - T_i)}\right] \qquad \text{for } Ti < t < Te$$

$$F(t) = \frac{6\ r_a}{\rho_p\ d_o}\ \frac{T_i + T_e}{2} \qquad \text{for } t \geq T_e$$

4.12

In addition to the assumptions that were made for the shrinking particle model, the following assumptions were also applied:

1. The pore propagation starts rapidly. All pores start from the particle surface, and the number of possible new pores formed within the particles is negligible.
2. Oxidation is confined to the leading face (closed end) of the pore. No oxidation of the pore walls take place.
3. The rate of mineral dissolution per unit surface area of the pore base, r_p, is constant throughout the leaching process.
4. All pores have equal diameters.
5. Mass transfer of nutrients, oxygen and carbon dioxide to the base of the pore, and the diffusion of the reaction products away from the base of the pore is not rate

limiting.

Again a comprehensive discussion of the model for batch conditions is given by Drossou, and will not be repeated here.

4.3.2 Continuous Reactor Operation.

The propagating pore model predicts three distinct regions for batch leaching, where different kinetics apply, thus making it difficult to convert this performance equation to describe a continuous system. This is due to the fact that one would expect a wide distribution of residence times for individual particles in a completely mixed tank, rather than a single residence time for all the particles fed to the reactor. For this reason one would expect that for any residence time, more than one kinetic expression would be valid. The difficulty lies in determining the degree to which each factor contributes to the rate of leaching that is observed.

If one considers the first relationship, as given in Equation 4.12, it follows that:

$$r_v = -\frac{dC}{dt} = \frac{6\ r_a}{\rho_p\ d_o} = k \qquad 4.13$$

where k is a constant, therefore zero order kinetics exists. From this, if a mass balance is performed for a continuous, single stage reactor, it follows that:

$$C = C_o - \tau\ k \qquad 4.14$$

or, alternatively,

$$F(\tau) = \frac{6\ r_a}{\rho_p\ d_o}\ \tau \qquad 4.15$$

where τ is the residence time (= V/Q). If one considers the relationship for the batch prediction, it follows that the predicted contact time for a similar degree of oxidation to have taken place is similar.

Therefore, to minimize reactor volume, Equation 4.15 predicts that a plugflow reactor should be used for at least the degree of oxidation, or fraction mineral leached, equal to that obtained for time T_1 predicted in the batch process.

However, in order to prevent biomass wash-out, bacterial kinetics demand essentially a CSTR type first stage.

If the second region of the kinetics proposed in the model is considered, a relationship to describe the substrate concentration in terms of the pore length, L, has to be found first, by considering the mass substrate removed when a pore is formed. Therefore for a pore length increment of dL, the change in the substrate concentration is given by:

dC = - (incremental volume of the pore)x(density)
x(the number of active pores per unit surface area)x(surface area per particle)x(number of particles)

$$= - \frac{3\ \pi\ d_p^{\,2}\ C_o}{2\ d_o}\ n_q\ dL \qquad 4.16$$

where n_q is the number of active pores an d_p the pore diameter.

Drossou derived the following equation to describe the number of active pores for the pore length range L_i and L_e which correspond to the contact times T_i and T_e in the batch model.

$$n_q = F(L) = \frac{n_{qo}}{(L_e - L_i)} (L - L_i) \qquad 4.17$$

Substituting this in Equation 4.16, and integrating for $C = C_i$ when $L = L_i$, the following is obtained after rearranging:

$$C - C_i = - \frac{3 \pi d_p^2 C_o n_{qo}}{2 d_o (L_e - L_i)} (L^2 - L_i L + \frac{L_i^2}{2}) \qquad 4.18$$

where n_{qo} is the maximum number of active pores per unit surface area (this corresponds to the number of pores active during the initial stage of the batch leach).

The concentration C_i can be expressed in terms of the pore length L_i as follows:

$C_i = C_o$ - (mass per unit volume that has been removed by all the pores with length L_i)

$$= C_o (1 - \frac{3 \pi}{2 d_o} n_{qo} d_p^2 L_i) \qquad 4.19$$

For the evaluation of the continuous fed reactor, the specific volumetric leach rate is also required. Drossou derived the following equation for the volumetric leach rate,

$$r_v = 6\, r_{a_o}\, \frac{C_o\, n_q}{\rho\, d_o\, n_{q_o}} \qquad 4.20$$

and on substituting n_q (Eq. 4.17), it follows that:

$$r_v = 6\, r_{a_o}\, \frac{C_o}{\rho\, d_o}\, \frac{(L - L_i)}{(L_o - L_i)} \qquad 4.21$$

Considering a single stage continuous fed reactor at steady state, a mass balance gives:

$$Q\, C_o = Q\, C + V\, r_v \qquad 4.22$$

Substituting Equations 4.18 and 4.21 in Equation 4.22 and rearranging gives:

$$\frac{S}{2} L^2 - \left(S\, L_i + 6\, \frac{r_{a_o}}{\rho\, d_o}\, \tau\right)L + L_i\left(6\, \frac{r_{a_o}}{\rho\, d_o}\, \tau + \frac{S}{2} L_i\right) + \left(1 - \frac{C_i}{C_o}\right)(L_o - L_i) = 0 \qquad 4.23$$

where $S = \dfrac{3\, \pi\, d_p^{\,2}}{2\, d_o}\, n_{q_o}$

For a given residence time, τ, let:

$$\alpha = \frac{S}{2}$$

$$\beta = SL_i + 6 \frac{r_{ao}}{\rho\, d_o} \tau$$

and

$$\gamma = L_i(6 \frac{r_{ao}}{\rho\, d_o} \tau + \frac{S}{2} L_i) + (1 - \frac{C_i}{C_e})(L_e - L_i)$$

Then a quadratic equation in L follows of the format:

$$\alpha L^2 - \beta L + \gamma = 0$$

solving L, and disregarding the negative radical gives

$$L = \frac{\beta + \sqrt{\beta^2 - 4\,\alpha\,\gamma}}{2\,\alpha} \qquad 4.24$$

This equation gives the pore length as a function of the residence time. By substituting this equation in Equation 4.18, the substrate concentration can be obtained as a function of the residence time. L_e can be found in a similar fashion to L_i. The model then gives the the substrate concentration as a function of the residence time and five constants, C_i, C_e, r_{ao}, n_{qo} and d_p, that need to be determined experimentally.

Considering the third region of kinetics in the propagating pore model, no further leaching occurs, therefore, for a residence time greater than τ_e a substrate concentration C_e will be obtained. A mass balance over a single stage continuous reactor then gives:

$$F(\tau) = 1 - C_e/C_o \qquad 4.25$$

4.4 The Logistic Growth Model.

Under the assumption that the rate of substrate consumption is directly related to the rate of bio-mass production according to Monod kinetics, that is :

$$\frac{dX}{dt} = - Y \frac{dC}{dt} \qquad 4.26$$

where X = biomass and C = substrate concentration, some relationships that describe bacterial growth can directly be applied to describe substrate consumption.

Pinches *et al.* (1987) proposed the use of the logistic growth model to directly predict the rate of pyrite oxidation.

4.4.1 Batch Operation.

Pinches *et al.* (1987) proposed the logistic growth model in the following oxidation rate format:

$$r_v = \frac{dF}{dt} = k_m F \left[1 - \frac{F}{F_m} \right] \qquad 4.27$$

where F_m is the maximum fraction pyrite that can be oxidized, and k_m is a rate constant. When F is small, that is when F/F_m is small, Equation 4.17 reduces to:

$$\frac{dF}{dt} = k_m F \qquad 4.28$$

therefore exhibiting first order kinetics. This is equivalent to the initial exponential growth exhibited by bacteria.

Equation 4.17 can be directly integrated to give the degree of oxidation in a batch reactor as a function of time. Solving this equation with the limitation that at t = 0, F = F_o and after rearranging, gives:

$$F(t) = \frac{F_o \exp(k_m t)}{1 - \frac{F_o}{F_m}\left[1 - \exp(k_m t)\right]} \qquad 4.29$$

To fit the model, three constants, F_o, F_m and k_m have to be determined. Equation 4.18 can be rearranged to give a linear form, which can then, if necessary, be used to determine these parameters from the experimental data. This linear form is as follows:

$$\ln\left[\frac{F(t)}{F_m - F(t)}\right] = k_m t - \ln\left[\frac{F_m - F_o}{F_o}\right] \qquad 4.30$$

thus plotting the left hand side of equation 4.19 against time with data experimentally obtained, a straight line is obtained by linear interpolation with F_m as a variable. The constants F_o and k_m can then be obtained from the y-intercept and the slope respectively.

Alternatively, a least squares method such as the Nelder-Mead routine can be used to directly determine the constants. This is the technique that will be employed in

the scope of this thesis to determine the constants for all the models fitted.

4.4.2 Continuous Reactor Operation.

To determine the reactor performance in a continuous fed reactor system, we first need to determine the expression for the specific leach rate, at a substrate concentration C.

The fraction of pyrite leached at any stage is given by:

$$F = \frac{C_o - C}{C_o} \qquad 4.31$$

therefore,

$$\frac{dF}{dt} = -\frac{dC}{C_o\, dt} \qquad 4.32$$

thus,

$$V\,(r_v) = -V\frac{dC}{dt} = V\frac{dF}{C_o\, dt} = F\,k_m\left[1 - \frac{F}{F_m}\right] \qquad 4.33$$

Consider a number of leach reactors in series and assume a volumetric flow rate, Q, (m^3/unit time) through the cascade. Then a mass balance over the n^{th} reactor in the cascade gives:

$$V_n\frac{dF_n}{dt} = Q\,F_{n-1} - Q\,F_n + V\,(r_v) \qquad 4.34$$

Assuming steady state conditions, and substituting r_v it follows that:

$$\tau_n F_{n-1} - \tau_n F_n + k_m F_n \left[1 - \frac{F}{F_m} \right] = 0 \qquad 4.35$$

where $\tau = Q / V_n$ (V_n is the volume of the n^{th} reactor).

Rearranging Equation 4.24 gives the following quadratic equation in F_n,

$$F_n^2 \frac{k_m \tau_n}{F_m} - F_n (k_m \tau_n - 1) - F_{n-1} = 0 \qquad 4.36$$

which can be solved for F_n to give:

$$F_n = \left\{ F_{n-1} \frac{F_m}{k_m \tau_n} + \left[\frac{F_m}{2} \left(1 - \frac{1}{k_m \tau_n} \right) \right]^2 \right\}^{1/2} + \frac{F_m}{2} \left[1 - \frac{1}{k_m \tau_n} \right] \qquad 4.37$$

If a single stage reactor is considered, then $F_{n-1} = 0$, and Equation 4.26 simplifies to:

$$F = F_m \left(1 - \frac{1}{k_m \tau} \right) \qquad 4.38$$

giving the fraction of pyrite leached for a single stage reactor in terms of the residence time, τ, and two model constants. To solve the two constants, the fraction of

pyrite leached can be plotted against the inverse of the residence time to give a straight line. The y-intercept will give the constant F_m, and the constant k_m can be determined from the slope of the curve.

It is clear from Equation 4.38 that when the retention time (τ) is equal to the inverse of the rate constant (k_m), (i.e. $\tau = 1/k_m$), then $F = 0$. This condition, therefore, will be equivalent to that of 'cell washout' in microbiological reactors when the dilution rate ($1/\tau$) is is equal to or greater than the maximum specific growth rate of the bacteria.

CHAPTER 5

MATERIALS, APPARATUS AND METHODS.

5.1 Materials.

5.1.1 Pyrite Concentrate: Description and Preparation.

The test sample was obtained from a single 240kg lot of flotation concentrate originating from the Crown Mines waste ore dumps. This material had previously been treated for gold recovery. The flotation concentrate was further upgraded on a WIFLEY shaking table to obtain 125kg of approximately 95% pure pyrite sample.

The total mass of concentrate was cyanide leached in order to remove all the free gold that might still be available for extraction. Using a standard roll bottle technique, a 50% slurry was used. The slurry pH was adjusted to 10.5 prior to cyanide addition, and maintained at that level during the leach period, using a 10% NaOH solution. Sodium cyanide was added to give a solution concentration of 2% (w/v) NaCN. The initial cyanidation period was 24 hours, after which the supernatant was replaced by a fresh 2% NaCN solution, and the slurry was rolled for a further 24 hour period. The concentrate was then filtered, and thoroughly washed with distilled water. In addition to this the concentrate was washed with a 5% hydrochloric acid solution, to remove all readily acid soluble impurities.

The concentrate was subsequently fractionated into three different particle size distributions, +53 -75μm, +38 -53μm and -38μm respectively, by using standard laboratory sieves and sieving techniques. In order to obtain a

normalized size distribution for the -38μm fraction, the concentrate was vigorously agitated at a solids concentration of 30%(w/v), allowed to settle for 1 minute, and decanted. This procedure was repeated twice to remove the very fine particles. The resulting material showed a more-or-less normalized size distribution on the Malvern size analyser, with a d_{50} of about 25μm. The respective fractions were then split in approximately 1kg lots and sealed in plastic bags for storage.

5.1.2 Bacteria.

The bacterial culture that was used was originally a pure strain of *Thiobacillus ferrooxidans*, (ATCC 33020), obtained from the Microbiology Department of the University of Cape Town. However, no attempt was made to maintain the culture under aseptic conditions, and it is therefore likely that contamination of the culture did take place.

5.2 Apparatus.

Drossou (1986) in her work on the same concentrate, observed a substantial particle size reduction over the leach period. She attributed this mainly to mechanical effects, since a high agitator speed was used for mixing. The possibility of a size reduction due to a shrinking particle mechanism was not considered. Therefore, in order to minimize particle-particle and particle-impellar interaction, i.e. particle size reduction due to mechanical action, it was decided to use an air agitated pachuca reactor.

A diagramatic scheme of the apparatus for batch and continuous reactor leaching, is given in Figure 5.1.

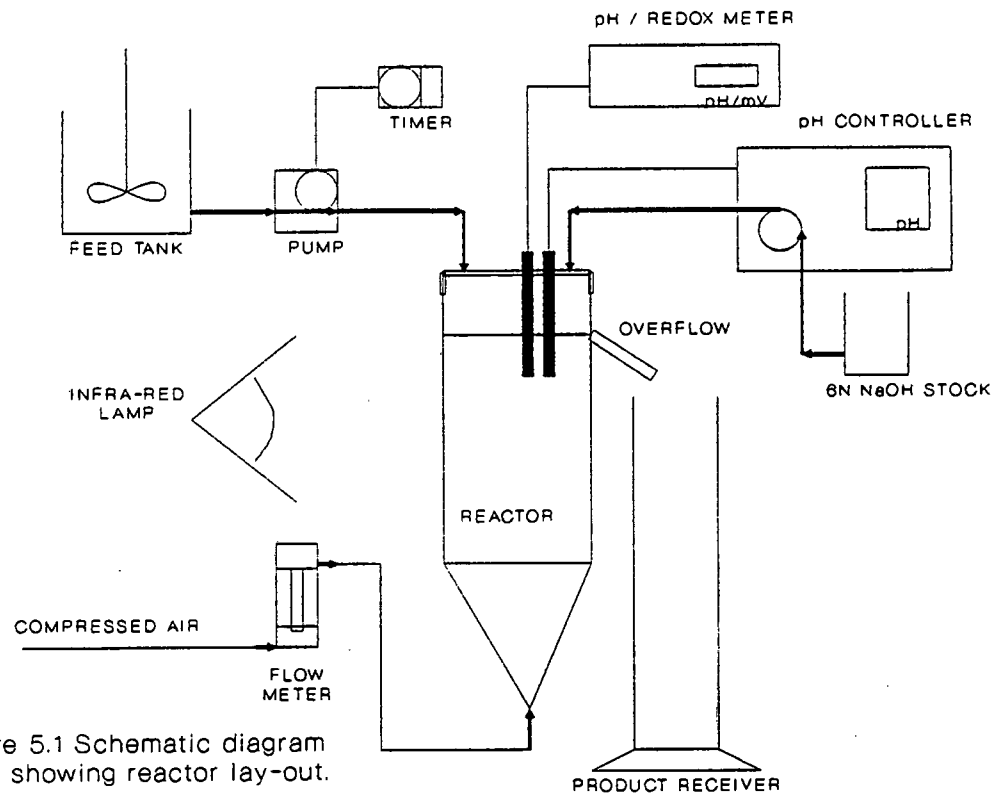

Figure 5.1 Schematic diagram showing reactor lay-out.

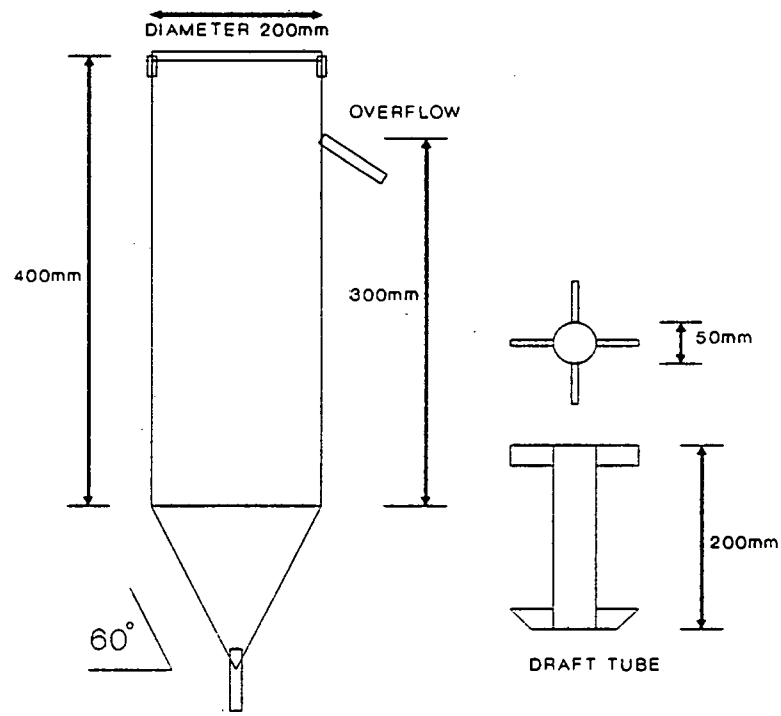

Figure 5.2 Reactor Dimensions.

The pachuca was made of clear perspex piping, 200mm in diameter, and cut to length. A conical section (60° apex) of P.V.C. was welded onto the pipe section to form the base of the reactor. A 3mm ID P.V.C. pipe section was fitted to the apex of the conical section to provide an aeration inlet. For improved solids suspension and fluid turnover the pachuca was fitted with a short draught tube made of clear perspex piping. The reactor was fitted with an overflow connection for level control. Figure 5.2 gives the overall dimensions of the reactor.

During batch leaching, residue samples for time course data were removed intermittently by vacuum suction into a glass sample receiver. For continuous leaching, the reactor top was sealed, thus directing all the effluent gases through the overflow port. This resulted in a blow-out effect, which removed any excess pulp rapidly, and proved to be adequate for level control. A tall glass cylinder was used as a sample receiver during this procedure.

Infra-red radiation was used for temperature control, and was found adequate to maintain the temperature at 30°C ± 1.5°C. Compressed air was used for aeration and was humidified prior to injection into the reactor, in order to minimize evaporation. The air was not enriched with carbon dioxide, as it was thought that the high aeration rate (1,0 vvm.), and the highly soluble nature of this gas would maintain concentrations in solution well above critical levels.

During continuously fed leaching test work, the pH was maintained automatically with a Gallenkamp modular fermentor pH controller, feeding a 6N sodium hydroxide solution. For batch leaching this addition was done manually on a daily basis.

During continuously fed experiments, solids were fed to the reactor in a 10 % (w/v) slurry suspended in a 5 litre P.V.C. container with a rubber-coated pitched blade agitator. The slurry was fed to the reactor with a Watson Marlow peristaltic pump, model 502S, activated by a Paladen Lanfer GMBH intermittent time switch to achieve the desired dilution rate.

Dissolved oxygen levels were measured with a Gallenkamp modular fermentor dissolved oxygen meter. A Zeiss Optical Instruments pH meter, model 300, was used for pH measurements.

5.3 Experimental Procedures.

5.3.1 Culture Maintenance and Growth Evaluation.

The culture was routinely maintained on the 9K medium of Silverman and Lundgren (1959) in which the ferrous sulphate was replaced by pyrite to give a 10% (w/v) solids concentration at a pH of 1.80. Table 5.3.1 Gives the composition of the medium used. The bacteria were harvested and re-inoculated onto fresh solids medium after a period of 15 days to ensure the continued existence of an active culture.

Table 5.3.1. Growth Medium.

Component	Quantity
$(NH_4)_2SO_4$	3,00g
K_2HPO_4	0,50g
KCl	0,10g
$MgSO_4$	0,50g
$Ca(NO_3)_2$	0,01g
H_2SO_4	Desired pH
Water	make up to 1,0 litre

Bacteria were harvested after 7 - 9 days of inoculating the culture maintenance vessel, when preparing an inoculum for experimental runs, as this corresponded to the late logarithmic growth phase. The following procedure was adopted:

The culture maintenance was left standing for a period of 4 hours in order to allow all the solids in suspension to settle. The supernatant was subsequently decanted carefully, so as not to disturb the solids on the bottom of the vessel, and then centrifuged at 10 000 rpm in a Beckman model J2-21 centrifuge. The bacterial pellet thus obtained was then re-suspended and washed with distilled water at a pH of 1.5 to dissolve any jarosite that might have been removed with the bacterial solution. The washing procedure was repeated. The bacterial pellet obtained after the second wash was re-suspended in distilled water at a pH of 1.80. The cell concentration in the washed suspension was determined by visual count and the aliquot required to inoculate the reactor at a bacterial concentration of 1.0×10^8 cells per cm^3 was calculated.

Only the growth of free in solution bacteria was evaluated. This was done by visual count using a Petroff-Hausser bacterial counting chamber and a Leitz Dialux 22-EB microscope. Phase contrast was used under a magnification of 400. Standard bacterial counting procedures were employed.

5.3.2 Leaching Techniques.

The concentrate to be used in the experiment was acid washed with a 5% hydrochloric acid solution at a 50% slurry concentration for 1 hour. This was done to remove any naturally oxidized material that might have formed between sample preparation and use. The slurry was filtered and washed well with distilled water. The resulting filter cake was then dried rapidly with the use of acetone. Preliminary investigations showed that the use of acetone to dry the filter cake had no adverse effect on leaching rates.

For the batch leaching studies, the required mass of concentrate was made up with 10 litres of iron-free medium. The slurry was aerated and the temperature was allowed to stabilize before inoculation. After inoculation, on a daily basis the following was done:

- The pulp level was maintained at the initial level by addition of distilled water.
- The pH was adjusted to 1.80
- A 5ml solution sample was taken to determine ferrous and ferric and free in solution bacteria levels.
- A 5ml pulp sample was taken, diluted at a 1:1 ratio with a 30% HCl solution and the total acid soluble ferrous and ferric levels were determined.
- The temperature, redox potential and dissolved

oxygen levels were measured and recorded.

On a longer interval basis, larger samples were taken (usually 500 to 700ml) to obtain sufficient solid residue to enable the correlation of the fraction pyrite leached with the daily samples taken. Normally six such residue samples were obtained during a batch run.The presence of silica (SiO_2) was used as an inert tracer in order to calculate the fraction of pyrite leached. These residues were also used to determine the refractory gold release curve. After such a large sample was taken, the new reactor level was recorded and maintained. In addition, the aeration rate was adjusted to maintain a rate of 1,0 vvm. The batch tests were performed over a period of 30 days.

One sterile control run was performed on the +38-53μm size fraction at 10%(w/v) solids concentration over a period of 30 days. The main objective of the sterile control run was to establish the effect of agitation on the size distribution of the solids under non leaching condition.

The gold release vs. fraction of pyrite leached data was also obtained from the batch experiments.

For the continuous fed experiments, the feed vessel was replenished on a daily basis to maintain a constant feed pulp level, giving a constant feed head, which ensured a steady pumping rate. For a set dilution rate, four reactor volume changes were allowed prior to assuming steady state conditions. During this period of "non-steady state" the temperature, redox potential and the dissolved oxygen level as well as the pumping rate were monitored on a daily basis. The pH was automatically controlled at 1.80.

After steady state had been attained, the overflow samples for four consecutive days were collected. The

residue samples were then acid washed with a 15% hydrochloric acid solution in a 50%(w/v) slurry for a period of 1 hour to dissolve excessive jarosite precipitation. The solid residue was then used to correlate the fraction of pyrite leached with that obtained from the leach supernatant. Silica was once again used as an inert tracer.

5.3.3 Analytical Procedures.

Iron analysis was performed by fusing the sample with sodium peroxide and leaching it in boiling water. The hydroxide precipitate was separated by filtration and redissolved in hydrochloric acid. The solution was then reduced with stannous chloride. The resulting solution was titrated with potassium dichromate using sodium diphenylamine as an indicator (Vogel, 1961).

The total sulphur analysis was performed in a Leco Sulphur Determinator, SC32 DB64, at 1350°C. Elemental sulphur was extracted from the sample by dissolving it in hot carbon tetrachloride. The liquid fraction was separated from the insoluble fraction by using a continuous Soxhlet type reflux system. The solvent was then evaporated and the sulphur was determined gravimetrically.

Gold was determined by standard fire assay method (Van Wyk and Dixon, 1983).

Ferrous iron in solution was determined by using the standard potassium dichromate titration with sodium diphenylamine as indicator. Total iron in solution was determined by reducing the ferric in solution and titrating with potassium dichromate and using sodium diphenylamine as an indicator. In addition, analyses for iron, arsenic, nickel and copper in the supernatant were performed by

atomic absorption spectrophotometry. A Varian, model AA-6, Atomic Absorption Spectrophotometer was used for the iron analysis, and a Varian, model 1275, for the arsenic, copper and nickel.

The calculations concerning the bacterial oxidation of the pyrite were based on the fraction iron extracted from the solid phase, rather than the fraction of iron observed in the liquid phase.

5.3.4 Miscellaneous Measurements.

The specific area of the different size fractions was determined by the standard B.E.T. method. The gas used for adsorption was Krypton.

The densities of the three different size fractions were obtained in a Quantachrome Spy-2 Stereopycnometer.

Feed and residue samples were examined with a Hitachi S450 Scanning Electron Microscope (S.E.M). The S.E.M has a 25kV accelerating voltage and a beam current of approximately $1x10^{-10}$ amps. The samples were prepared by mounting the particles on a microscope stub, and gold coating in a Polaron E 5000 Sputter Coater to a thickness of approximately 25nm. In addition to this the polished sections of the feed and residue were examined by reflective light microscopy.

CHAPTER 6

RESULTS AND DISCUSSION

6.1 Introduction.

In this chapter, the results obtained for the batch and continuous bacterial leaching tests are presented and discussed. The objective of the experimental work was to obtain kinetic data for the bacterial leaching of a pyrite concentrate. The kinetic data obtained were tested against three models in the case of the batch test results, (i.e. the shrinking particle, propagating pore and logistic growth models), and, against two models in the case of the continuous test results (i.e. the shrinking particle and the logistic growth models).

6.2 Batch Test Results.

It has already been established in the literature survey that a surface area oxidation rate will be used as an estimation of the bacterial leaching performance in the current study.

Using a median particle diameter, the specific surface area ($m^2\ kg^{-1}$) for the respective size fractions was calculated. This was then used to calculate the required solids concentration ($kg\ l^{-1}$) to give a constant initial surface area concentration ($m^2\ l^{-1}$) in the batch tests. The specific surface areas and solids concentrations are summarized in Table 6.1.

Table 6.1 Calculated Specific Areas and Solids Concentrations for Batch Experiments.

Particle size distr. (μm)	Esst. d_{50} (μm)	Specific surface area		Calculated solids conc. % (w/v)
		calculated $m^2\ kg^{-1}$	B.E.T $m^2\ kg^{-1}$	
+53 -75	64.0	19.62	240	14.07
+38 -53	45.5	26.81	200	10.00
-38	25.0	48.80	560	5.50

An unusually high specific surface area measurement, using the B.E.T. method, was observed for the +53-75μm fraction. This did not follow the trend observed for the smaller size fractions using the B.E.T. method of surface area determination. Closer examination of this size fraction with a scanning electron microscope (Fig. 6.1), revealed that the majority of the particles in this size fraction were pitted. The etching appears to be superficial in nature, and explains the unusually high B.E.T. specific surface area observed for this size fraction. The pitting or superficial etching was not as prominent in the smaller size fractions.

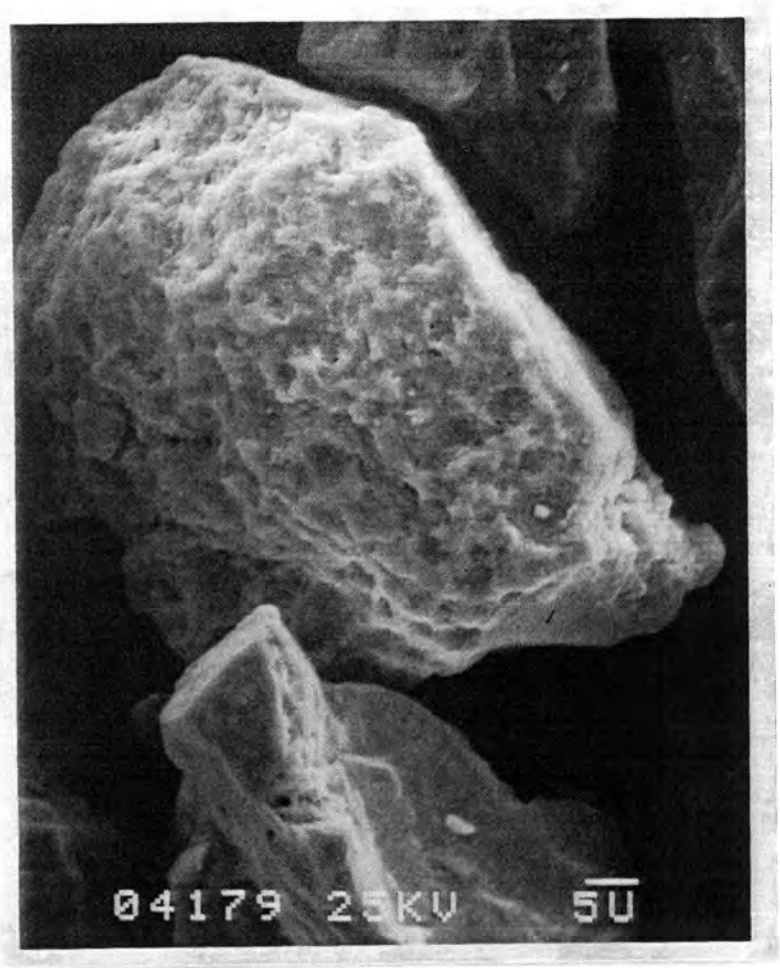

Figure 6.1 Superficial etching and pitting of pyrite particles in the +53-75μm size fraction.

6.2.1 Experimental Results.

The experimental results obtained from the daily samples for the batch tests, are summarized in Appendix A. Total acid soluble iron analyses provided a useful measure for determining the daily reactor performance, because it was not practical to remove large pulp samples for residue analysis. The intermittent pulp samples on the other hand, provided a means of checking the accuracy of the daily total acid soluble iron determinations. The total acid soluble iron leached for the three batch runs are shown in Figure 6.2, while Table 6.2 summarizes the analyses and the calculated fractions iron leached for the intermittent samples. The fractions of iron leached for these intermittent samples were calculated using the SiO_2 concentration in the residues as an inert tracer (See Appendix A). Table 6.2 also includes the equivalent fractions of iron leached calculated from the measured total acid soluble iron.

For the initial stages of each run, the fraction of iron leached (calculated from the total acid soluble iron), compares favourably with that obtained from the residue analyses (Table 6.2). However, towards the end of the leach period, the fraction of iron leached calculated from the total acid soluble iron is less than that calculated from the residue analyses. This discrepancy was especially prominent in the +53-75μm size fraction. In general, the difference between these two calculated values did not exceed 5%. A maximum error of 8% was observed for day 15 of the +53-75μm size fraction (37.4% iron leached, calculated from the residue vs. 29.4%, calculated from the total acid soluble iron).

Overall mass balances for iron and SiO_2 were obtained for each batch experiment and are shown in Appendix A. These balances considered the accountability for total mass of SiO_2 associated with the residue samples, in comparison to the total SiO_2 in the initial feed. The iron balance on the other hand, also considered the soluble iron that was removed with each sample. In general, the overall accountability for these components were good, and did not provide any explanation for the observed discrepancy in the calculated fractions iron leached. For this reason it was decided to compare the total iron concentration (residue + solution) in each pulp sample with that of the initial feed (Table 6.3).

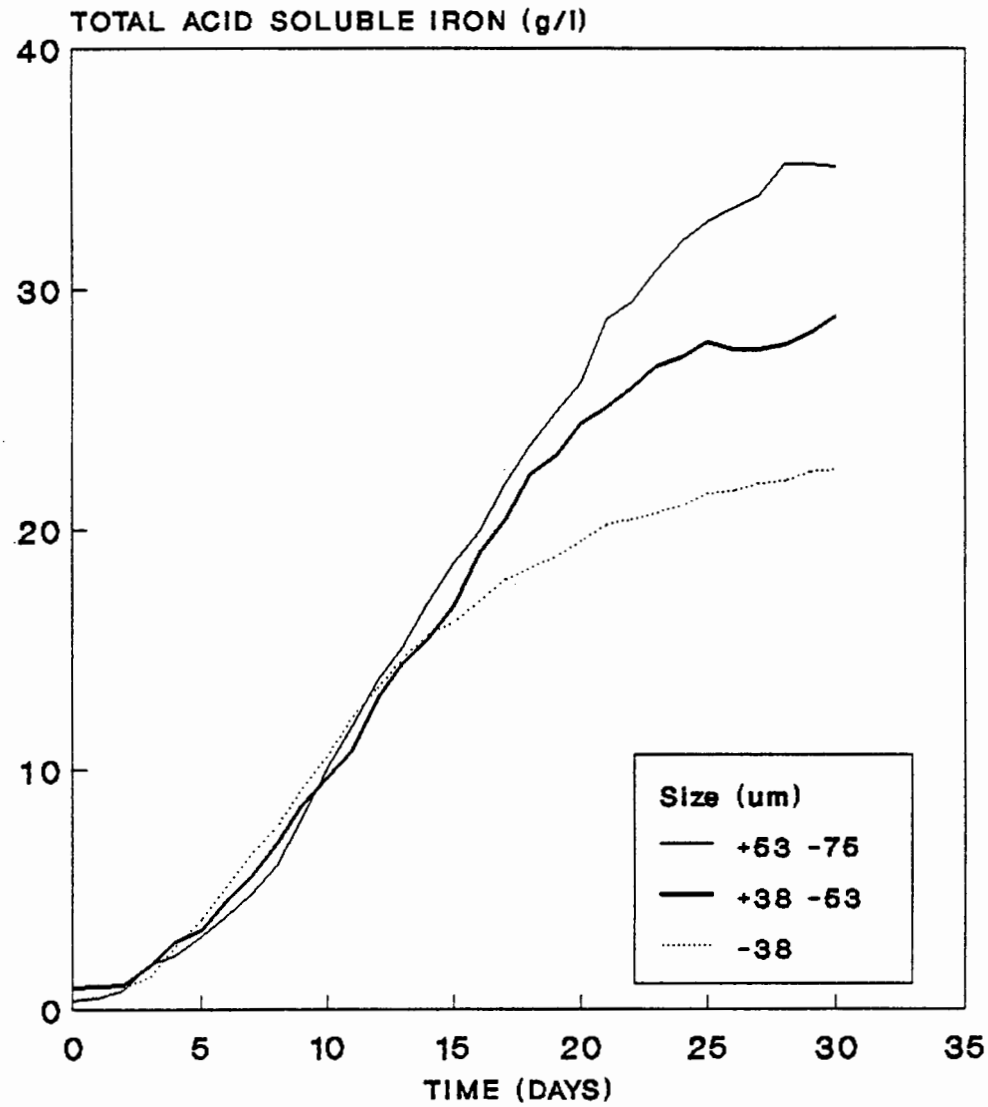

Figure 6.2 Total acid soluble iron leached during batch bacterial leaching of the respective size fractions.

Table 6.2 Batch Test Results. Analysis of unreacted solid residues, calculated fractions of iron and sulphide leached and the equivalent fraction iron leached calculated from the total acid soluble iron.

Size μm	Day	Residue Analysis (%)			Fraction Leached		Supernatant	
		Fe	S^{2-}	SiO_2	Fe	S^{2-}	Fe_T g l^{-1}	Fraction Leached
+53 -75	Feed	44.9	48.9	2.78				
	3	44.9	48.8	2.89	0.038	0.040	2.2	0.029
	6	44.8	49.4	2.95	0.060	0.048	3.9	0.062
	10	44.3	49.2	3.35	0.181	0.165	10.1	0.160
	15	42.9	48.9	4.24	0.374	0.344	18.6	0.294
	21	43.0	48.5	5.25	0.493	0.475	28.8	0.456
	30	39.8	45.8	6.26	0.606	0.584	35.1	0.556
+38 -53	Feed	45.3	50.4	1.75				
	6	43.8	49.9	1.85	0.085	0.063	4.5	0.099
	8	44.0	49.7	2.00	0.150	0.137	6.9	0.152
	12	43.5	49.4	2.35	0.285	0.270	13.0	0.287
	17	43.3	48.4	3.45	0.515	0.512	20.4	0.450
	22	42.1	48.0	4.17	0.610	0.600	25.9	0.572
	30	41.4	47.4	4.80	0.667	0.657	28.9	0.638
-38	Feed	44.9	50.2	3.50				
	4	43.0	49.0	3.71	0.097	0.079	2.6	0.105
	6	42.3	48.1	4.15	0.204	0.192	5.1	0.206
	10	42.1	48.0	5.61	0.415	0.404	10.6	0.429
	15	37.2	39.8	8.52	0.660	0.674	16.1	0.659
	21	26.5	28.9	16.90	0.878	0.881	20.2	0.818
	30	18.3	16.2	24.90	0.943	0.955	22.5	0.911

Analyses are of acid (HCl) washed residues.

Fe_T refers to total acid soluble iron.

Table 6.3 Mass balances for iron obtained from the individual pulp samples.

Size	Day	Mass Fe in res. (g)	Mass Fe in soln. (g)	Soln. vol. (l)	Total Fe conc. (g l^{-1})	Initial Fe conc (g l^{-1})
+55	3	51.64	1.62	0.875	60.86	
-75	6	45.47	3.49	0.895	54.70	
	10	37.85	8.28	0.820	56.25	60.26
	15	30.10	14.69	0.790	56.69	
	21	35.93	31.39	1.090	61.76	
	30	131.34	204.63	5.830	57.63	
+38	6	39.03	4.10	0.910	47.39	
-55	8	35.86	6.56	0.950	44.65	
	12	34.15	15.86	1.220	40.99	44.00
	17	21.84	20.60	1.010	42.02	
	22	17.58	28.10	1.085	42.10	
	30	76.40	147.97	5.120	43.82	
-38	4	20.86	2.56	0.985	23.77	
	6	17.55	5.07	0.995	22.73	
	10	16.59	10.68	1.008	27.05	24.29
	15	10.08	16.66	1.035	25.83	
	21	5.01	21.11	1.045	24.99	
	30	6.02	114.64	5.095	23.72	

Mass of iron in the residue is calculated from the mass and analysis of the residue.
Mass of iron in the solution is calculated from the concentration of the total acid soluble iron and the volume of the solution.
The total iron concentration is the total mass of iron (residue + solution) divided by the solution volume.
The initial iron concentration is obtained from the total mass of iron in the feed, divided by the total volume of liquid added to the reactor.

The data in Table 6.3 shows that the total iron concentrations for the smaller size fractions compare well with the initial iron concentration. However, a more marked discrepancy is observed for the large size fraction. This leads to the conclusion that non-ideal mixing existed in the reactors, especially when it is considered that the reactors had a height (overall) to diameter ratio of approximately 2,2 : 1 and aeration was the only means of agitation. The non-ideal mixing subsequently led to erroneous sampling, which would explain the discrepancy in the total iron concentrations. However, considering the margin of error, the observed discrepancies are negligible and the data as presented in Table 6.2 will be accepted as sufficiently accurate for the purposes of the current study.

From Figure 6.2 it can be seen that the linear sections for the iron leach curves of the three batch runs co-incide, confirming that a constant surface area oxidation rate is observed. This also suggests that the surface area oxidation rate is independent of the solids concentration and the particle size, for at least within the limitations of the present study. The surface area and volumetric oxidation rates for the three batch runs were determined by obtaining the slope of a straight line fitted through the linear sections of each leach curve, and are given in Table 6.4.

Table 6.4 Surface oxidation rates calculated for geometric and B.E.T. specific surface areas from the maximum oxidation rates. The maximum oxidation rates were obtained from the linear section of the batch leach curves.

Size	Volumetric oxidation rate (mg $l^{-1}h^{-1}$)		Surface oxidation rate for pyrite (kg $m^{-2}day^{-1}$)	
	Iron	Pyrite	Geometric	B.E.T.
+53-75	70.67	151.65	1.357×10^{-3}	1.077×10^{-5}
+38-53	62.40	133.97	1.199×10^{-3}	1.608×10^{-5}
-38	57.70	123.88	1.107×10^{-3}	9.653×10^{-5}

The maximum volumetric oxidation rates for the two smaller size fractions are very similar, reflecting a constant surface area oxidation rate, based on the calculated geometric specific surface areas for the solids. This was not reflected in the calculated surface area oxidation rates, using the B.E.T. specific surface areas. However, the geometric surface area oxidation rate for the +53-75μm size fraction is markedly higher than that for the smaller size fractions, indicating that the specific surface area available for leaching in this size fraction was underestimated. This was confirmed by the B.E.T. measurement and is consistent with the scanning electron microscopic observations for the feed material of this size fraction, as discussed previously.

Figure 6.2 suggests that because the volumetric leach rate is constant for a constant initial surface area concentration, that the volumetric oxidation rate is dependent on the surface area concentration. This is in agreement with the literature, where it has been shown that the volumetric leach rate is linearly dependent on the

surface area concentration. In the following paragraphs, the surface oxidation rates obtained in the present study will be compared with those reported in the literature. However, in order to compare surface oxidation rates, it must be noted that different methods of obtaining surface area concentrations have been used in the literature and therefore direct comparison is not always possible. In addition to this, only a few studies on the leach kinetics of pyrite, with sufficient data to enable the calculation of the surface area oxidation rate, have been published. It would not be logical to compare the surface oxidation rate of pyrite with other base metal sulphides, since it has already been shown in the literature that different minerals leach at different rates.

Pinches (1972) obtained the volumetric iron leach rate as a function of pyritic surface area concentration. A linear relationship was observed over the range of surface area concentrations, indicating a constant surface oxidation rate of $0,90 \times 10^{-4}$ kg Fe m^{-2} day^{-1}. This is equal to a pyritic oxidation rate of $1,90 \times 10^{-4}$ kg FeS_2 m^{-2} day^{-1}. This surface oxidation rate is an order of magnitude lower than that ($1,20 \times 10^{-3}$ kg FeS_2 m^{-2} day^{-1}) found in the present study. The lower value observed by Pinches (1972) may be due to :

a)the preferential oxidation of the arsenopyrite in the sulphide concentrate at the cost of the pyrite, which should result in a lower volumetric oxidation rate of the pyrite, or,

b) the differences in the mineralogical characteristics of the pyrite in the Pinches and the present study.

In a more recent study, Helle and Onken (1987) reported the leach kinetics of a pyrite concentrate. The

pyrite concentrate used in the study had a size distribution of 90% (w/w) less than 60 μm, and contained 83% pyrite. By calculating the initial geometric surface area for the 10% (w/v) pulp used in their experimental work, the volumetric oxidation rate reported can be converted to a surface area oxidation rate. This is equivalent to a surface area oxidation rate of 1,56 x 10^{-3} kg m^{-2} day^{-1}. (Compare this to the surface oxidation rate of approximately 1,20 x 10^{-3} kg m^{-2} day^{-1} observed in the present study.)

In addition, Pinches *et al.* (1987) reported on the leach kinetics of a 80% (w/w) less than 38μm pyrite concentrate, containing 54% pyrite. At an initial solids concentration of 15% (w/v), the initial available pyritic surface area can be calculated to convert the volumetric oxidation rate into a surface area oxidation rate. This was found to be 1,49 x 10^{-3} kg m^{-2} day^{-1}, which compares favourably with the findings in the present study.

On the other hand, Drossou (1987) observed a much lower pyritic surface oxidation rate of 0,66 x 10^{-3} kg m^{-2} day^{-1}. Drossou did not report any dissolved oxygen data. In addition, it does not appear that the method of aeration used, was adequate to provide sufficient oxygen in solution to maintain the oxidation rate. It is possible that the investigator may have worked under oxygen limiting conditions, explaining the comparatively low oxidation rate.

A final observation on the batch data is that the extent of pyrite oxidation was found to increase with a decrease in the particle size (Table 6.2). This is in agreement with data presented by Drossou (1987), Bruynesteyn and Duncan (1974), and Malouf and Prater (1961).

Two of the three models described in Chapter 5 are mechanistically based, whilst the third is an empirical relationship. The first two, the shrinking particle and the propagating pore models are described and discussed comprehensively by Drossou (1987), and therefore will not be discussed here. The agreement of the three models to the experimental data was determined by obtaining the model parameters from the experimental data, using a Nelder-Mead parameter optimization routine. This routine gives the best fit of the model to the data, by minimizing the sum of the errors squared between the experimental data and that predicted by the model.

6.2.2 Comparison of the Propagating Pore and the Shrinking Particle Models.

The model parameter estimates obtained with the Nelder-Mead parameter optimization routine, are given in Table 6.5. The variable parameters in each of the models were as follows :

-Shrinking particle model : surface oxidation rate, r_a; lag time T_L
-Propagating Pore Model : surface oxidation rate, r_{a_o}; lag time, T_L; time at which pore deactivation starts, T_i; time at which all pores have become inactive, T_e.

The surface oxidation rates are based on the oxidation of pyrite, calculated from the fraction iron oxidized. Included in Table 6.5 are the sum of errors squared for each size fraction, indicating the degree with which the model corresponds to the experimental data. The leach curves predicted by each model as well as the experimental data for each size fraction are shown in Figures 6.3, 6.4 and 6.5 respectively.

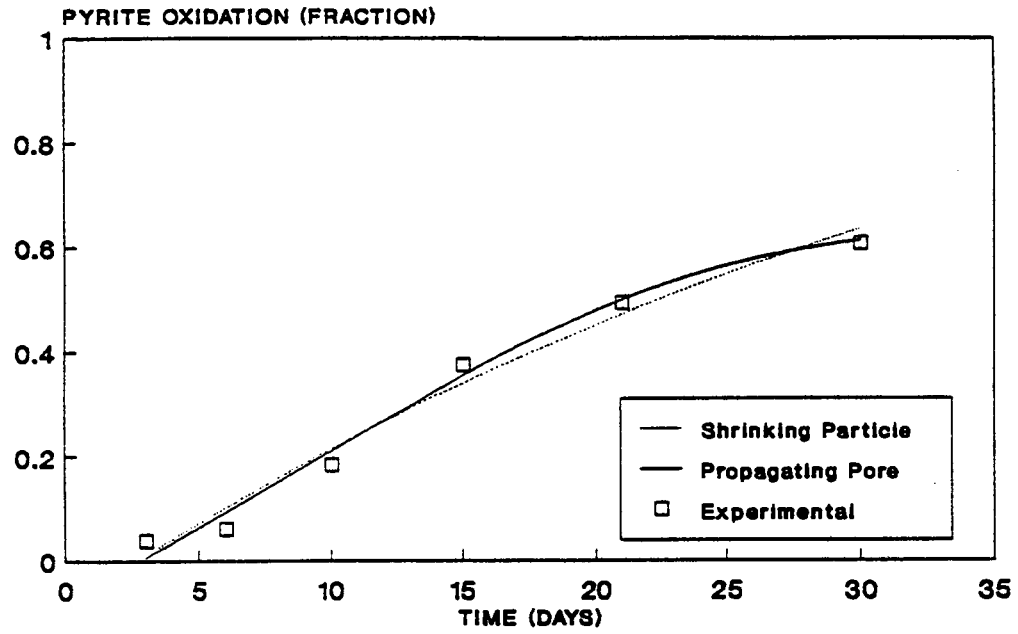

Figure 6.3 Experimental data and leach curves predicted by the shrinking particle and propagating pore models.

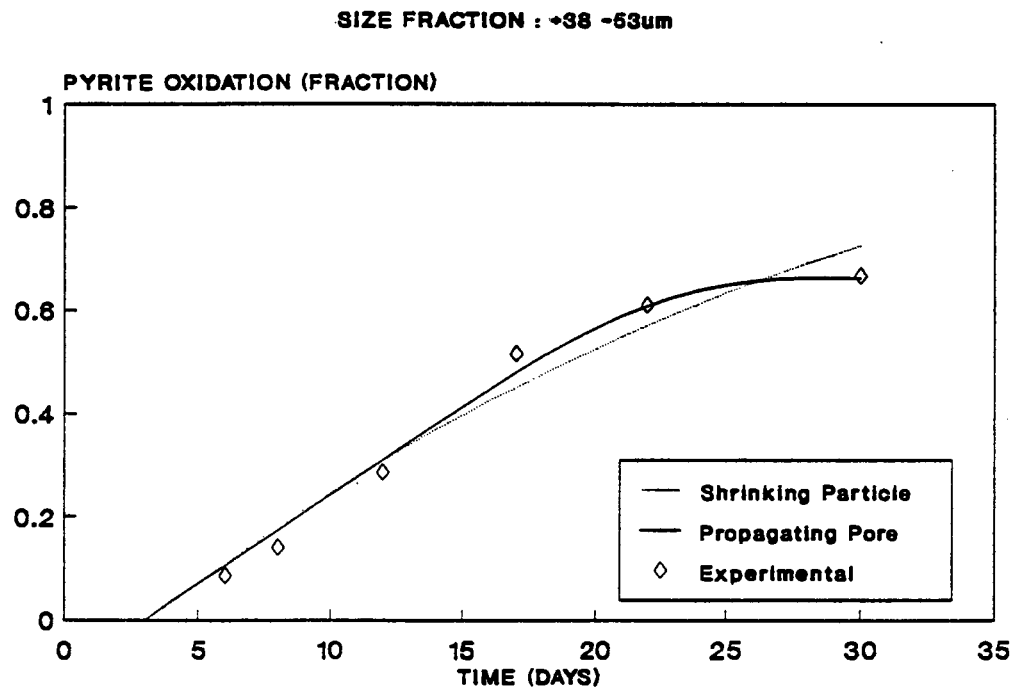

Figure 6.4 Experimental data and leach curves predicted by the shrinking particle and propagating pore models.

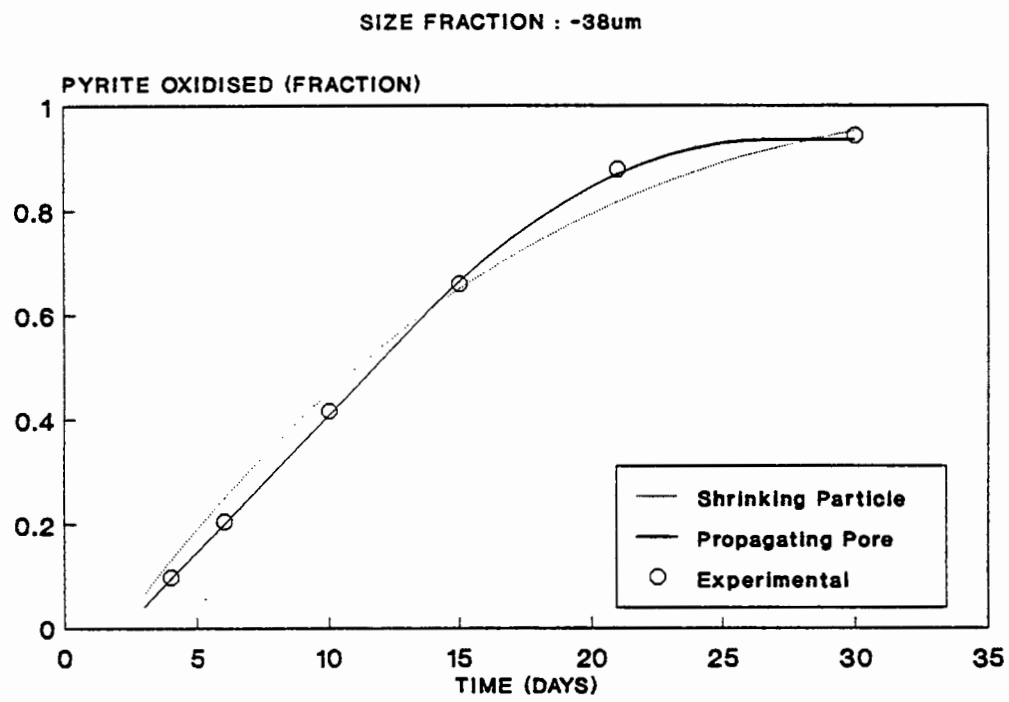

Figure 6.5 Experimental data and leach curves predicted by the shrinking particle and propagating pore models.

Table 6.5 Model parameters estimated for the shrinking particle and propagating pore models by least squares method from the batch data. Oxidation rates were obtained from pyrite leach data.

Shrinking particle model			
Size μm	Lag period days	Surface oxidation rate kg m^{-2} day^{-1}	Sum of errors squared
+53-75	2.6	1.67×10^{-3}	5.97×10^{-3}
+38-75	3.1	1.48×10^{-3}	1.10×10^{-2}
-38	2.0	1.42×10^{-3}	8.44×10^{-3}

Propagating pore model					
Size (μm)	Lag period (days)	T_i (days)	T_e (days)	Surface oxidation kg $m^{-2}day^{-1}$	Sum of errors squared
+53 -75	2.8	12.08	30.85	1.55×10^{-3}	3.28×10^{-3}
+38 -53	2.9	13.91	25.06	1.29×10^{-3}	2.80×10^{-3}
-38	2.2	11.09	24.66	1.09×10^{-3}	1.09×10^{-3}

It can be seen from Figures 6.3, 6.4 and 6.5 that the propagating pore model correlates better with the experimental data than does the shrinking particle model. Similarly, using the sum of the errors squared as an indicator of the degree of correlation of the models to the data, it is evident from Table 6.5 that the propagating pore model correlates better.

The two parameter shrinking particle model is less

versatile than the propagating pore model. Essentially the shrinking particle model, using a constant surface oxidation rate as a rate parameter, can be used to predict the mean particle size as a function of leach time or fraction leached. The size distributions obtained with the Malvern particle size analyser, for the three particle size fractions before and after leaching, as well as for the sterile control, are shown in Figures 6.6, 6.7 and 6.8.

For the +38 -53μm size fraction, Drossou observed a decrease in the d_{50} (calc.) from 46,5 to 32,8μm over a 28 day leach period (38% pyrite leached). The author attributed this particle size diminution to effects arising from mechanical agitation. In the present study, aeration was the only means of agitation, reducing the effects mechanical agitation might have on the particle size distribution. In Figure 6.7 it can be seen that only a slight shift in the particle size distribution was observed for the sterile control. Therefore, the particle-particle attrition contribution to particle size diminution is not a major consideration.

Figure 6.7 shows a 6,2μm decrease in the d_{50} (calc.), for the +38 -53μm size fraction, from 49,8 to 43,6μm over a 30 day leach period whilst 66% of the pyrite is leached. For this degree of oxidation, the shrinking particle model predicts a 17,8μm reduction in the d_{50} from 49,8μm to 32μm (Equation 4.10). Even though only a third of the predicted particle size reduction was observed, it should be noted that the fraction of inert particles, which should remain at a constant size distribution, increased almost threefold as a result of the fraction pyrite leached. The particle size distribution could therefore be closer to that predicted by the model. This may indicate that the shrinking particle mechanism may take an active part in the bacterial leaching of pyrite.

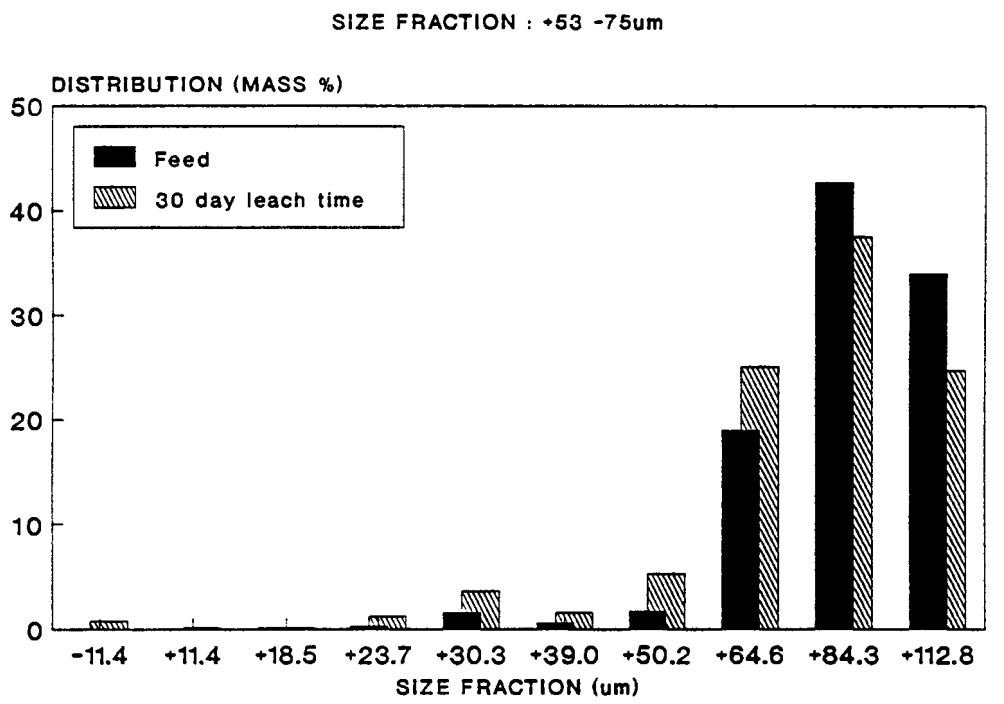

Figure 6.6 Particle size distribution obtained on the Malvern size analyser before and after 30 days leach time.

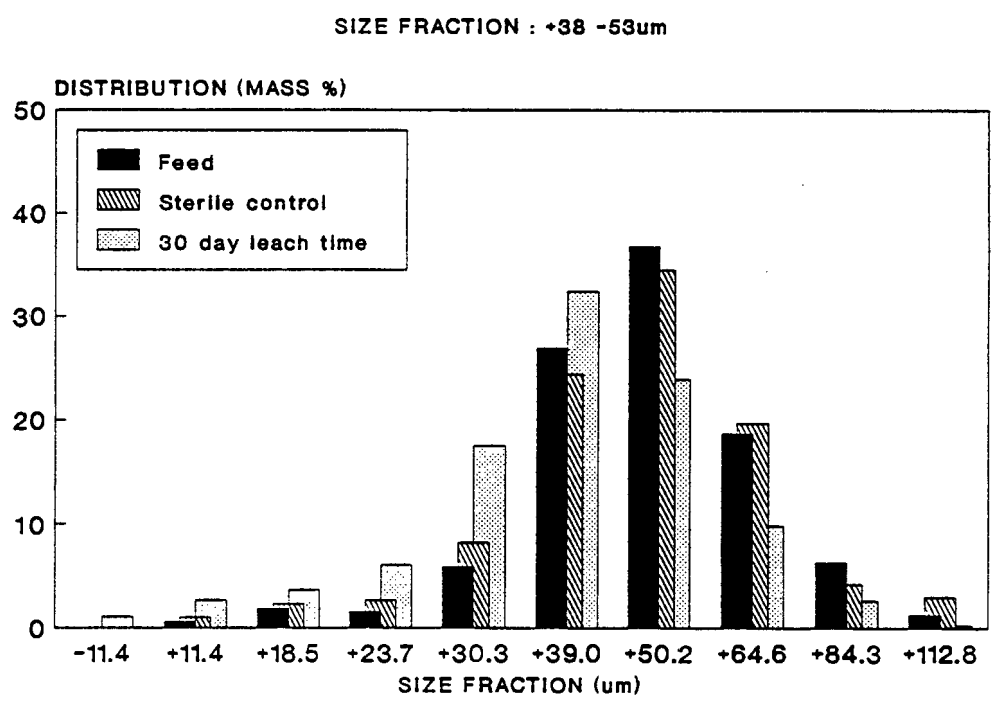

Figure 6.7 Particle size distribution obtained on the Malvern size analyser before and after 30 days leach time.

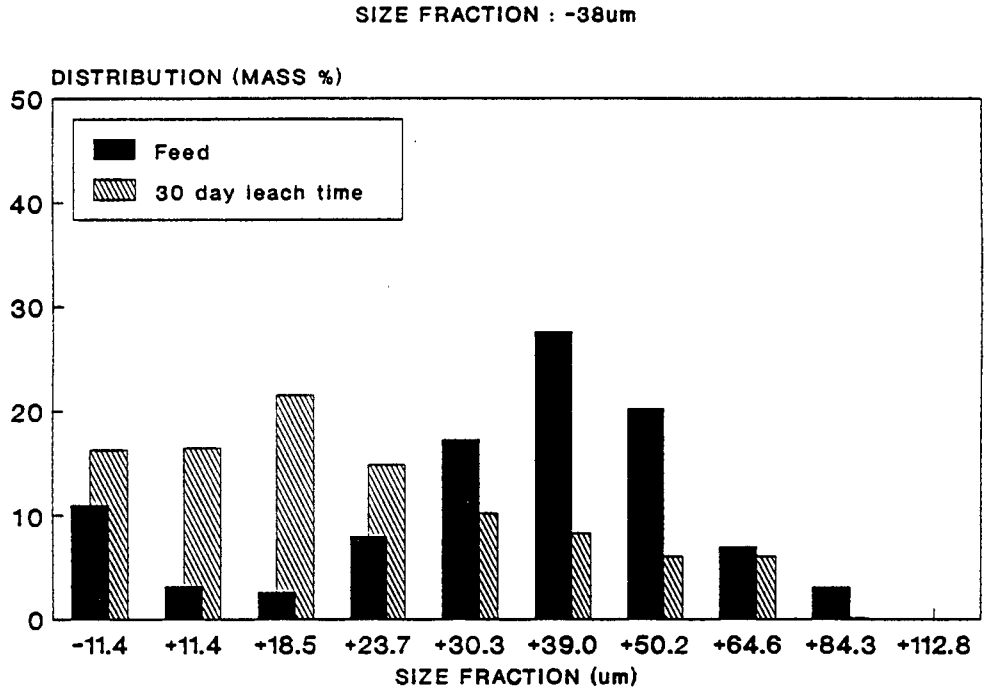

Figure 6.8 Particle size distribution obtained on the Malvern size analyser before and after 30 days leach time.

Even though the shrinking particle mechanism may actively contribute to the leaching mechanism, it should be kept in mind that the shrinking particle model is unable to adequately describe the experimental data (Figures 6.3, 6.4 and 6.5). On the other hand, the propagating pore model presents a much better correlation with the leach curves obtained for the three different size fractions.

The propagating pore and the shrinking particle models differ from each other in that the surface area available for oxidation is modified according to the mechanism involved. The surface area for the shrinking particle model decreases proportionally with the fraction pyrite oxidized, reaching zero when the substrate is completely oxidized. However, the surface area available for oxidation in the propagating pore model, is limited to that represented by the cumulative number of active pores at any time. This surface area modification, by describing the deactivation of the pores at any time, better enables the propagating pore model to describe the leach curves obtained. The linear phase predicted by the propagating pore model, during which all pores are active, generally correlates well with the data. The second order phase, during which pore deactivation takes place, also provides a good correlation with the data. It is this phase, which in effect requires a decrease in the surface area available for oxidation, resulting in the observed reduced volumetric oxidation rate, that the shrinking particle model is unable to adequately describe. Unfortunately, there is not sufficient experimental data available to confirm the zero order phase predicted by the propagating pore model, after total pore deactivation has occurred.

Perhaps a shortcoming in both models is the use of the lag time parameter T_L to accommodate the initial lag phase observed. The iron leach data presented in Figure 6.2

suggests that initially the leach rate is accelerated exponentially from zero at inoculation, to the maximum leach rate observed. This initial phase is therefore not a phase of zero leach rate as assumed for the derivation of these mechanistic models.

To illustrate the propagating pore mechanism, Drossou (1987) presented an extensive selection of scanning electron micrographs, illustrating mainly leached surfaces of pyrite particles. These surface observations provided evidence of pore formation during the bacterial leaching process. The scanning electron micrograph presentation by Drossou (1987) is quite comprehensive. The observations made by Drossou were confirmed in the current study, and will not be repeated.

However, certain surface characteristics not shown by Drossou (1987), were observed in the current study. Illustrated in Figure 6.9(a) is a typical leach residue. The dark unetched particle to the top and right of centre is a quartz particle. The pyrite particle to the right of centre shows a long branched surface 'furrow'. This 'furrowed' surface defect is repeated in the extensively pitted particles shown in the top left corner of this photograph. Similarly, Figure 6.9(b) illustrates a single particle repeating the 'furrowed' surface defect observed, as well as the extensive pit and pore formation on which the derivation of the propagating pore model is based. A surface 'furrow' is shown in Figure 6.9(c) at greater magnification. This 'furrow' measures approximately 4μm across and appears to be slanted into the particle. This indicates that these 'furrows' may be pores formed close to the surface of the particle, running parallel or almost parallel with the surface. This will result in a pore cut in half along its' length and would thus appear as a furrow.

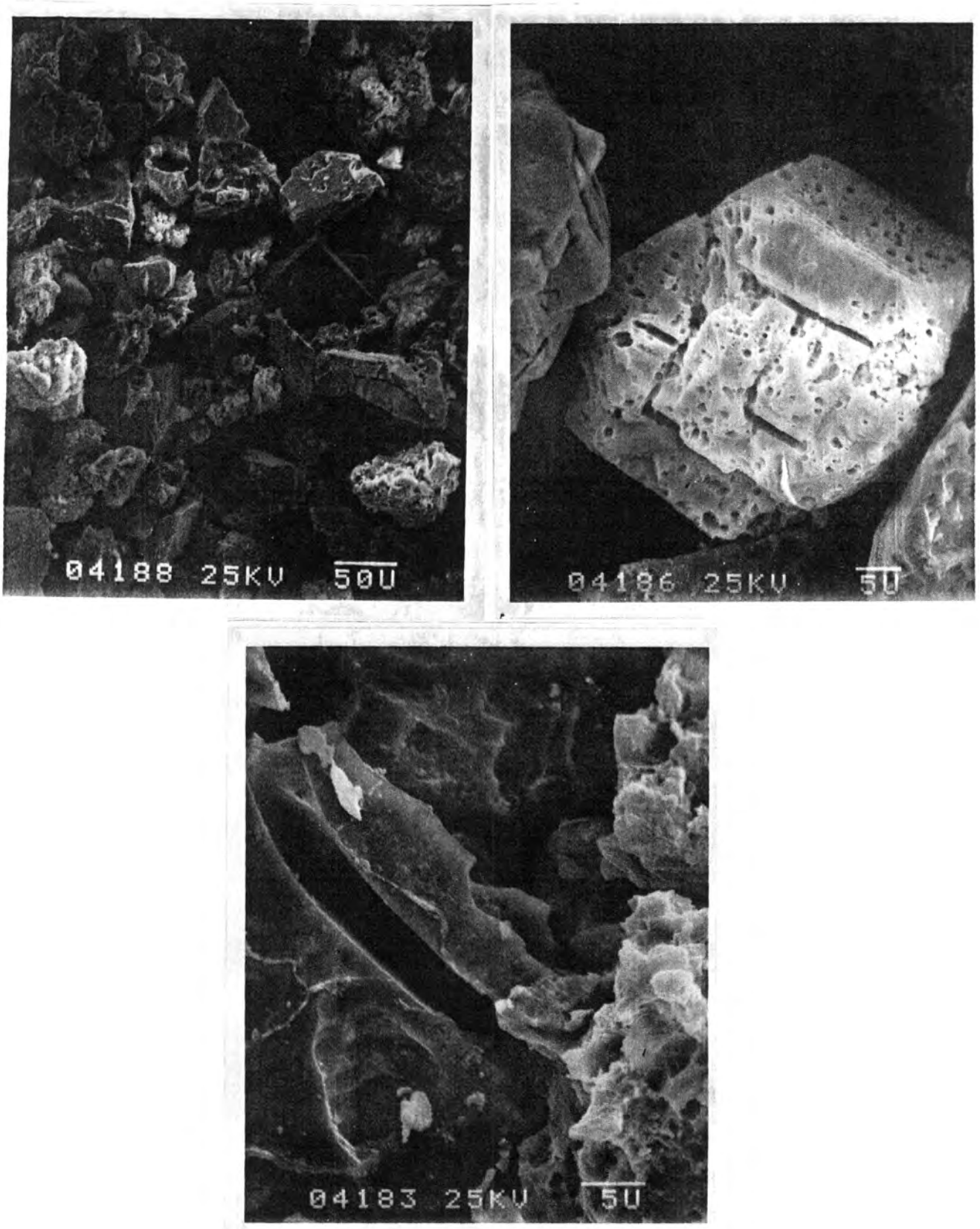

Figure 6.9 Scanning electron micrographs of:
a) bacterially leached residue; +53 -75μm
b) single pyrite particle showing pitted surfaces and 'furrowed' appearance.
c) furrow or disected pore shown at greater magnification.

Even though scanning electron microscopic observations provide significant and useful information in connection with the leach mechanism, they do not reveal anything about what happens inside the particle, once a pore has been initiated. For this reason polished cross sections of bacterially leached particles were examined using reflective light microscopy.

Some photographs of polished sections typifying bacterial leach residues are presented in Figures 6.10 and 6.11. The observations from the photographs of the polished sections can be summarized as follows:

Figure 6.10 (a) Pores ±1μm in diameter are seen at right angles to each other. No pitting is observed on the particle periphery.

(b) Pores (± 1μm in diameter) exhibit angular orientation. This photograph shows pore branching. Pitting and cracks are observed.

(c) Both narrow and wide pores are observed. The particle to the right of centre exhibits no pore orientation and branching appears to be occurring.

(d) Extremely long narrow, branched pores are observed. Pores are ±0,5μm in diameter.

(e) A bending pore ±2μm in diameter is seen.

Figure 6.11 (a) It is not clear whether pits or pores are being observed, however the large variation in diameters is notable.

(b) Both narrow and wide pores are observed. Pore propagation does not appear to be in a straight line.

(c) Pitting on the particle periphery is evident, approximating a shrinking core

mechanism.

(d) The holes are most likely pores. Of note is the hexagonal cross section some of the pores exhibit.

(All micrographs were taken in plane polarised, vertically incident light, using oil immersion objectives.)

Southwood and Southwood (1985) studying polished sections of extensively leached pyrite particles with the use of reflective light microscopy, observed similar pore formations.

The polished sections revealed significant information concerning the shape, length, orientation and branching of pores after initiation. It would appear that pore propagation is not always in a straight line. Furthermore, it would appear that branching of pores does occur. Some pores were observed to be orientated at right angles and others were observed to bend at right angles. However, in contrast to this, pore orientation in some particles did not exist. Southwood and Southwood (1985) concluded from their observations that the pores are preferentially orientated parallel to the three crystallographic axes of the cubic pyrite lattice, but this does not always appear to be the case.

In addition to this, pores observed to be initiated from a common surface are shown to be at different lengths, suggesting that not all pores are initiated at the same time, or alternatively, that not all pores propagate at the same rate.

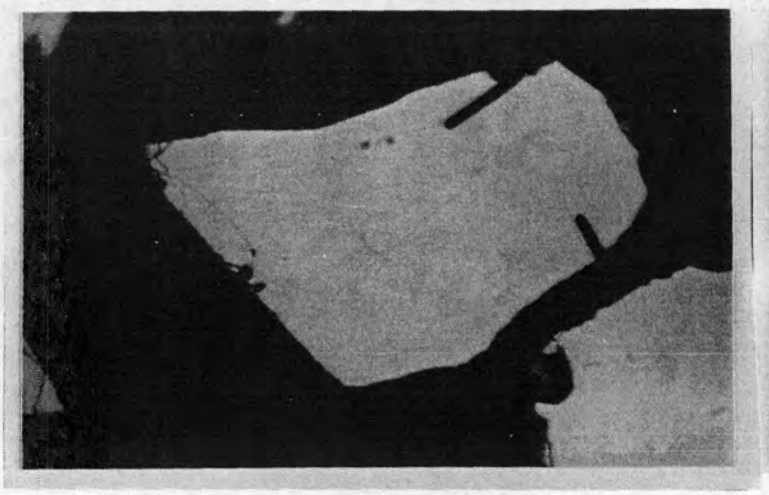

(a)

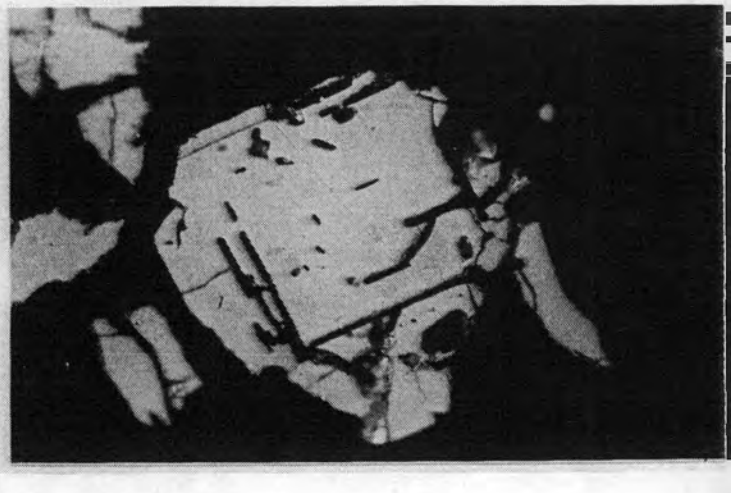

(b)

(c)

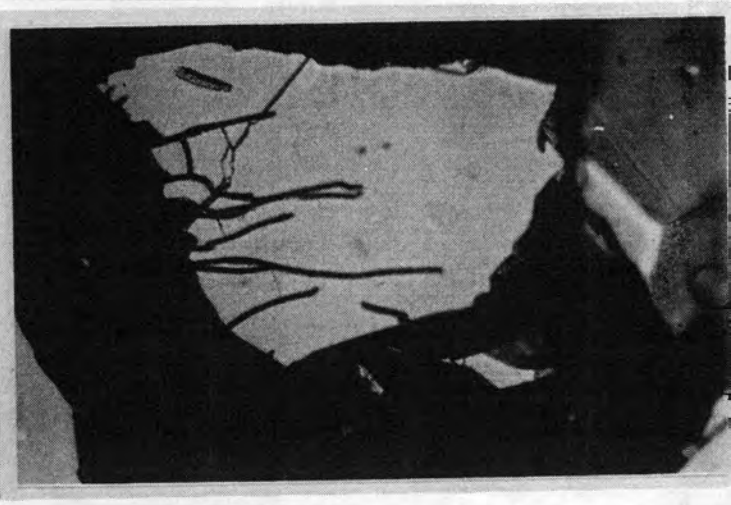

(d)

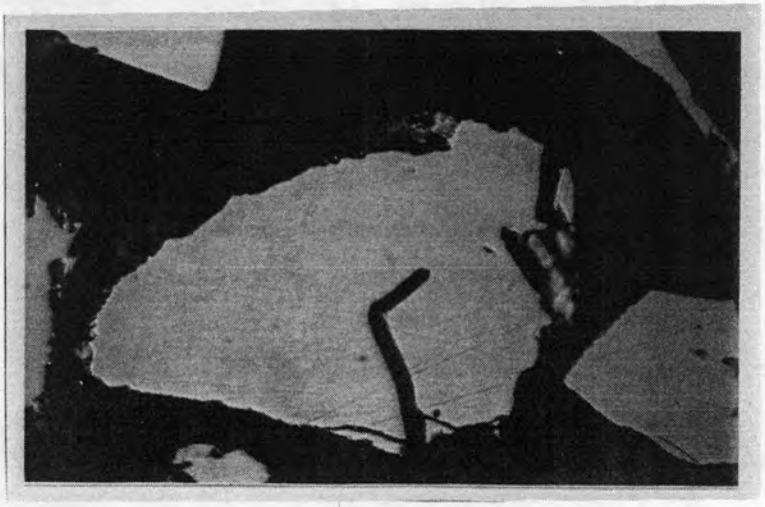

(e)

Figure 6.10 Photograhps of polished sections of pyrite particles illustrating pore formation and characteristics.

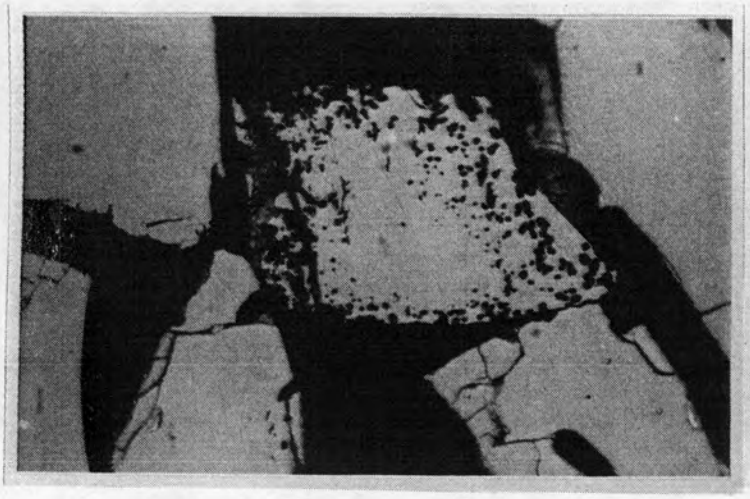

(a)

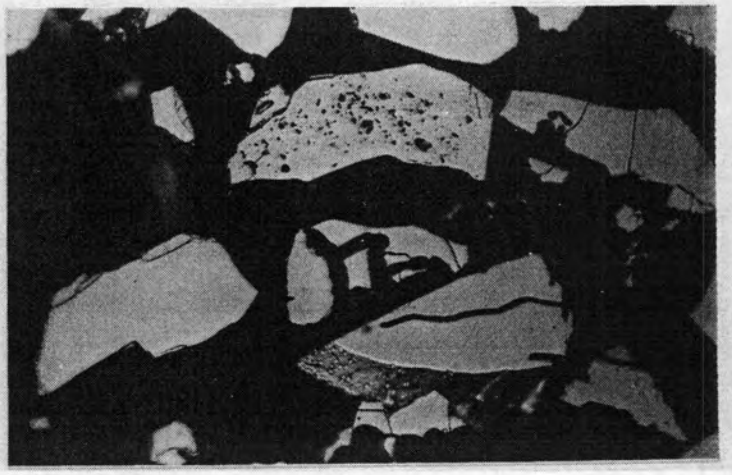

(b)

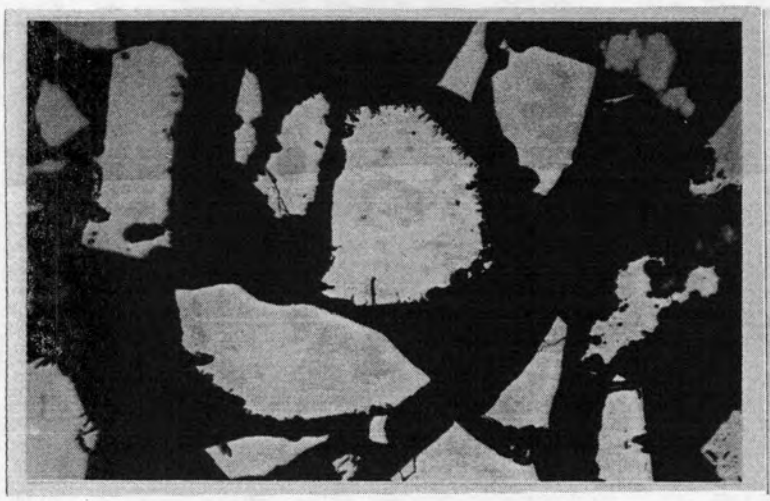

(c)

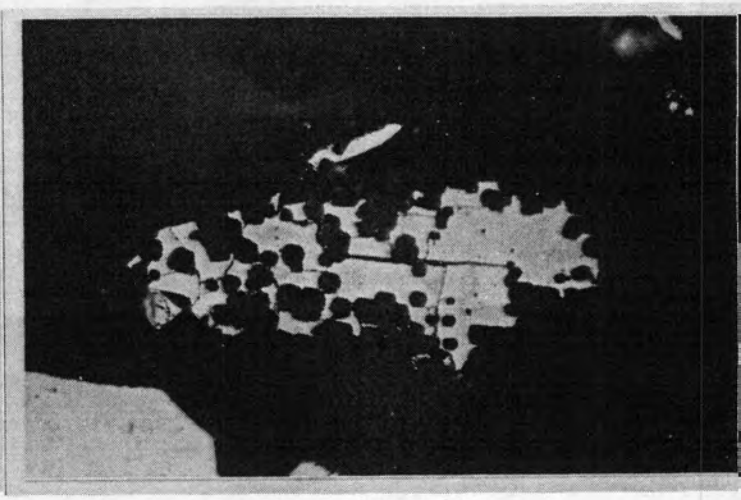

(d)

Figure 6.11 Photographs of polished sections of pyrite particles illustrating pore formation and characteristics.

Pore formation in a solid spherical particle, where the original diameter is maintained, should result in an increased overall specific surface area of the particle if the internal surface area is measured. A technique such as the B.E.T. method of specific surface area determination is capable of measuring this internal surface area. The specific surface area of a solid substrate obtained by the B.E.T. method can therefore be used as a means of tracking the degree of pore formation in a leach residue. The specific surface areas for the leach residues of the respective size fractions were obtained. The time course results are illustrated in Figure 6.12. Figure 6.13 illustrates the equivalent increase in specific surface area as a function of the total sulphide oxidation.

As can be seen from Figures 6.12 and 6.13, all the size fractions show an increase in the specific surface areas, substantiating pore formation in all the size fractions. The +53 -75μm size fraction showed the least increment in the specific surface area. This can probably be attributed to the unusually high initial specific surface area exhibited by this size fraction.

In the light of the information obtained from the polished sections, it would appear that the assumptions made for the derivation of the propagating pore model are possibly oversimplified. The actual leach mechanism appears to be more complex than that suggested in the derivation of this model. In addition to this, the degree of particle size reduction observed during the batch leach tests, suggests that the shrinking particle mechanism contributes a major part in the overall leach mechanism. This suggests that a hybrid model, which combines both the propagating pore and shrinking particle mechanisms, should be more successful if a mechanistic approach is to be pursued.

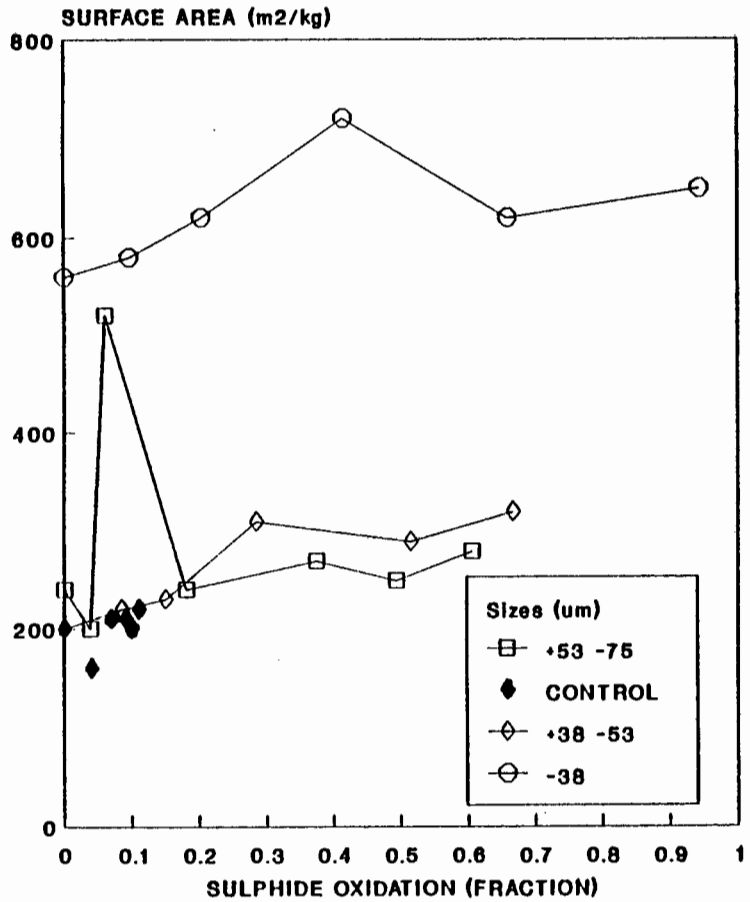

Figure 6.13 B.E.T. specific surface areas as a function of total sulphide oxidation for batch leach residues.

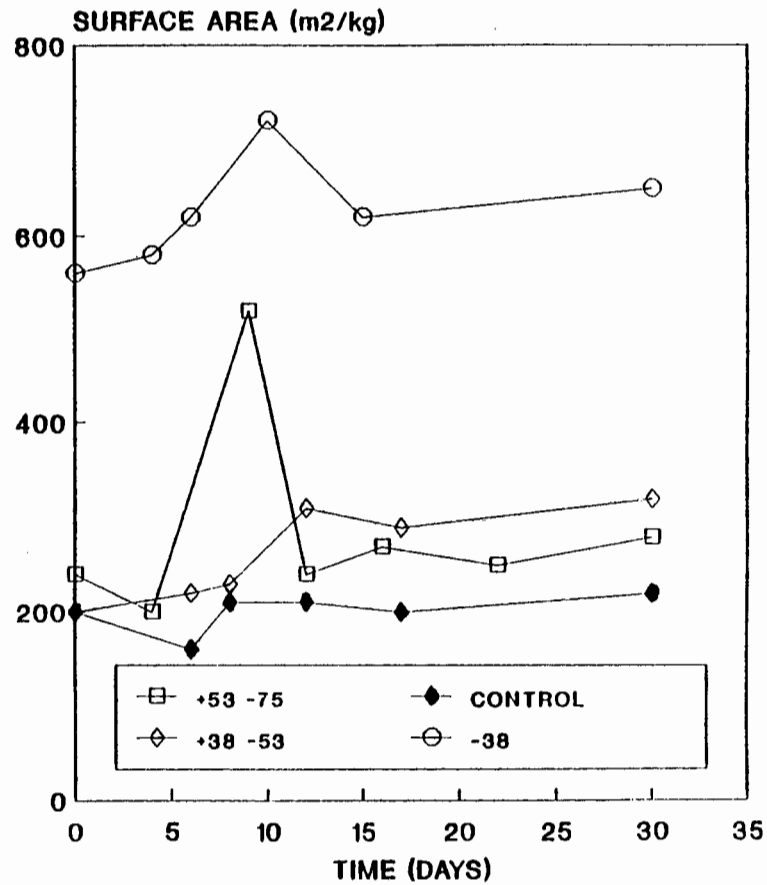

Figure 6.12 B.E.T. specific surface areas as a function of leach time obtained for the batch leach residues.

6.2.3 The Logistic Growth Model - Discussion, and Fitting the Model to the Experimental Data.

The format of the empirical logistic growth model simulates the characteristic sigmoid of batch culture. To fit the model, three constants, F_o, F_m and k_m have to be determined. Figure 6.14 illustrates the time course plot of the logistic model.

The model parameter F_o, as illustrated in figure 6.14, is equivalent to the fraction of oxidation at time zero. Even though the fraction of mineral oxidation may be zero at time zero, this parameter cannot be set equal to zero, since this will reduce Equation 4.29 to zero. If F_o is set to zero, the system can be considered uninoculated and therefore leaching will not commence. This parameter essentially dictates the length of the lag time observed for the leach curve. The smaller the numeric value assigned to this parameter, the longer the resulting lag period will be.

The model parameter F_m corresponds to the maximum fraction of the mineral oxidisable during the batch leach. Therefore, if the mineral is totally oxidisable during the batch leach, this parameter would be equal to 1,0. However, as the results obtained in the present study indicate, the maximum fraction of pyrite oxidisable appears to be dependent on the particle size, indicating that this parameter would not necessarily be equal to 1,0.

The rate parameter, k_m, primarily determines the slope of the linear section of the leach curve illustrated in Figure 6.14, and is dependent on the time scale within which leaching goes to completion. An increase in the rate parameter would result in an increase in the slope. Therefore, this parameter would largely be determined by the

maximum leach rate observed in batch culture.

Both F_o and F_m are given as fractions and are therefore dimensionless. The units of the rate constant, k_m, is the inverse of the time scale used (i.e. if the time scale is reported in days, the units of k_m will be given in $days^{-1}$).

The Nelder-Mead parameter optimisation routine was used to obtain parameter values that gave the best model correlation with the time course kinetic data obtained for the oxidation of pyrite. The model parameters are summarised in Table 6.6, and includes the sum of errors squared. The fitted model curves for the three respective size fractions are illustrated in Figure 6.15, 6.16 and 6.17.

Table 6.6 Parameters estimated for the logistic model by least squares method from the experimental data obtained for batch culture.

Size (μm)	F_o	F_m	k_m (day^{-1})	$\Sigma(errors)^2$
+53 -75	0.018	0.597	0.259	2.09×10^{-3}
+38 -53	0.018	0.662	0.277	1.44×10^{-4}
-38	0.048	0.942	0.265	4.13×10^{-3}

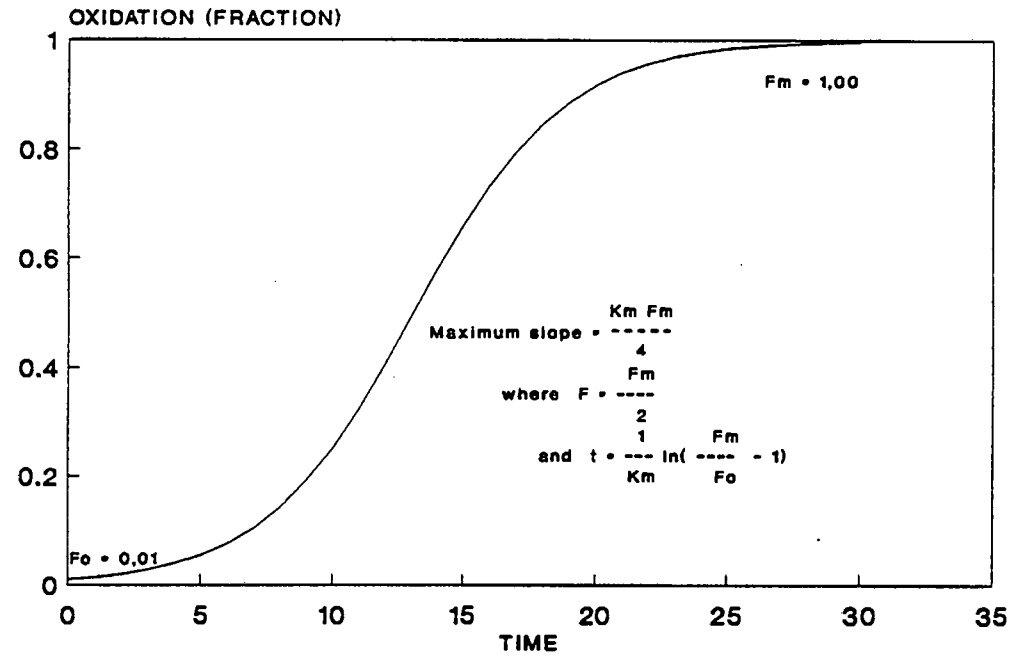

Figure 6.14 Typical oxidation as a function of time prediction by the logistic model.

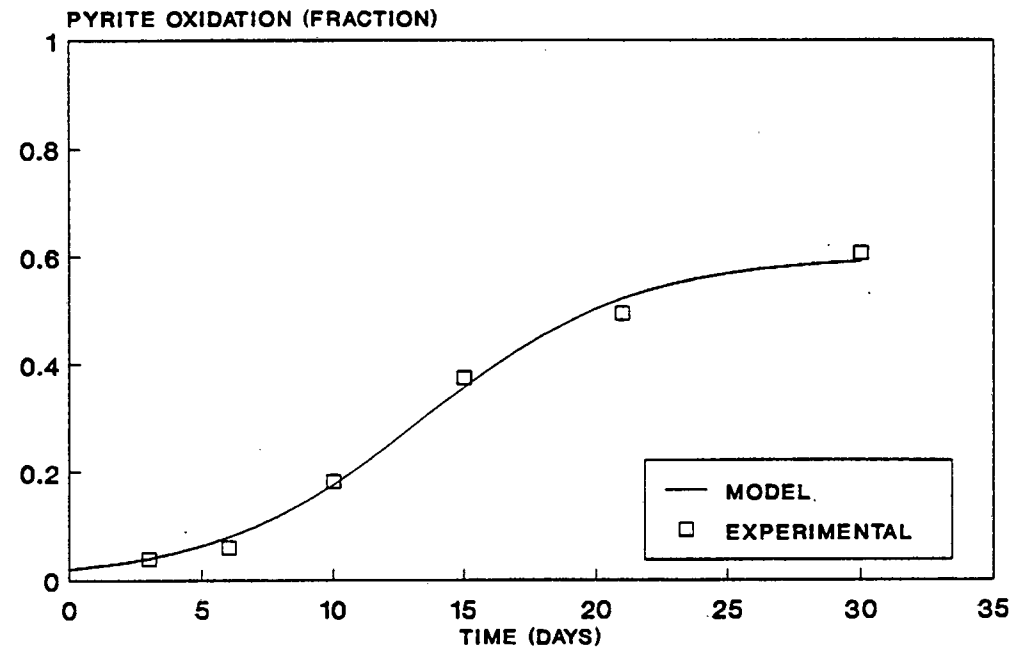

Figure 6.15 Experimental data and leach curve predicted by the logistic model.

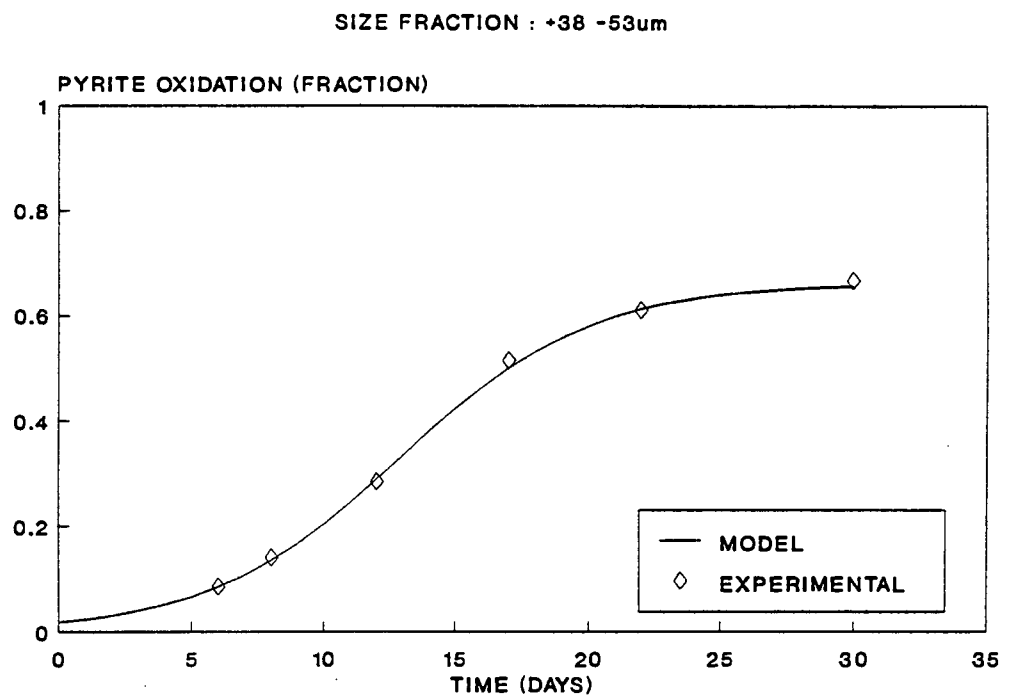

Figure 6.16 Experimental data and leach curve predicted by the logistic model for total pyrite oxidation.

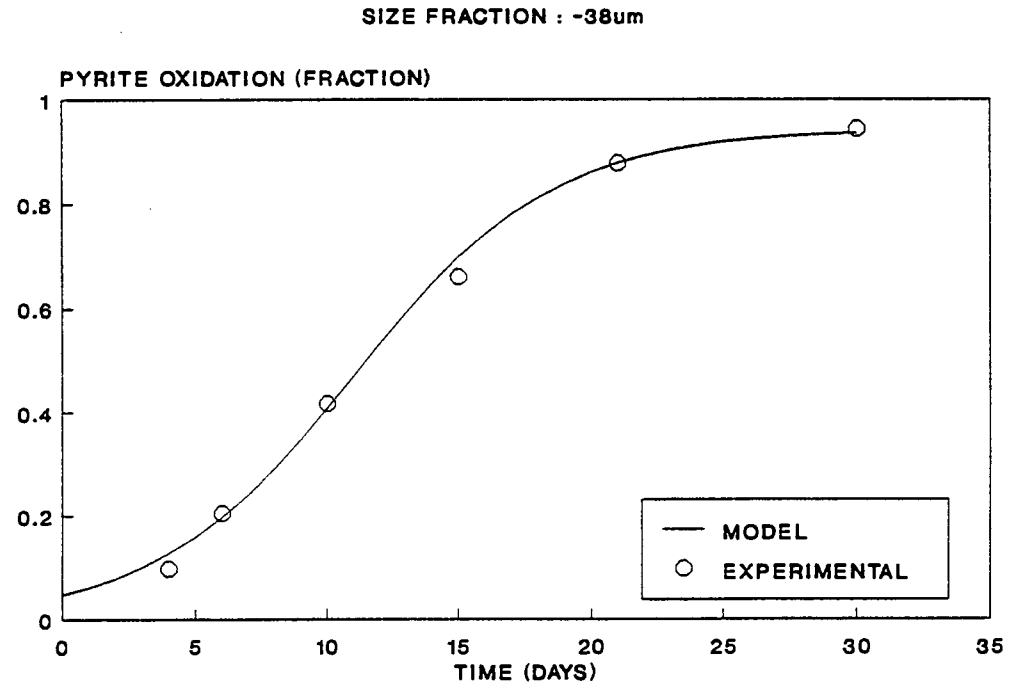

Figure 6.17 Experimental data and leach curve predicted by the logistic model for total pyrite oxidation.

It is evident in Figures 6.15, 6.16 and 6.17 that the logistic model, even though it is empirical in nature, provides the best correlation with the experimental data. The sum of the errors squared given in Table 6.6 confirms this observation.

The parameter F_o varied inversely according to the lag periods observed for the three batch runs. The largest F_o observed, was for the -38μm size fraction which exhibited the shortest lag time. Pinches *et al.* (1987) found F_o to be equal to 0,008 in their study.

The F_m, or maximum fraction of pyrite that can be oxidised, for the -38μm size fraction was found to be 0,942. Pinches *et al.* (1987) found this parameter to be equal to 0,944 for a pyrite concentrate with a particle size distribution of 80% less than 38μm. A wide variation in this parameter was found for the respective size fractions. This may indicate that a consistent or universal correlation could exist between the particle size distribution of the mineral being leached and this parameter (F_m) of the logistic model.

The rate constant was found to remain approximately constant at 0,265 day^{-1} for the three size fractions. Pinches *et al.* (1987) found this parameter to be equal to 0,482 day^{-1}. As previously established, a direct correlation exists between the oxidation rate and the surface area concentration. Since k_m is a rate parameter, it is not totally excluded that a direct correlation may exist between the rate parameter k_m and the initial pyritic surface area concentration. The greater k_m value reported by Pinches *et al.* (1987) would then be taken up in this effect, since the initial pyritic surface area in their study substantially exceeded that of the present study.

It would therefore appear that there may be a connection between the physical conditions in the leach, such as surface area concentration and particle size, and the various parameters of the logistic model. Additional experimental work needs to be done to establish any such relationship.

The logistic model is able to accommodate all the characteristics that typify a sigmoidal batch leach curve. This model holds the advantage over previously discussed models in that it is contained in one single equation, thus eliminating the cumbersome nature of separate equations describing different regions of the leach curve. This simplifies equation manipulation required for the description of reaction kinetics in the industrial application of this technology.

6.3 Continuous Reactor Test Results.

6.3.1 Experimental Results.

The analytical results obtained for the steady state products of the respective size fractions at various residence times, are summarized in Table 6.7. This table includes the analyses of the unreacted products as well as the solutions. In Table 6.7 two residence times are shown. The first was obtained from the volumetric feed rate. However, because a difference between the feed and product volumes was observed due to evaporation, the solids retention time was calculated using the SiO_2 in the feed and the product as an inert tracer (See Appendix B). Similarly, the fraction oxidation, as shown for the residues, was calculated from the residue analysis by using SiO_2 as an inert tracer (Appendix B). The iron analysis shown for the solution is the total acid soluble iron concentration in

grams per litre. The equivalent oxidation shown for the solution analysis was calculated as the fraction iron in the feed solubilized.

A summary of the mass balances obtained for iron at steady state operation, is shown in Table 6.8 for the respective size fractions. These averages were obtained over a four day period after steady state had been reached. Included in Table 6.8 is a ratio of the iron in the feed to the iron in the product. As can be seen, this ratio is consistently close to 1,0, indicating a good accountability for iron during the continuous operation of the single stage reactor. A more complete mass balance, which includes that for SiO_2, is given in Appendix B.

Table 6.7 Continuous Leaching Test Results. Residence times are given in days. The fraction leached is calculated on a mass basis. For the supernatant the total acid soluble iron analysis is given and the equivalent fraction leached is calculated.

Size (μm)	Residence time		Residue analysis (%)			Fraction Leached		Supernatant	
	Pumping rate	SiO_2 tracer	Fe	S^{2-}	SiO_2	Fe	S^{2-}	Anal. (g/l)	Fract'n leached
+ 53 - 75	4.43	4.66	43.6	46.6	3.47	0.142	0.14	7.1	0.136
	7.66	7.87	42.9	47.9	4.70	0.361	0.36	15.9	0.305
	10.38	10.34	41.6	45.4	5.39	0.462	0.47	27.4	0.464
	15.16	14.27	39.7	45.7	7.01	0.567	0.55	31.5	0.564
+ 38 - 53	4.20	4.29	45.1	48.3	2.96	0.136	0.13	7.7	0.149
	6.82	6.87	43.8	47.9	2.81	0.395	0.41	19.3	0.364
	10.13	9.84	43.1	46.5	3.05	0.481	0.50	28.0	0.486
	13.53	14.27	43.4	46.0	3.36	0.587	0.61	33.3	0.615
- 38	4.48	4.52	42.5	48.3	4.34	0.298	0.29	14.2	0.280
	7.54	7.09	41.8	45.3	4.99	0.450	0.47	24.2	0.458
	10.80	11.12	40.9	45.9	6.14	0.598	0.60	30.3	0.562
	13.81	13.70	40.7	45.3	7.03	0.637	0.64	35.9	0.590

Table 6.8 Steady state mass balances obtained for iron during the continuous operation of the single stage reactor. Average iron balances over a period of four days, after steady state had been achieved, are shown.

Size (μm)	Residence Time (days)	Fe in feed (g day^{-1})	Fe in product (g day^{-1})	Fe in feed / Fe in prod.
+ 53 - 75	4.43	102.8	102.5	1.00
	7.66	59.5	56.4	1.05
	10.38	45.4	45.8	0.99
	15.16	30.1	30.2	0.99
+ 38 - 53	4.20	108.7	110.4	0.98
	6.82	66.5	64.7	1.03
	10.13	44.9	45.4	0.98
	13.53	33.5	34.7	0.97
- 38	4.48	101.2	99.9	1.01
	7.54	60.6	61.5	0.98
	10.80	42.1	40.8	1.03
	13.81	32.8	31.5	1.04

The leach results obtained for the single stage continuous reactor have been plotted as the fraction of pyrite oxidised, $F(\tau)$, versus the residence time, τ, and is shown in Figure 6.18. The surface area oxidation rates calculated based on the surface area concentration in the feed to the reactor, are shown in Table 6.9. Also shown are the surface area oxidation rates based on the B.E.T. specific area estimations.

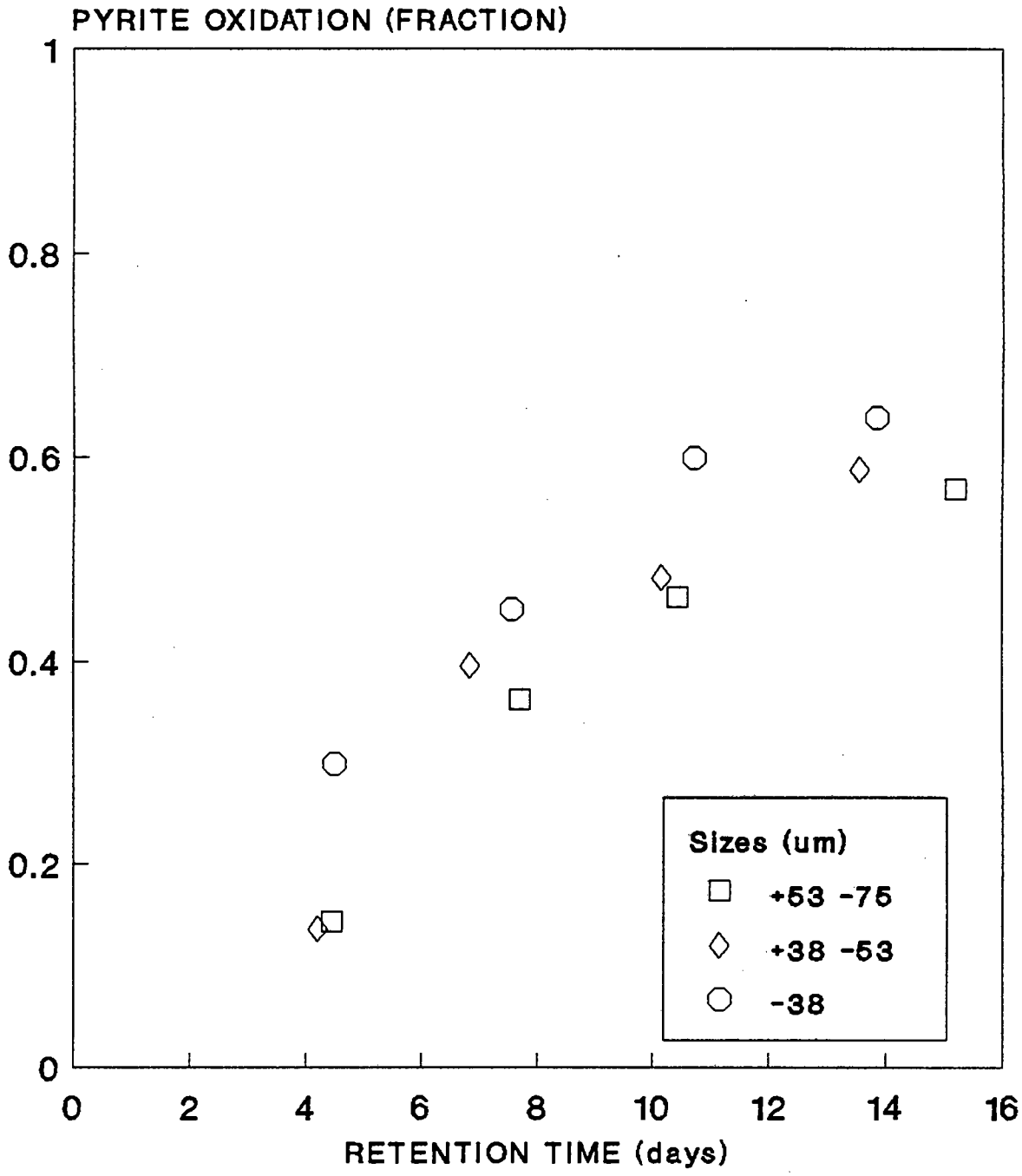

Figure 6.18 Pyrite oxidation obtained from the continuous reactor study for the respective size fractions.

Table 6.9 Volumetric and surface oxidation rates observed for the single stage continuous leaching reactor. The surface oxidation rate is obtained from the surface area concentration in the feed.

Size (μm)	τ (days)	Volumetric oxidation rate (mg l^{-1} h^{-1})		Surface oxidation rate for pyrite ($kgm^{-2}day^{-1}$)	
		Iron	Pyrite	Geometric	B.E.T.
+ 53 - 75	4.43	59.5	127.8	1.564×10^{-3}	1.277×10^{-4}
	7.66	76.7	164.8	2.016×10^{-3}	1.648×10^{-4}
	10.38	89.2	191.6	2.344×10^{-3}	1.913×10^{-4}
	15.16	71.4	153.4	1.876×10^{-3}	1.533×10^{-4}
+ 38 - 53	4.20	67.0	143.9	1.288×10^{-3}	1.726×10^{-4}
	6.82	90.6	194.6	1.742×10^{-3}	2.331×10^{-4}
	10.13	92.2	198.1	1.773×10^{-3}	2.374×10^{-4}
	13.53	86.8	186.5	1.696×10^{-3}	2.236×10^{-4}
- 38	4.48	130.4	280.1	1.378×10^{-3}	1.199×10^{-4}
	7.54	117.4	252.2	1.240×10^{-3}	1.079×10^{-4}
	10.80	99.5	213.6	1.051×10^{-3}	9.154×10^{-5}
	13.81	81.6	175.2	0.862×10^{-3}	7.509×10^{-5}

Chang and Meyerson (1982) in their study of the continuous bacterial leaching of a pyrite concentrate, used B.E.T. measurements to estimate the specific surface area. They reported surface area oxidation rates that varied from $0,10 \times 10^{-5}$ kg m^{-2} day^{-1} to $3,30 \times 10^{-5}$ kg m^{-2} day^{-1} for retention times of 0,7 to 3,5 days. The surface area oxidation rates based on B.E.T. determinations in the current study varies from $7,51 \times 10^{-5}$ to $23,7 \times 10^{-5}$ kg m^{-2} day^{-1}. Unfortunately, Chang and Meyerson presented insufficient data to be able to determine the equivalent geometric surface area oxidation rates.

Helle and Onken (1987) observed an increase of steady state iron in solution with an increase in the retention time. The fraction of pyrite oxidation increased from 0,062 at a retention time of 2,08 days, to 0,102 at a 4,17 day retention time. The steady state surface area oxidation rate for pyrite, calculated from the geometric surface area and the iron solubilized, ranged from $0,60 \times 10^{-3}$ kg m^{-2} day^{-1} to $2,06 \times 10^{-3}$ kg m^{-2} (volumetric oxidation rates of 218 to 977 mg l^{-1} h^{-1}). In the current study, the geometric surface area oxidation rates ranged from $0,86 \times 10^{-3}$ kg m^{-2} day^{-1} to $2,34 \times 10^{-3}$ kg m^{-2} day^{-1}.

Pore formations, similar to those observed in the batch leached residues of the respective size fractions, were observed for the leach residues of the continuous reactor tests. B.E.T. specific surface areas were obtained for the leach residues of the continuous reactor tests for the respective size fractions and are illustrated in Figure 6.19. Compared with the batch test results, a greater increase in the specific surface areas for all the particle size fractions was observed for equivalent fractions sulphide oxidation.

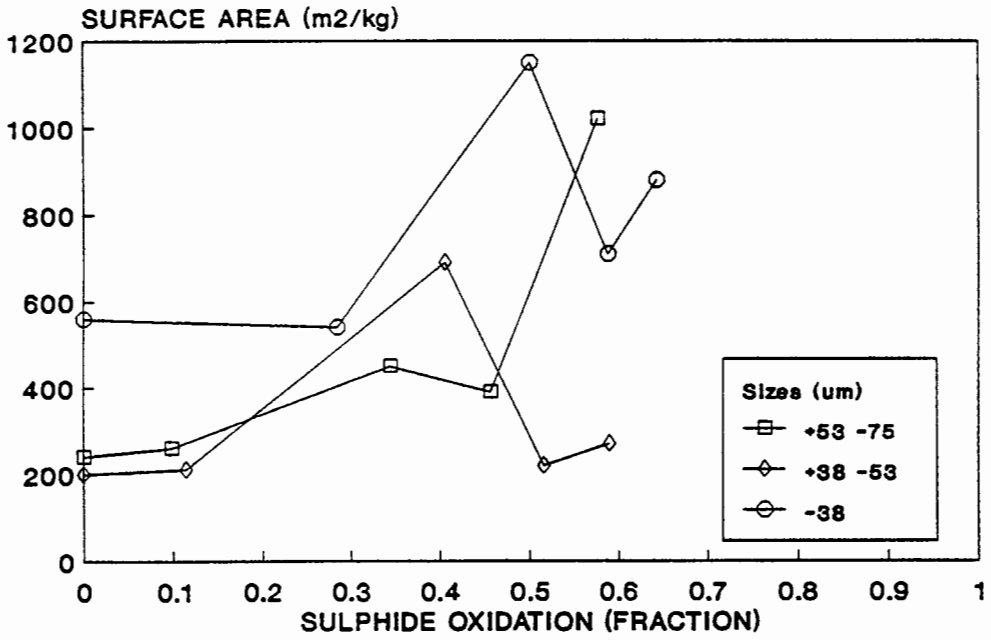

Figure 6.19 B.E.T. specific surface areas as a function of total sulphide oxidation from continuous reactor data.

6.3.2 Fitting the Models to the Experimental Data.

The model parameters for the logistic growth and shrinking particle models derived for single stage continuous reactor description, were obtained by using the Nelder-Mead parameter optimisation routine. However, in the case of the propagating pore model derived for a single stage continuous reactor, a total of five parameters need to be solved from only four data points. This will result in more than one possible solution to the parameters. Therefore, the parameters of this model were not determined.

The values estimated for the various parameters of the shrinking particle and logistic models are given in Table 6.10. Also included in Table 6.10 are the sum of the errors squared, indicating the degree with which the models correlate with the experimental data. In the case of the shrinking particle model, the parameters were obtained from the model format given in Equation 4.11, where the retention time is given as the independent variable (as opposed to the fraction of sulphide oxidation in the case of the logistic model). The sum of the errors squared obtained for these two models are therefore not comparable, which explains the substantial difference in numeric values.

Table 6.10 Model parameters estimated by least squares method from single stage continuous reactor data. The surface oxidation rates given are for pyrite oxidation.

Shrinking particle model			
Size (μm)	τ_w (days)	Oxidation rate (kg m^{-2} day^{-1})	$\Sigma(errors)^2$
+53-75	2.0	4.23×10^{-3}	1.459
+38-53	2.2	3.66×10^{-3}	1.589
-38	0.4	2.03×10^{-3}	1.180
Logistic model			
Size (μm)	F_m	k_m (day^{-1})	$\Sigma(errors)^2$
+53 -75	0.725	0.276	7.91×10^{-4}
+38 -53	0.769	0.290	1.13×10^{-3}
-38	0.792	0.348	2.16×10^{-3}

The correlation with the experimental data obtained for the shrinking particle model is illustrated in Figures 6.20, 6.21 and 6.22. A much closer correlation with the data was achieved when using the washout term, than when this term was omitted. This substantiates the importance of using a washout parameter, if a mechanistic approach is to be pursued.

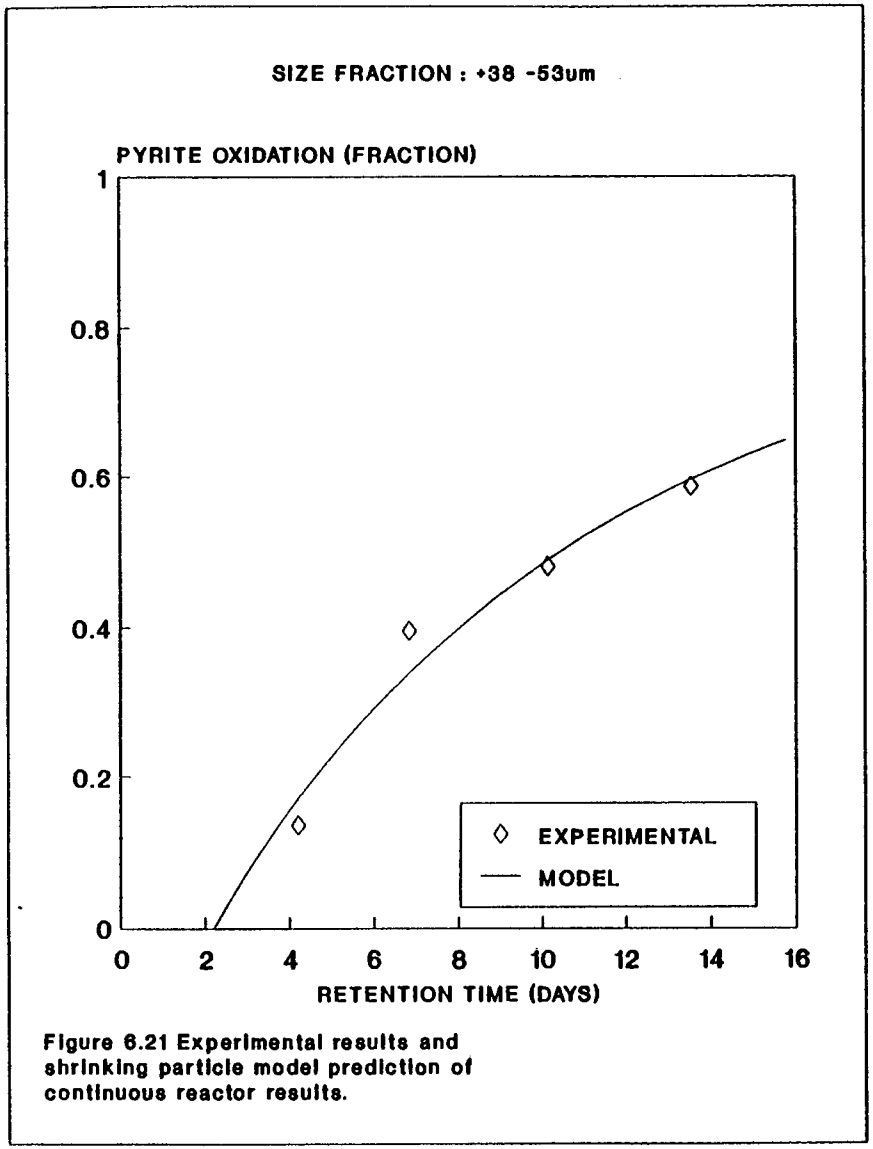

Figure 6.21 Experimental results and shrinking particle model prediction of continuous reactor results.

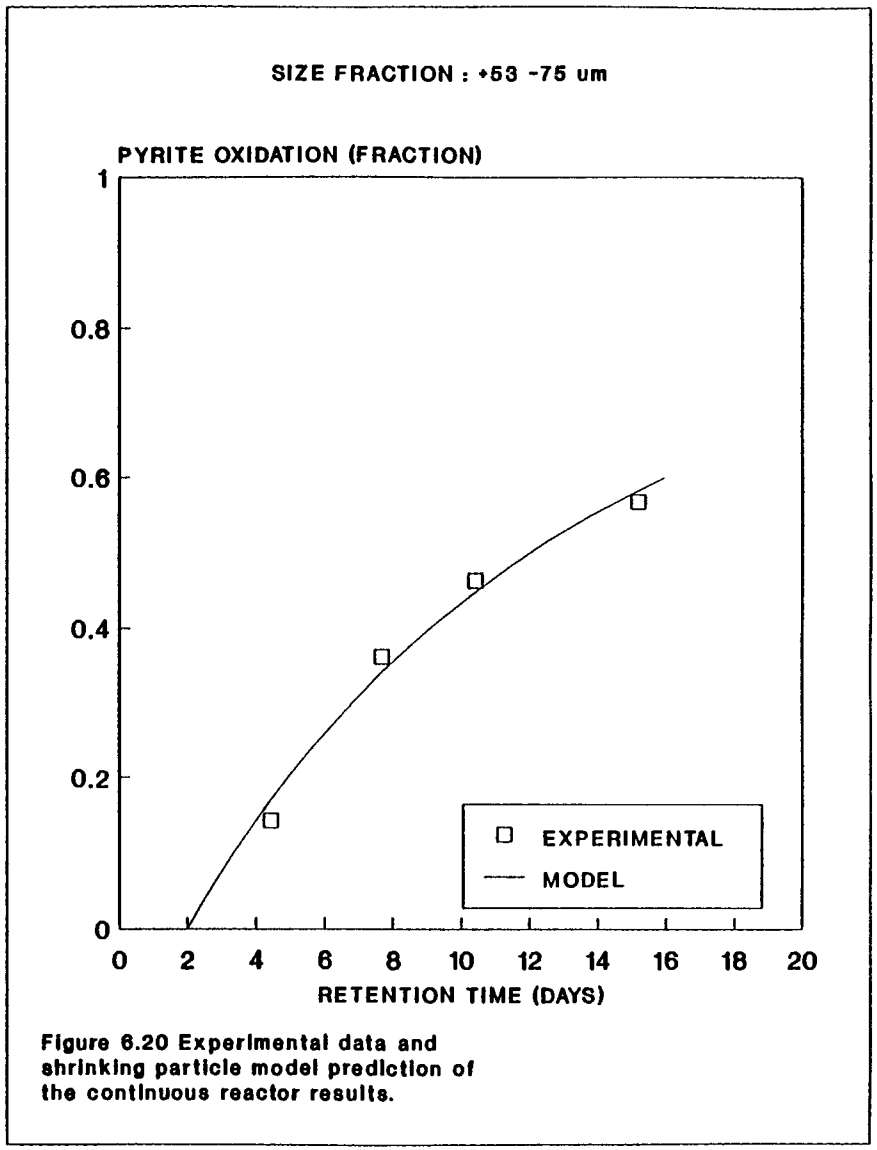

Figure 6.20 Experimental data and shrinking particle model prediction of the continuous reactor results.

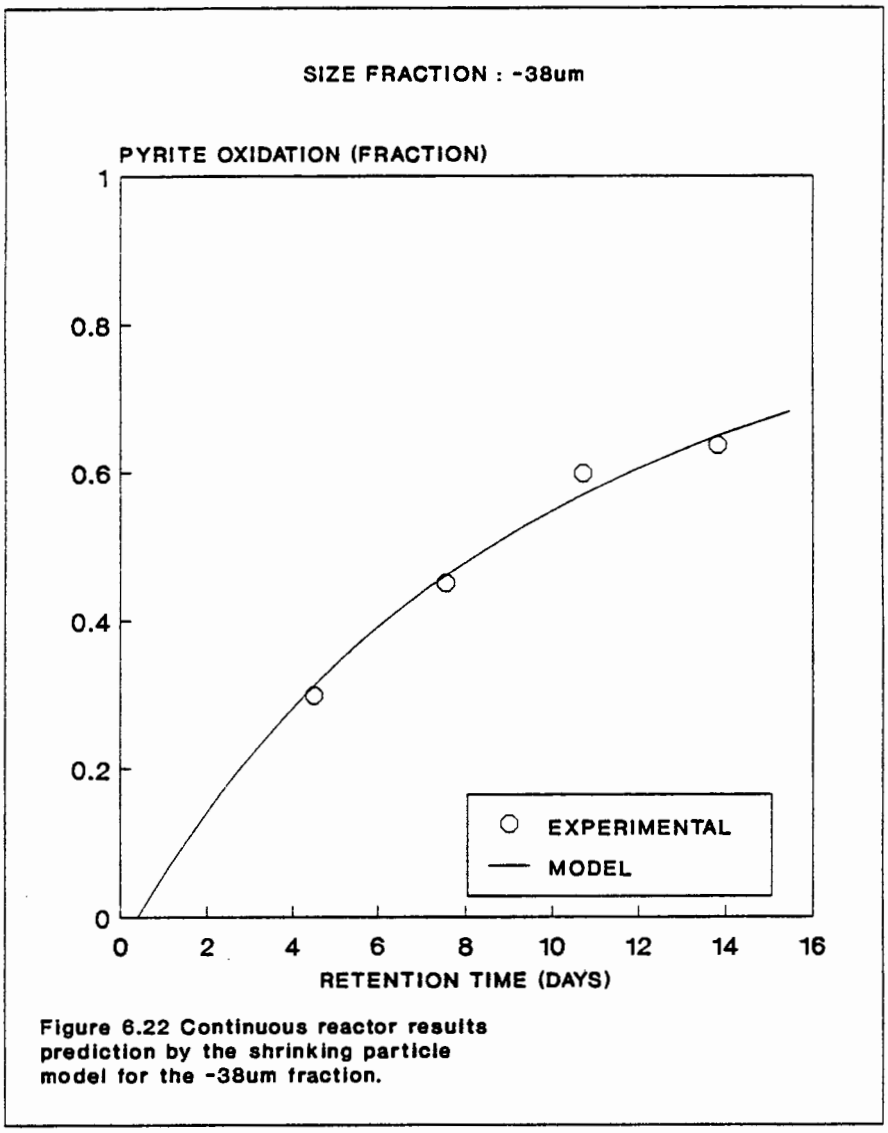

Figure 6.22 Continuous reactor results prediction by the shrinking particle model for the -38um fraction.

Equation 4.11(b) derived for the continuous reactor description in the case of the shrinking particle model, shows an asymptote, as F approaches 1,0. The model predicts that an infinite retention time will be required for complete oxidation of the pyrite. However, it is evident, as was also illustrated by the batch test results, that the shrinking particle model does not provide a good correlation with the experimental data.

Figure 6.23 gives a typical plot of the fraction of pyrite oxidised as a function of the retention time, for a single continuous reactor, as described by the logistic growth model (Eq. 4.38). This plot gives the anomaly between the model parameters and the physical observations for the continuous operation of a single stage reactor. As can be seen from this plot, similar to the batch description, F_m indicates the maximum fraction of pyrite that can be oxidised in a reactor with an infinitely long retention time.

The rate parameter, k_m, as previously discussed, is equal to the inverse of the retention time at which the condition of zero oxidation (or equivalent cell washout in a biological growth description) will occur. The ability of the logistic growth equation, as applied in the present context to describe this condition, is of prime importance, since this is a common phenomenon observed in biological systems. Furthermore, it is an important criterium in the successful operation of any biological system. Even though washout was not illustrated in the current study, sufficient evidence of this phenomenon is given in the literature.

Figures 6.24, 6.25 and 6.26 show plots of the model correlated with the experimental results for the respective size fractions.

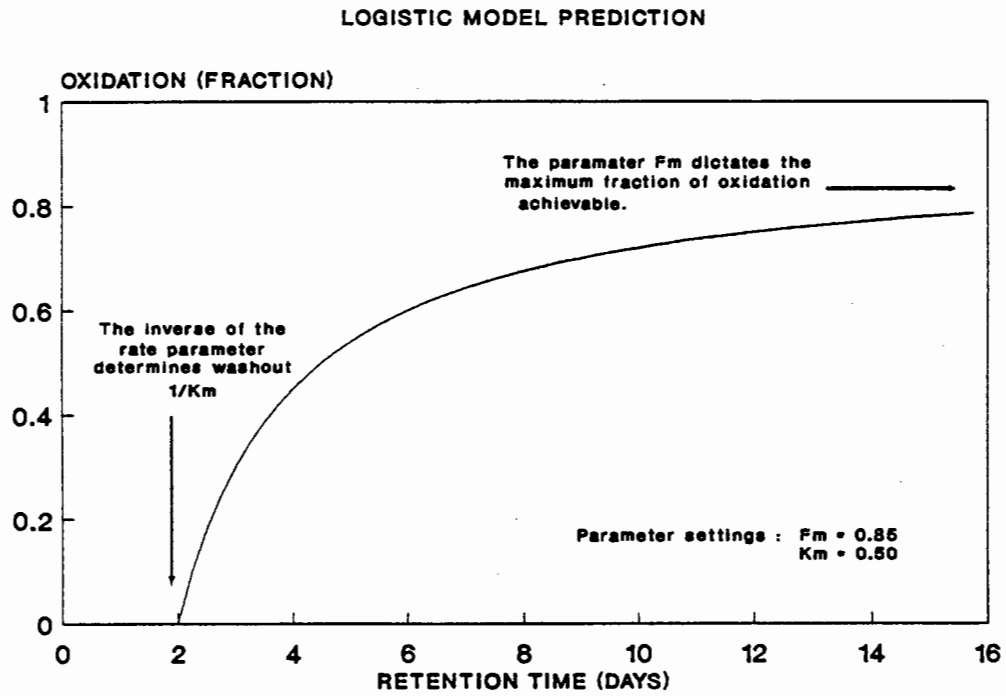

Figure 6.23 Typical oxidation vs retention time profile prediction by the logistic model.

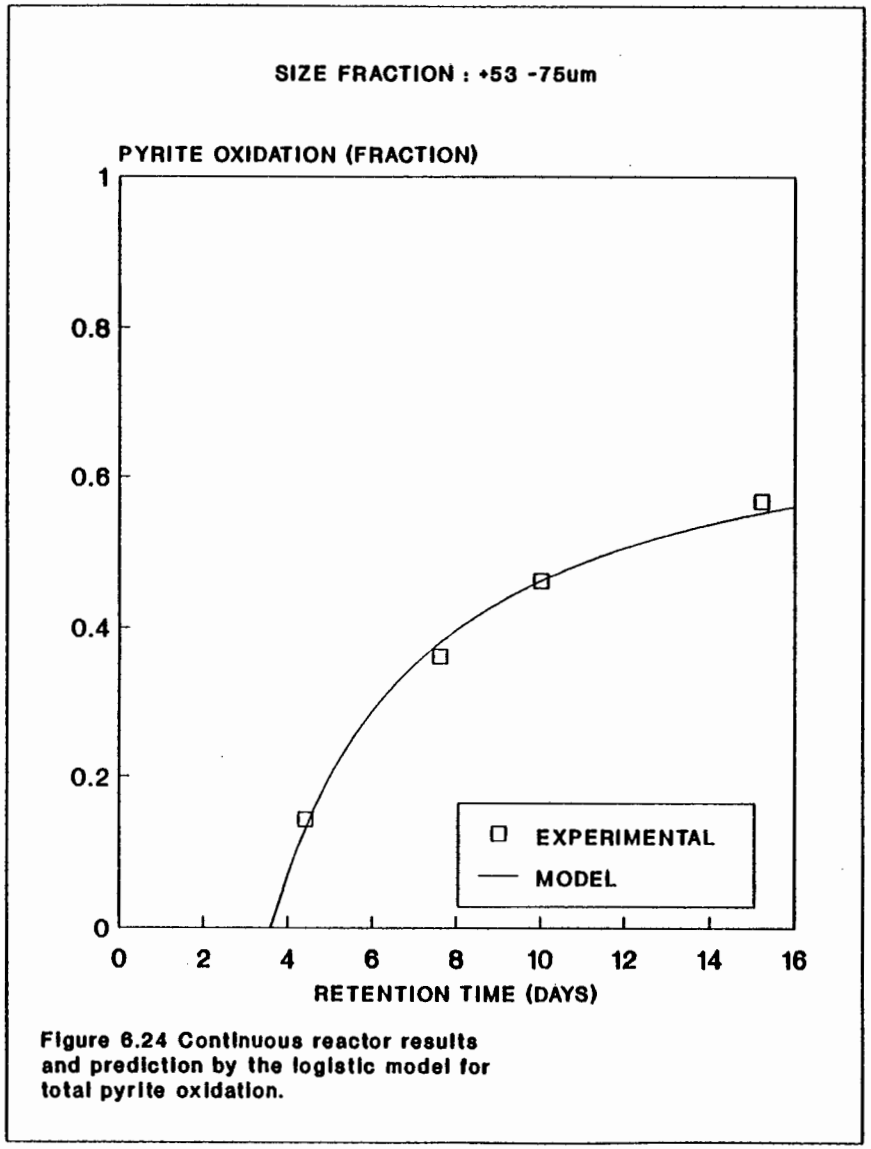

Figure 6.24 Continuous reactor results and prediction by the logistic model for total pyrite oxidation.

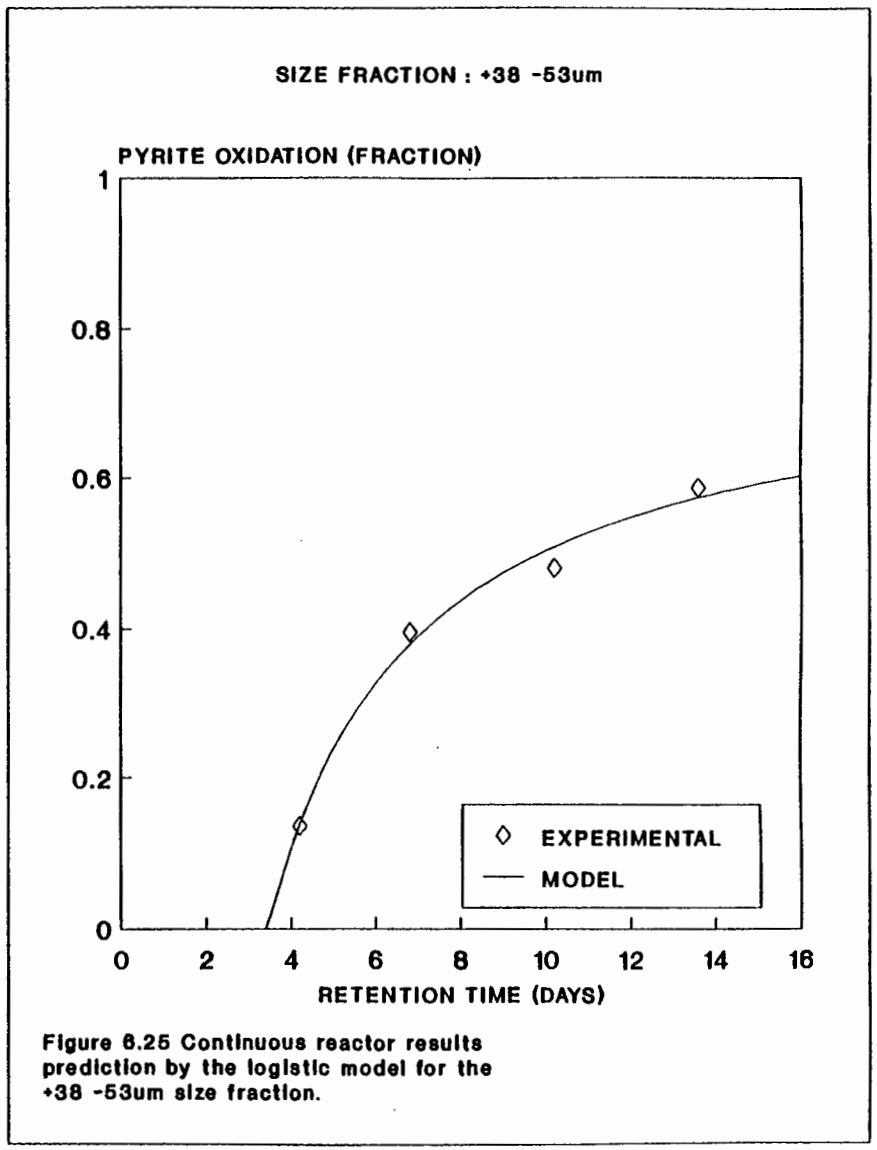

Figure 6.25 Continuous reactor results prediction by the logistic model for the +38 -53um size fraction.

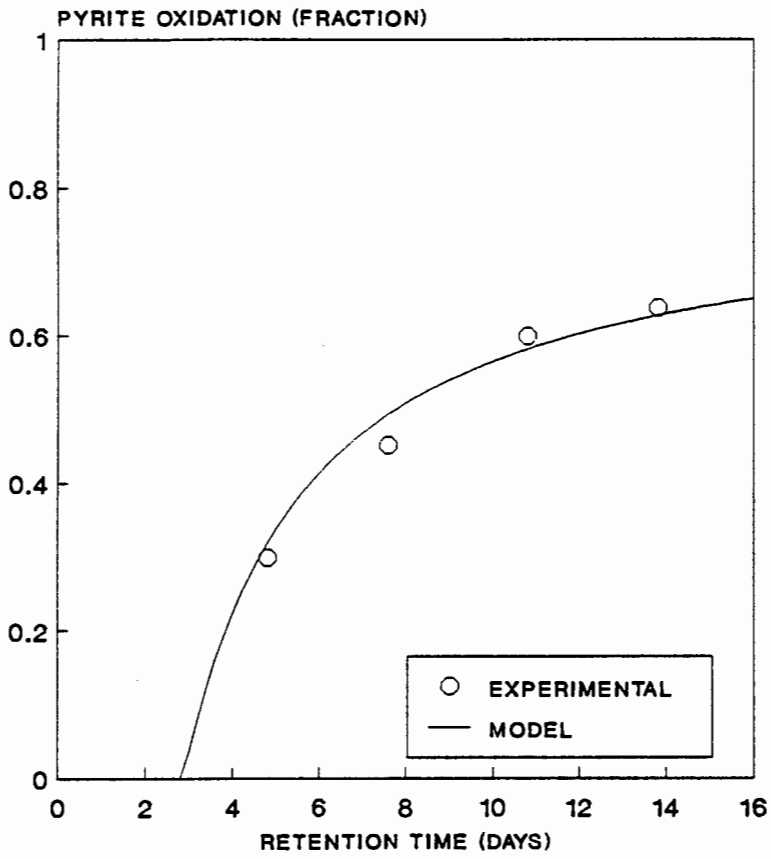

Figure 6.26 Continuous reactor results prediction by the logistic model for the -38um size fraction.

It is clear from these graphical representations that the logistic model correlates accurately with the experimental data obtained for the single stage continuously operated reactor. Similar to the results obtained for the batch reactor study, the results indicate that the model parameter F_m is related inversely to the particle size. An increase for F_m was observed for a decrease in the particle size. The rate parameter, which is equal to the inverse of the washout retention time, was observed to increase with an increased surface area concentration in the feed pulp. This would suggest that a direct relationship exists between the rate of pyrite oxidation and the surface area concentration.

Since the logistic model description is limited to three parameters for batch oxidation of pyrite, and only two parameters for continuous reactor description, it presents a powerful tool which can be implemented in the scale-up and multiple reactor configuration description, which would especially be useful in the industrial application of bacterial leaching.

6.4. Gold Extraction.

The gold extraction results for the three size fractions, obtained from both the batch and continuous reactor tests, are summarised in Table 6.9. Since the respective size fractions were cyanide leached prior to bacterial oxidation, all the gold present in the feed appears as refractory gold. The respective bacterial leach residue samples taken during the batch tests were insufficient to enable gold analyses of the material before and after cyanidation, therefore, only the bacterial - cyanide leached residue analyses are shown. The SiO_2 concentration in the feed and final residue was therefore used to calculate the gold recovery, assuming the ratio of

the inert SiO_2 to gold was maintained. This assumption was confirmed by the gold analysis of the bacterial leach solutions, which never exceeded a gold concentration of 0.002 g m^{-3}.

The gold extraction as a function of the sulphide oxidation obtained from the batch tests, is illustrated in Figure 6.27. Similarly, the results obtained from the continuous reactor tests are shown in Figure 6.28. Partial sulphide oxidation of the sterile control was observed, which resulted in increased gold extraction. However, this increased gold extraction corresponds with the overall gold extraction to sulphide oxidation relationship observed for this sulphide concentrate. Similar gold extraction to sulphide oxidation profiles were observed for both batch and continuous reactor tests. The fraction gold extraction to fraction sulphide oxidation relationship is non-linear for all the size fractions and appears to be independent of the particle size distribution over the size range examined. However, the initial gold analyses, and thus the refractory gold content, does appear to be dependent on the particle size distribution. A gold analysis of 2.39 g t^{-1} was observed for the +53 -75 μm size fraction, which decreased to 1.20 g t^{-1} for the -38 μm size fraction. This would suggest that any decrease in the particle size distribution would result in additional gold extraction. Similarly, pore formation would also lead to additional gold extraction. However, it would be extremely difficult to separate the contribution of these two factors towards additional gold extraction. Thus, only the gross gold extraction will be discussed here.

The non-linear gold extraction to sulphide oxidation relationship observed confirms the data obtained by Drossou (1986). The enhanced fractional gold extraction above sulphide oxidation suggests that the gold does not appear in

solid solution in the pyrite structure. Microprobe analysis of the pyrite particles did not reveal particulate gold, but did show a random occurrence of the the gold. This suggests that preferential oxidation of the sulphide mineral may occur in the gold rich areas, resulting in enhanced gold extraction.

Similar to the findings of Drossou (1986), a linear relationship was observed for the the fraction arsenic leached and the fraction gold extraction. These results are illustrated in Figure 6.29 which shows the data obtained from both the batch and continuous reactor test results.

Microprobe analysis of the pyrite concentrate showed that some of the arsenic occurred in solid solution and some occurred as arsenopyrite. However, it was not possible to determine a direct correlation between the gold and the arsenic and/or arsenopyrite occurrence. In the absence of any direct observation, the gold extraction to fraction arsenic leached relationship suggests that the gold probably is associated with the arsenopyrite or the arsenic phase in the pyrite. It has been shown in the literature that arsenopyrite leaches at a more rapid rate than pyrite (Pinches, 1972). Even though the arsenic phase in solid solution in the pyrite is less refractory than the non-arsenic phase (Southwood, 1985), this phase would not always be readily available at a particle surface for oxidation to occur. It would therefore appear that the included gold is more likely to be associated with the arsenopyrite, similar to the Sao Bento concentrate (Haines (1986)). However, it is difficult to compare the mineralogy of one concentrate with another because of the varying conditions under which these minerals are formed thus dictating different characteristics. The gold mineralogy of sulphide minerals should be evaluated on an individual basis.

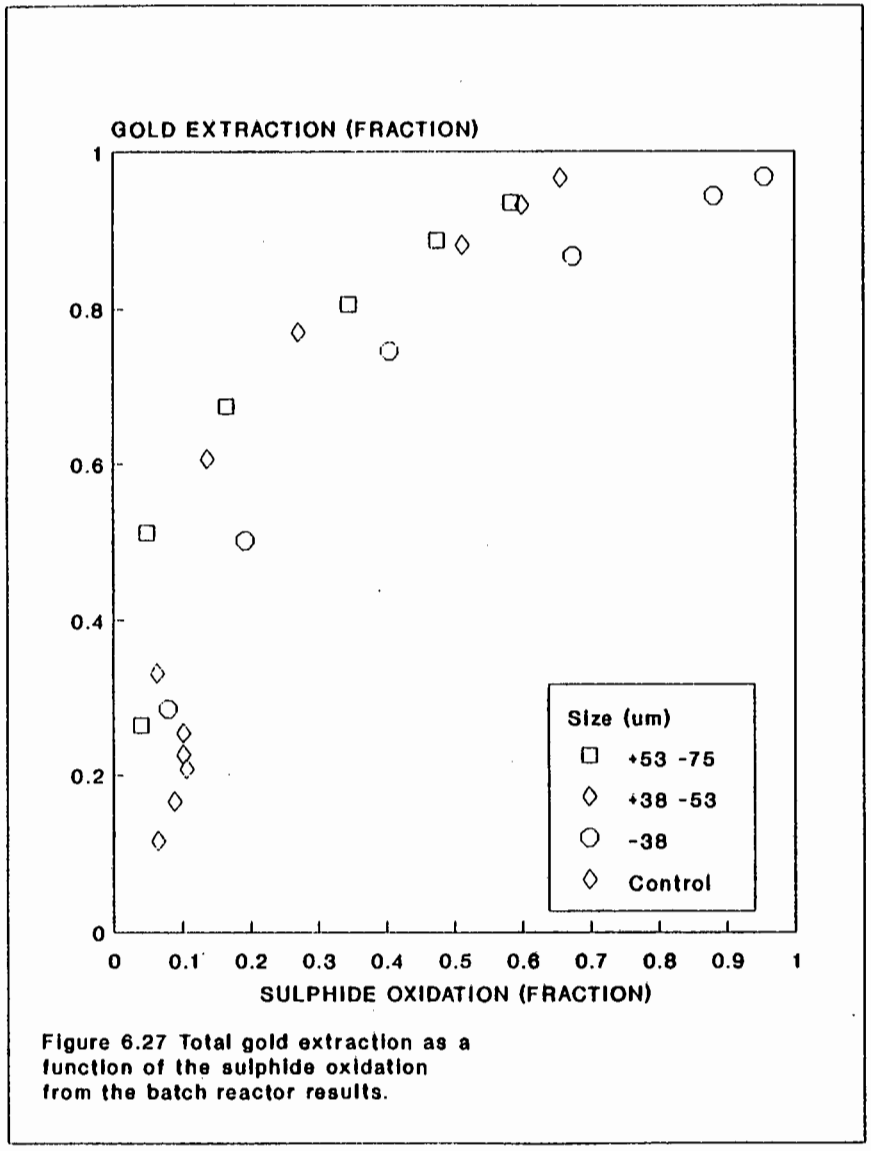

Figure 6.27 Total gold extraction as a function of the sulphide oxidation from the batch reactor results.

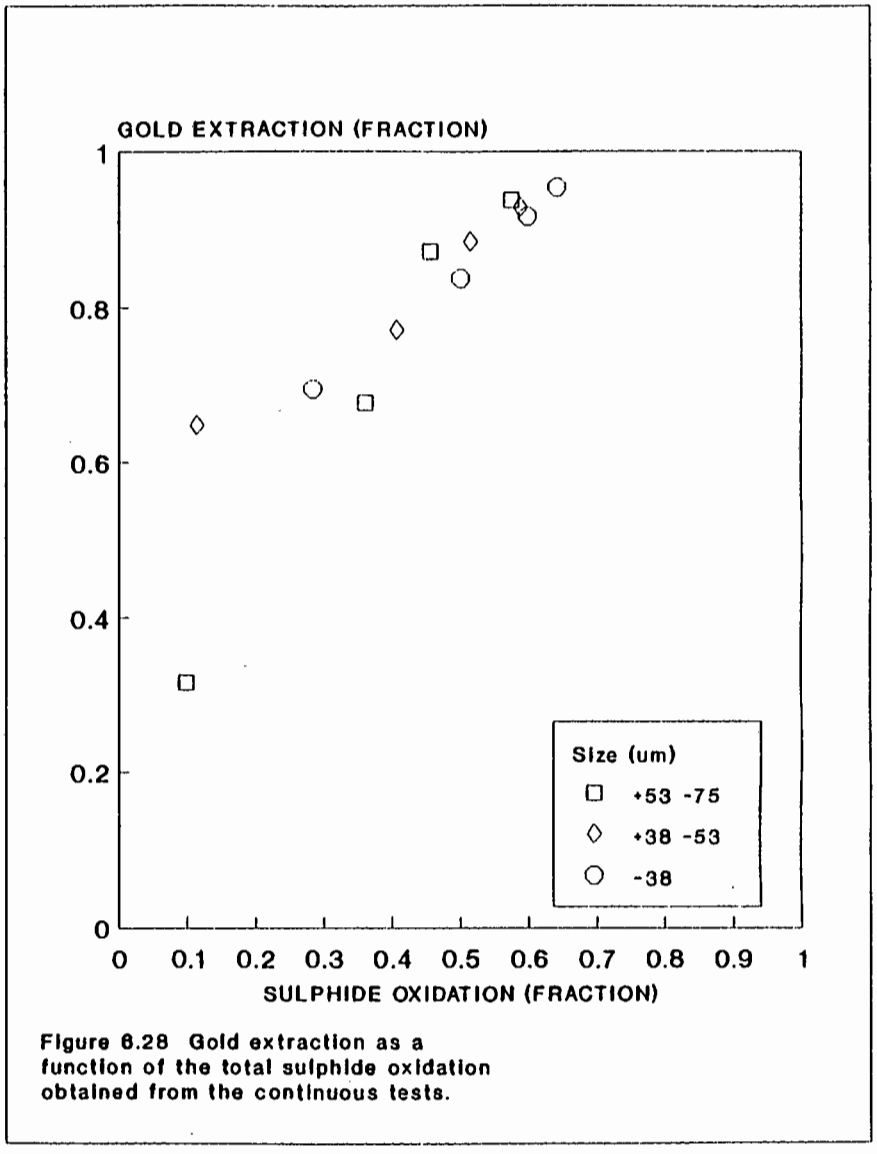

Figure 6.28 Gold extraction as a function of the total sulphide oxidation obtained from the continuous tests.

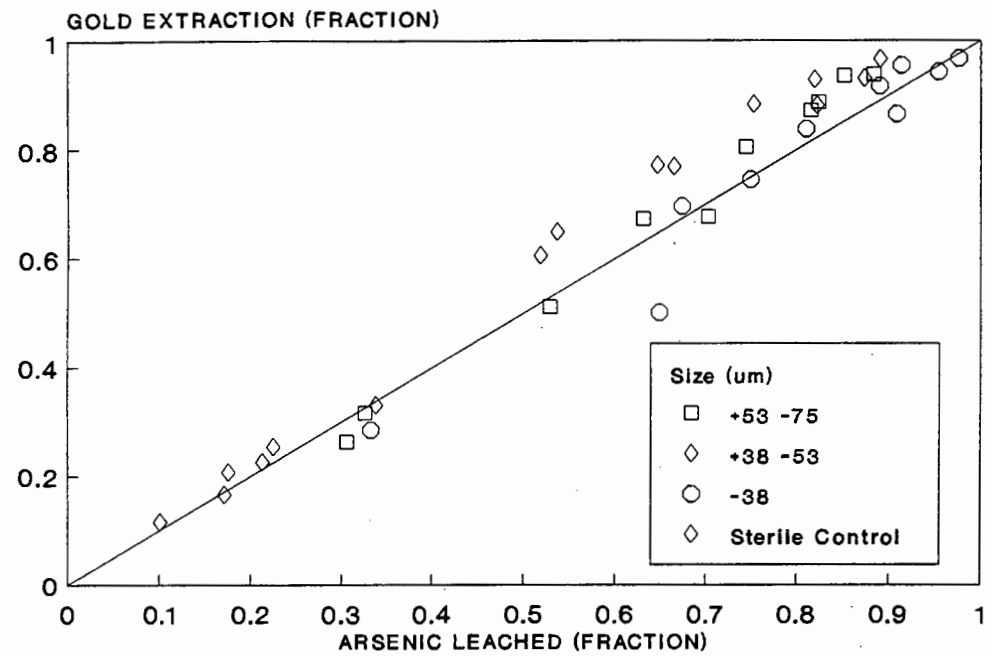

Figure 6.29 Gold extraction as a function of total arsenic leached for both batch and continuous test results.

CHAPTER 7

CONCLUSIONS AND RECOMMENDATIONS

7.1. Conclusions.

The main objectives of the study as outlined in Chapter 1, were:

- to investigate the bacterial oxidation kinetics of a pyrite concentrate in batch and continuous processes

- testing the mechanistic based shrinking particle and propagating pore models against the time course data obtained for the bacterial oxidation of the pyrite concentrate

- testing the empirical logistic growth model against the time course data obtained for the three narrow size fractions.

- to establish the relationship between gold extraction and total sulphide oxidation as well as the fraction arsenic leached.

The observations made in this study, and the conclusions drawn from the results can be summarised as follows:

1. In batch bacterial leaching of the sulphide concentrate, the maximum rate of pyrite oxidation was found to be approximately constant for a constant initial surface area

concentration, irrespective of initial particle size or solids concentration, suggesting that constant global surface area oxidation rate may be applied.

2. The continuous reactor test results indicated that the total pyrite oxidation rate increased proportionally with an increase in the surface area concentration of the feed pulp. In addition, the oxidation rates observed in the continuous reactor tests, substantially exceeded the performance of the batch reactors, for similar initial surface concentrations in the feed.

3. The reduction in particle size distribution observed during leaching was inadequate to confirm a shrinking particle mechanism. However, results indicated that this mechanism cannot be completely discounted.

4. Scanning Electron Microscopic observations confirmed the pore formations observed by Drossou (1986). However, reflective light microscopy observations revealed that pores do not always propagate in a straight line. In addition, branching of pores was observed. It appears that not all pores are initiated at the same time, or alternatively, do not propagate at an equal rate.

5. Both the B.E.T. and geometric methods of predicting the oxidation surface area appear to to be inadequate. The geometric method is unable to accommodate additional surface area provided by particle etching and the internal surfaces of micro fissures present. On the other hand, the B.E.T. method provides an overestimate of the surface area available for leaching, since it includes both internal (micro pores and cracks that may not necessarily provide sites where leaching could occur) as well as external surface areas.

6. The extent (fraction) of pyrite oxidation was found to be dependent on the particle size distribution of the concentrate (at least for the limitations of this study). This along with the pore formation observations, suggests that a constant pore density per unit surface area will be initiated, irrespective of the particle size. At a constant pore diameter and pore density, the fraction of the particle leached will vary inversely with the particle size.

7. Of the mechanistic based models fitted to the experimental batch data, the propagating pore model proved to simulate the results better than the shrinking particle model. However, the empirical logistic model, based on bacterial growth description, proved to give the best correlation with the experimental batch results.

8. Of the two mechanistic models derived to describe a single stage continuous reactor, only the shrinking particle model was fitted to the experimental results. This model did not correlate well with the experimental data.

9. The derivation of the logistic model to describe a single stage continuous reactor correlated well with the experimental data.

10. The relationship between gold extraction and total sulphide oxidation was observed to be non-linear and independent of particle size. However, the refractory gold content of the concentrate was observed to be directly dependent on the particle size.

11. A directly proportional relationship was observed to exist between the gold extraction and the fraction arsenic leached. Even though no direct observation of gold occurring with arsenic and/or arsenopyrite was made, it is suspected that the gold occurred with arsenopyrite.

7.2. Recommendations.

The following recommendations for future research work can be made:

1. If a mechanistic approach is to be pursued, it is recommended that perhaps a combination of the shrinking particle and propagating pore mechanisms be used to provide a hybrid model, because even though considerable evidence in favour of the propagating pore mechanism has been presented, the shrinking particle mechanism could not be totally discounted. In addition, it is believed that a growth factor related to bacterial reproduction, should be incorporated.

2. The logistic model correlated the best with the experimental data of both the batch and continuous reactor studies. In addition, this model consists of a single mathematical relationship, which can easily be manipulated to describe different continuous reactor configurations. Even though this model is empirical in nature, it is strongly recommended that a complete study of this model in the application of bacterial leaching be undertaken.

3. Since the study showed that the geometrical and B.E.T. methods of predicting the surface area available for oxidation were not completely accurate, it is suggested that an alternative method for obtaining this parameter should be investigated.

4. It is also recommended that the leach kinetics of pyrite concentrates from different origins be investigated and compared, to establish whether or not a universal leach parameter can be applied.

REFERENCES.

ATKINS, A.S. (1978), Studies on the Oxidation of Sulphide Minerals (Pyrite) in the Presence of Bacteria. In L.E. MURR, A.E. TORMA and J.A. BRIERLEY (Eds) Metallurgical Applications of Bacterial Leaching and Related Microbiological Phenomena. Academic Press, New York, 403-426.

AMELINCKX, S. (1964), The Direct Observations of Dislocations. In F. SEITZ and D. TURNBULL (Eds), Solid State Physics, 6, Academic Press.

BENNETT, J.C. and H. TRIBUTSCH (1978), Bacterial Leaching Patterns on Pyrite Crystal Surfaces. *J. Bacteriol.*, 134, (1), 310-317.

BERRY, V.K. and L.E. MURR (1978), Direct Observations of Bacteria and Quantitive Studies of their Catalytic Role in the Leaching of Low-Grade, Copper-Bearing Waste. In L.E. MURR, A.E. TORMA and J.A. BRIERLEY (Eds), Metallurgical Applications of Bacterial Leaching and Related Microbiological Phenomena. Academic Press, New York, 103-135.

BLANCARTE-ZURITA, M.A., R.M.R. BRANION and R.W. LAWRENCE (1985), Application of a Shrinking Particle Model to the Kinetics of Microbiological Leaching. Paper presented at the 5th International Symposiuum on Biohydrometallurgy, Vancouver (August 1985).

BOYLE, R.W. (1979), the Geochemistry of Gold and its Deposits. *Geol. Surv. Can. Bull.*, 280, 584.

BRIERLEY, C.L. (1977), Thermophilic Microorganisms in

Extraction of Metals from Ores. *Dev. Ind. Microbiol.*, 18, 273.

BRIERLEY, C.L. (1978), Bacterial Leaching. *CRC Crit. Rev. Microbiol.*, 6, (3), 207-262.

BRIERLEY, C.L. (1982), Microbiological Mining. *Sci. Am.*, 247, 42-51.

BRUYNESTEYN, A. (1984), Bioleaching of Refractory Gold-Silver Ores and Concentrates. Paper presented at the 14th Annual CIM Hydrometallurgical Meeting, Ontario (October 1984).

BRUYNESTEYN, A. and D.W. DUNCAN (1971), Microbiological Leaching of Sulphide Concentrates. *Can. Metall. Q.*, 10, 57.

BRUYNESTEYN, A. and D.W. DUNCAN (1974), Effect of Particle Size on the Microbiological Leaching of Chalcopyrite Bearing Ore. In F.F. APLAN, W.A. McKINNEY and A.D. PERNICHELE (Eds), Solution Mining Symposium 1974. The American Institute of Mining, Metallurgical and Petroleum Engineers, New York, 324-337.

BRYNER, L.C. and R. ANDERSON (1957), Microorganisms in Leaching Sulphide Minerals. *Ind. Eng. Chemistry*, 49, (10), 1721-1724.

CHANG, Y.C. and A.S. MYERSON (1982), Growth Models of the Continuous Bacterial Leaching of Iron Pyrite by *Thiobacillus ferrooxidans*. *Biotechnol. Bioeng.*, 24, 889-902.

CHANT, K. (1975), Gold Recovery from Refractoty Arsenopyrite by Roasting, Bacterial Leaching and Sodium Carbonate Pressure Leaching. Report to Charter Consolidated Limited, (July 1975).

COLMER, A.R. and M.E. HINKLE (1947), The Role of Micro-organisms in Acid Mine Drainage: a Preliminary Report. *Science*, 106, 253-256.

CORRANS, I.J. (1974), Kinetic and Mechanistic Studies on the Biological and Chemical Leaching of Nickel from Sulphide Ores. Ph.D Thesis, University of Natal, South Africa.

CORRANS, I.J., B. HARRIS and B.J. RALPH (1972), Bacterial Leaching: an Introduction to its Application and Theory and a Study on its Mechanism of Operation. *J. S. Afr. Inst. Min. Metall., 72,* 221-230.

DE NOOY, D. (1987), Personal communication.

DISPIRITO, A.A. and O.H. TUOVINEN (1982), Kinetics of Uranous Ion and Ferrous Iron Oxidation by *Thiobacillus ferrooxidans. Arch. Microbiol.* 133, 33-37.

DROSSOU, M (1986), The Kinetics of the Bioleaching of a Refractory Gold Bearing Pyrite Concentrate, M.Sc. Thesis, University of Cape Town.

DUGAN, P.R. and W.A. APEL (1978), Microbiological Desulphurisation of Coal. In L.E. MURR, A.E. TORMA and J.A. BRIERLEY (Eds), Metallurgical Applications of Bacterial Leaching and Related Microbiological Phenomena. Academic Press, New York, 223-250.

DUNCAN, D.W. and A.D. DRUMMOND (1973), Microbiological Leaching of Porphyry Copper Type Mineralization: Post-Leaching Observations. *Can. J. Earth Sci.*, 10, 476-484.

DUNCAN, D.W., J. LANDESMAN and C.C. WALDEN (1967), Role of *Thiobacillus ferrooxidans* in the Oxidation of Sulphide

Minerals. *Can. J. Microbiol.*, 13, 397-403.

DUNCAN, D.W., C.C. WALDEN and P.C. TRUSSELL (1966), Biological Leaching of Mill Products. *Can. Min. Metall. Bull.* , 59, 1075-1079.

DUTRIZAC, J.E. (1974), Ferric Ion as a Leaching Medium. *Miner. Sci. Eng.*, 6, 69-100.

EHRLICH, H.L. (1963), Bacterial Action on Orpiment. *Econ. Geol.*, 58, 991-994.

EHRLICH, H.L. and S.I. FOX (1967), Environmental Effects on Bacterial Copper Extraction from Low-Grade Copper Sulphide Ores. *Biotechnol. Bioeng.*, 9, 471-485.

ERICKSON, L.E., L.T. FAN, P.S. SHAH and M.S.K. CHEN (1970), Growth Models of Cultures with two Liquid Phases: 4. Cell Adsorption, Drop Size Distribution and Batch Growth. *Biotechnol.* and *Bioeng.*, 12, 713-746.

GORMELLY, L.S. (1973), Continuous Microbiological Leaching of a Zinc Sulphide Concentrate. Ph.D Thesis, University of British Columbia, Vancouver.

GORMELLY, L.S. and D.W. DUNCAN (1974), Estimation of *Theobacillus ferrooxidans* Concentrations. *Can. J. Microbiol.*, 20, 1453.

GORMELLY, L.S., D.W. DUNCAN, R.M.R. BRANION and K.L. PINDER (1975), Continuous Culture of *Theobacillus ferrooxidans* on a Zinc Sulphide Concentrate. *Biotechnol. Bioeng.*, 17, 31-49.

GROUDEV, S.N. (1979), Mechanism of the Bacterial Oxidation of Pyrite. *MiKrobiolojia.* no.1, 75-87.

GROUDEV, S.N. (1982), Leaching of Nickel from Sulphide Minerals by Pure and Mixed Cultures of Chemolithotrophic Bacteria. *Dokl. Bolg. Akad. Nauk.*, 35, (8), 1113-1116.

GROUDEV, S.N., F.N. GENCHEV and S.S. GAIDARJIEV (1978), Observations on the Microflora in an Industrial Copper Dump Leaching Operation. In L.E. MURR, A.E. TORMA and J.A. BRIERLEY (Eds), Metallurgical Applications of Bacterial Leaching and Related Microbiological Phenomena. Academic Press, New York, 253-274.

GUAY, R., M. SILVER and A.E. TORMA (1976), Microbiological Leaching of a Low-Grade Uranium Ore by *Thiobacillus ferrooxidans. Eur, J. Appl. Microbiol.*, 3, 157-167.

HANSFORD G.S. and M. DROSSOU, (1987), A Propagating Pore Model for the Batch Bioleach Kinetics of Refractory Gold-Bearing Pyrite. In the Proceedings of the International Biohydrometallurgy Symposium, Warwick, Edited by P.R. NORRIS and D.P. KELLY, Science and Technology Letters, 1988.

HARRISON, V.F., W.A. GOW and M.R. HUGHSON (1966), 1. Factors Influencing the Application of Bacterial Leaching to a Canadian Uranium Ore. *J. Met.*, 18, 1189-1194.

HELLE, U. and U.ONKEN (1987), Continuous Bacterial Leaching of a Pyrite Flotation Concentrate by Mixed Cultures. In the Proceedings of the International Biohydrometallurgy Symposium, Warwick, Edited by P.R. NORRIS and D.P. KELLY, Science and Technology Letters, 1988.

HENLEY, K.J. (1975), Gold-Ore Mineralogy and its Relation to Metallurgical Treatment. *Miner. Sci. Eng.*, 7, (4), 289-312.

HERBET, D., R. ELSWORTH and R.C. TELLING (1956), The Continuous Culture of Bacteria: a Theoretical and Experi-

mental study. *J. Gen. Microbiol.*, 14, 601-622.

HUBERTS, R. (1986), M.Sc. Thesis, University of Witwatersrand.

KARAVAIKO, G.I., S.I. KUZNETSOV and A.I. GOLONIZIK (1977), (Eds), The Bacterial Leaching of Metals from Ores. Technicopy Ltd, England.

KELLER, L. and L.E. MURR (1982), Acid-bacterial and Ferric Sulfate Leaching of Pyrite Single Crystals. *Biotech. and Bioeng.*, XXIV, 83-96.

KELLY, D.P., P.R. NORRIS and C.L. BRIERLEY (1979), Microbiological Methods for the Extraction and Recovery of Metals. In A.T. BULL, D.C. ELLWOOD and C. RUTLEDGE (Eds), Microbial Technology: Current State, Future Prospects. 29th Symposium of the Society of General Microbiology, 263-308.

LAWRENCE, R.W. (1974), Bacterial Extraction of Metals from Sulphide Concentrates. Ph.D Thesis, University of Wales, Cardiff.

LAWRENCE, R.W. and A. BRUYNESTEYN (1983), Biological Preoxidation to Enhance Gold and Silver Recovery from Refractory Pyritic Ores and Concentrates. *CIM Bull.*, 76, (857), 107-110.

LAWRENCE, R.W. and J.D. GUNN (1985), Biological Preoxidation of Pyritic Gold Concentrate. Paper presented at the A.I.M.E. Annual Meeting, New York (February 1985).

LE ROUX, N.W., A.A. NORTH and J.C. WILSON (1973), Bacterial oxidation of Pyrite. Paper presented at the 10th International Mineral Processing Congress, London.

LEVENSPIEL, O. (1972), Chemical Reaction Engineering. John Willey and Sons, USA.

LIVESEY-GOLDBLATT, E., P. NORMAN and D.R. LIVESEY-GOLDBLATT (1983), Gold Recovery from Arsenopyrite/Pyrite Ore by Bacterial Leaching and Cyanidation. In G. ROSSI and A.E. TORMA (Eds), Recent Progress in Biohydrometallurgy. Associazone Mineraria Sarda, Italy, 627-641.

LUNDGREN, D.G. and E.E. MALOUF (1983), Microbial Extraction and Concentration of Metals. *Advan. Biotechnol. Processes*, 1, 223-249.

MALOUF, E.E. and J.D. PRATER (1961), Role of Bacteria in the Alteration of Sulphide Minerals. *J. Met.*, 13, 353-356.

MARCHANT, P.B. (1985), Continuous Vat Biooxidation of a Refractory Arsenical Sulphide Concentrate. Paper presented at the 17th Canadian Mineral Processors Conference, Ottawa (January 1985).

McELROY, R.O. and A. BRUYNESTEYN (1978), Continuous Biological Leaching of Chalcopyrite Concentrates: Demonstation and Economic Analysis. In L.E. MURR, A.E. TORMA and J.A. BRIERLEY (Eds), Metallurgical Applications of Bacterial Leaching and Related Microbiological Phenomena. Academic Press, New York, 441-462.

McGORAN, C.J.M., D.W. DUNCAN and C.C. WALDEN (1969), Growth of *Thibaccillus ferrooxidans* on Various Substrates. *Can. J. Microbiol.*, 15, 135-138.

MIRONOV, A.G., S.M. ZHMODIK and E.A. MAKSIMOVA (1981), An Experimental Investigation of the Sorption of Gold by Pyrites with Different Thermoelectric Properties. *Geochem. Int.*, 18, (2), 153-160.

MONOD, J. (1949), The Growth of Bacterial Cultures. *Ann. Rev. Microbiol.*, 3, 371-394.

MURR, L.E. and V.K. BERRY (1976), Direct Observations of Selective Attachment of Bacteria on Low-Grade Sulphide Ores and Other Mineral Surfaces. *Hydrometall.*, 2, 11-24.

MYERSON, A.S. and P.C. KLINE (1984), Continuous Bacterial Coal Desulphurisation employing *Thiobacillus ferrooxidans*. *Biotechnol. Bioeng.*, 26, 92-99.

NELDER, J.A. and R. MEAD (1965), A Simplex Method for Function Minimisation. *Comput. J.*, 5, 308-313.

NORRIS P.R. and L. PARROTT (1985), High Temperature, Mineral Concentrate Dissolution with *Sulpholobus*. Paper presented at the 5th International Symposium on Biohydrometallurgy, Vancouver (August 1985)

PENMAN, D.W. (1985), Metallurgical Aspects of the Treatment of Refractory Ores from Barberton. Paper presented at the 5th International Symposium on Biohydrometallurgy, Vancouver (August 1985).

PINCHES, A. (1972), The Role of Microorganisims for the Recovery of Metals from Mineral Materials. Ph.D Thesis, University of Wales, Cardiff.

PINCHES, A., F.O. AL-JAID and D.J.A. WILLIAMS (1976), Leaching of Chalcopyrite Concentrates with *Thiobacillus ferrooxidans* in Batch Culture. *Hydrometall.*, 2, 87-103.

PINCHES, A., J.T. CHAPMAN, W.A.M. TE RIELE and M. VAN STADEN, (1987), The performance of bacterial Leach Reactors for the Pre-oxidation of Refractory Gold-Bearing Sulphide

Concentrates. In the Proceedings of the International Biohydrometallurgy Symposium, Warwick, Edited by P.R. NORRIS and D.P. KELLY, Science and Technology Letters, 1988.

POLKIN, S.I., G.I. KARAVAIKO, Z.A. TAUZHNYANSKAYA and V.V. PANIN (1970), Bacterial Selective Extraction of Arsenic and Copper from Oxidised Sulphide Tin Concentrates (Engl. transl.). 9th International Mineral Processing Congress, Prague, 347.

RANGACHARI, P.N., V.S. KRISHNAMACHAR, S.G.PATIL, M.N. SAINANI and H. BALAKRISHNAN (1978), Bacterial Leaching of Copper Sulphide Ores. In L.E. MURR, A.E. TORMA and J.A. BRIERLEY (Eds), Metallurgical Applications of Bacterial Leaching and Related Microbiological Phenomena. Academic Press, New York, 427-439.

RAZZELL, W.E. and P.C. TRUSSELL (1963), Microbiological Leaching of Metallic Sulphides. *Appl. Microbiol.*, 11, 105-110.

RENNER, C.W., M.T. ERRINGTON and F.D. POOLEY (1984), Economics of Bacterial Leaching. Paper presented at the 23rd Annual Conference of Metallurgists, Quebec (August 1984).

SAKAGUCHI, H., A.E. TORMA and M. SILVER (1976), Microbiological Oxidation of Synthetic Chalcocite and Covellite by *Thiobacillus ferrooxidans*. *Appl. Environ. Microbiol.*, 31, 7.

SANMMUGASUNDERAM, V. (1981), Kinetic Studies on the Biological Leaching of a Zinc Sulphide Concentrate in two Stages Continuous Stirred Tank Reactors. Ph.D Thesis, University of British Columbia, Vancouver.

SANMMUGASUNDERAM, V., R.M.R. BRANION and D.W. DUNCAN (1985),

A Growth Model for the Continuous Microbiological Leaching of a Zinc Sulphide Concentrate by *Thiobacillus ferrooxidans*. Paper presented at the 5tth International Symposium on Biohydrometallurgy, Vancouver (August 1985).

SCHAEFFER, W.I., P.E. HOLBERT and W.W. UMBREIT (1963), Attachment of *Thiobacillus thiooxidans* to Sulphur Crystals. *J. Bacteriol.*, 85, 137-140.

SCHARTZ, G.M. (1944), The Host Minerals of Native Gold. *Econ. Geol.*, 39, 371-411.

SILVERMAN, M.P. (1967), Mechanism of Bacterial Pyrite Oxidation. *J. Bacteriol.*, 94, (4), 1046-1051.

SILVERMAN, M.P. and H.L. EHRLICH (1964), Microbial Formation and Degradation of Minerals. *Advan. Appl. Microbiol.*, 6, 153-206.

SILVERMAN, M.P. and D.G. LUNDGREN (1959), Studies on the Chemoautotrophic Iron Bacterium *Ferrobacillus ferrooxidans*, 1. An improved Medium and a Harvesting Procedure for Securing High Cell Yields. *J. Bacteriol.*, 77, 642.

SILVERMAN, M.P., M.H. ROGOFF and I. VENDER (1961), Bacterial Oxidation of Pyrite Materials in Coal. *Appl. Micobiol.* 9, 491-496.

SOUTHWOOD, M.J. (1985), The Mode of Occurrence of Gold in Pyrite and Arsenopyrite and its Implications for the Release of Gold during Bacterial Leaching. Technical Memorandum, no. 13255, MINTEK, Randburg, South Africa.

SOUTHWOOD, M.J. (1986), Personal communication.

SOUTHWOOD, M.J. and A.J. SOUTHWOOD (1985), Mineralogical

Observations on the Bacterial Leaching of Auriferous Pyrite: A New Mathematical Model and Implications for the Release of Gold. Paper presented at the 5th International Symposium on Biohydrometallurgy, Vancouver (August 1985).

TORMA, A.E. (1977), The Role of *Thiobacillus ferrooxidans* in Hydrometallurgical Processes. In T.K. GHOSE, A. FIECHTER and N.BLAKEBROUGH (Eds), Advances in Biochemical Engineering. New substrates. Springer-Verlag, New York, 6, 1-37.

TORMA, A.E. (1978), Complex Lead Sulphide Concentrate Leaching by Microorganisms. In L.E. MURR, A.E. TORMA and J.A. BRIERLEY (Eds), Metallurgical Applications of Bacterial Leaching and Related Microbiological Phenomena. Academic Press, New York, 375-387.

TORMA, A.E. and K.N. SUBRAMANIAN (1974), Selective Bacterial Leaching of a Sulphide Concentrate. *Int. J. Miner. Process.*, 1, 125-134.

TORMA, A.E., C.C. WALDEN and R.M.R. BRANION (1970), Microbiological Leaching of a Zinc Sulphide Concentrate. *Biotechnol. Bioeng.*, 12, 501-517.

TORMA, A.E., C.C. WALDEN, D.W. DUNCAN and R.M.R. BRANION (1972), The effect of Carbon Dioxide and Particle Surface Area on the Microbiological Leaching of a Zinc Sulphide Concentrate. *Biotechnol. Bioeng.*, 14, 777-786.

TUOVINEN, O.H. and D.P. KELLY (1972), Biology of Thiobacillus ferrooxidans in Relation to the Microbiological Leaching of Sulphide Ores. *Z. Allg. Mikrobiol.*, 12, 331-346.

TUOVINEN, O.H., S.I. NIEMELA and H.G. GYLLENBERG (1971), Effect of Mineral Nutrients and Organic Substances on the Development of *Thiobacillus ferrooxidans. Biotechnol. Bio-*

eng., 13, 517-527.

VAN WYK, E. and K. DIXON (1983), The Recovery of Platinum Group Metals and Gold by the Lead-Collection Step of the Fire-Assay Procedure. Report M88, MINTEK, Randburg, South Africa.

VOGEL, A.I. (1961), Quantitative Inorganic Analysis. Longmans, 309.

VOGLER, K.G. and W.W. UMBREIT (1941), The Necessity for Direct Contact in Sulphur Oxidation by *Thiobacillus Thiooxidans*. *Soil. Sci.*, 51, 331-337.

WAKAO, N., M. MISHINA, Y. SAKURAI and H. SHIOTA (1982), Bacterial Pyrite Oxidation. 1. The Effect of Pure and Mixed Cultures of *Thiobacillus ferrooxidans* on Release of Iron. *J. Gen. Appl. Microbiol.*, 28, (4), 331-343.

WAKAO, N., M. MISHINA, Y. SAKURAI and H. SHIOTA (1984), Bacterial Pyrite Oxidation. 3. Adsorption of *Thiodacillus ferrooxidans* Cells on Solid Surfaces and its Effect on Iron Release from Pyrite. *J. Gen. Appl. Microbiol.*, 30, (1), 63-77.

WEISS, R.L. (1973), Attachment of Bacteria to Sulphur in Extreme Environments. *J. Gen. Microbiol.*, 77, 501-507.

APPENDIX A

Unreacted solid residue analyses and mass balance calculations for batch reactor tests.

In the following tables, the complete residue analyses are given for the batch reactor tests performed on the respective size fractions. Included are the calculated fractions leached for the different elements in the sulphide concentrate. In addition, the overall mass balance calculations for each batch test is shown.

Fraction Leached Calculation.

Because a mass loss in the sulphide concentrate is observed during bacterial leaching and only representative samples were taken from the reactor at various intervals, it is necessary to use SiO_2 as an inert tracer to correct for this effect in the calculation of the fraction leached for each component in the concentrate. The following mass balance equations were used :

Let x_i = the initial concentration of SiO_2 in the sulphide concentrate

and

x_r = the SiO_2 concentration in the leached residue

Similarly, let M_i and M_r be the total mass before and at the time the sample was taken, then the total mass at the time of the sample can be calculated as follows :

$$M_i x_i = M_r x_r$$

$$M_r = M_i \frac{x_i}{x_r} \qquad \text{A1}$$

The mass loss can then be calculated :

$$\text{Mass loss} = \frac{M_i - M_r}{M_i}$$

and substituting Equation A1 gives :

$$\text{Mass loss} = 1 - \frac{x_i}{x_r} \qquad \text{A2}$$

The fraction leached of any component (Fe, As, S^{2-}

and Au) can now be calculated in the following manner :

Let y_i and y_r be the fraction of any component A in the initial concentrate and in the sample residue respectively. The fraction leached therefore is given by :

$$\text{Fraction A Leached} = \frac{M_A)_i - M_a)_i}{M_A)_i}$$

$$= \frac{M_i y_i - M_r y_r}{M_i y_i}$$

Substituting M_r from Equation A1 gives :

$$\text{Fraction A Leached} = 1 - \frac{y_r \; x_i}{y_i \; x_r} \qquad \text{A3}$$

Equations A 1-3 were used to calculate the fractions leached as given in the following tables.

Table A1.1 Analyses of unreacted solid residues and calculated fractions leached.
Size fraction : +53 -75um

		BACTERIAL LEACH RESIDUE ANALYSES						FRACTIONS LEACHED			
	Leach Time (days)	SiO2 (%)	Fe (%)	S2- (%)	S(TOTAL) (%)	As (%)	Au cyanide leached (g/t)	S2-	Fe	Au	As
FEED	0	2.78	44.90	48.90	49.10	0.18	2.39	0.000	0.000	0.000	0.000
	3	2.89	44.90	48.80	52.60	0.13	1.83	0.040	0.038	0.263	0.305
	6	2.95	44.80	49.40	51.40	0.09	1.24	0.048	0.060	0.511	0.529
	10	3.35	44.30	49.20	51.60	0.08	0.94	0.165	0.181	0.674	0.631
	15	4.24	42.90	48.90	51.50	0.07	0.71	0.344	0.374	0.805	0.745
	21	5.25	43.00	48.50	50.00	0.06	0.51	0.475	0.493	0.887	0.823
	30	6.26	39.80	45.80	47.40	0.06	0.36	0.584	0.606	0.933	0.852

Table A1.2 Mass balance calculations for iron and SiO2.
Size fraction : +53 -75um

Leach Time (days)	Residue Mass (g)	Mass SiO2 (g)	Mass Fe (g)	Liquid Sample Volume (l)	Total Fe conc. (g/l)	Mass Fe in Liquid (g)	Solids conc. (%)
0	1407.0	39.1	631.7	10.000			
3	115.0	3.3	51.6	0.875	1.85	1.6	13.1
6	101.5	3.0	45.5	0.895	3.90	3.5	11.3
10	85.5	2.9	37.9	0.820	10.10	8.3	10.4
15	70.2	3.0	30.1	0.790	18.60	14.7	8.9
21	83.6	4.4	35.9	1.090	28.80	31.4	7.7
30	330.0	20.7	131.3	5.830	35.10	204.6	5.7
TOTAL		37.2	332.3	10.300		264.1	

Total mass Fe accounted for = (Fe in residues) + (Fe in solution)
= 596.442
Total mass iron in feed = 631.743

Error = 5.6 %

Total mass SiO2 accounted for = 37.20
Total mass SiO2 in feed = 39.11

Error = 4.9 %

Table A2.1 Analyses of unreacted solid residues and calculated fractions leached.
Size Fraction : +38 -53um

	Leach Time (days)	RESIDUE ANALYSES SiO2 (%)	Fe (%)	S2- (%)	S(TOTAL) (%)	As (%)	Au Cyanide Leached (g/t)	FRACTIONS S2- leached	Fe leached	Au leached	As leached
FEED	0	1.75	45.30	50.40	52.20	0.20	1.71	0.000	0.000	0.000	0.000
	6	1.85	43.80	49.90	52.00	0.14	1.21	0.063	0.085	0.331	0.338
	8	2.00	44.00	49.70	52.10	0.11	0.77	0.137	0.150	0.606	0.519
	12	2.35	43.50	49.40	51.90	0.09	0.53	0.270	0.285	0.769	0.665
	17	3.45	43.30	48.45	51.10	0.07	0.40	0.512	0.515	0.881	0.822
	22	4.17	42.10	48.01	50.90	0.06	0.28	0.600	0.610	0.931	0.874
	30	4.80	41.40	47.40	49.80	0.06	0.16	0.657	0.667	0.966	0.891

Table A2.2 Mass balance calculations for iron and SiO2
Size Fraction : +38 -53um

Leach Time (days)	Mass (g)	Mass SiO2 (g)	Mass Fe (g)	Volume Liquid Sample (l)	Total soluble Fe (g/l)	Mass iron (g)	Solids conc. (%)
0	1000	17.5	453.0	10.000			
6	89	1.6	39.0	0.910	4.50	4.1	9.79
8	82	1.6	35.9	0.950	6.90	6.6	8.58
12	79	1.8	34.1	1.220	13.00	15.9	6.43
17	50	1.7	21.8	1.010	20.40	20.6	5.00
22	42	1.7	17.6	1.085	25.90	28.1	3.85
30	185	8.9	76.4	5.120	28.90	148.0	3.60
TOTAL		17.5	224.9	10.295		223.2	

Total mass Fe accounted for = (Fe in residues) + (Fe in solution)
= 448.0
Total mass iron in feed = 453.0

Error = 1.1 %

Total mass SiO2 accounted for = 17.46
Total mass SiO2 in feed = 17.50

Error = 0.2 %

Table A3.1 Analyses of unreacted solid residues and calculated fractions leached.
Size Fraction : -38um.

		RESIDUE ANALYSES						FRACTIONS LEACHED			
	Leach Time (days)	SiO2 (%)	Fe (%)	S2- (%)	S(TOTAL) (%)	As (%)	Au cyanide leached (g/t)	S2-	Fe	Au	As
FEED	0	3.50	44.90	50.20	51.40	0.24	1.20	0.000	0.000	0.000	0.000
	4	3.71	43.00	49.00	50.90	0.17	0.91	0.079	0.097	0.285	0.332
	6	4.15	42.40	48.10	50.00	0.10	0.71	0.192	0.204	0.501	0.649
	10	5.61	42.10	48.00	49.90	0.10	0.49	0.403	0.415	0.745	0.750
	15	8.52	37.20	39.80	42.00	0.05	0.39	0.674	0.660	0.866	0.909
	21	16.90	26.50	28.90	29.70	0.05	0.33	0.881	0.878	0.943	0.954
	30	24.90	18.30	16.20	21.90	0.05	0.28	0.955	0.943	0.967	0.974

Table A3.2 Mass balance calculations for iron and SiO2.
Size Fraction : -38um

Leach Time (days)	Mass (g)	Mass SiO2 (g)	Mass Fe (g)	Volume Liquid Sample (l)	Total Soluble Fe (g/l)	Mass Fe (g)	Solids conc. (%)
0	550.0	19.3	247.0	10.000			
4	48.5	1.8	20.9	0.985	2.60	2.6	4.92
6	41.4	1.7	17.6	0.995	5.10	5.1	4.16
10	39.4	2.2	16.6	1.008	10.60	10.7	3.91
15	27.1	2.3	10.1	1.035	16.10	16.7	2.62
21	18.9	3.2	5.0	1.045	20.20	21.1	1.81
30	33.9	8.4	6.2	5.095	22.50	114.6	0.67
TOTAL		19.7	76.3	10.163		170.7	

Total mass Fe accounted for = (Fe in residues) + (Fe in solution)
= 247.0
Total mass iron in feed = 247.0

Error = 0.0 %

Total mass SiO2 accounted for = 19.7
Total mass SiO2 in feed = 19.3

Error = -2.2 %

Table A4.1 Analyses of the unreacted solid residue and and calculated fractions leached.
Size fraction : +38 -53um STERILE CONTROL

		RESIDUE ANALYSES						FRACTIONS LEACHED			
	Leach Time (days)	SiO2 (%)	Fe (%)	S2- (%)	S(TOTAL) (%)	As (%)	Au cyanide leached (g/t)	S2-	Fe	Au	As
FEED	0	1.75	45.30	50.40	52.20	0.20	1.71	0.000	0.000	0.000	0.000
	6	1.85	44.40	49.85	52.20	0.19	1.60	0.064	0.073	0.115	0.101
	8	1.90	44.50	49.90	52.20	0.18	1.55	0.088	0.095	0.165	0.171
	12	1.91	44.60	49.20	52.30	0.18	1.48	0.106	0.098	0.207	0.175
	17	1.89	44.10	48.90	51.10	0.17	1.43	0.102	0.099	0.226	0.213
	30	1.92	44.00	49.70	52.60	0.17	1.40	0.101	0.115	0.254	0.225

Table A4.2 Mass balance calculations for iron and SiO2.
Size Fraction : +38 -53um STERILE CONTROL

Leach Time (days)	Mass (g)	Mass SiO2 (g)	Mass Fe (g)	Volume Liquid Sample (l)	Total Soluble Fe (g/l)	Mass Fe (g)	Solids conc. (%)
0	1000.0	17.5	453.0	10.000			
6	91.4	1.7	40.6	0.900	0.28	0.3	10.16
8	98.1	1.9	43.7	1.010	0.42	0.4	9.71
12	110.5	2.1	49.3	1.200	0.50	0.6	9.21
17	102.5	1.9	45.2	1.080	0.85	0.9	9.49
30	540.0	10.4	237.6	5.800	1.30	7.5	9.31
TOTAL		18.0	416.3	9.990		9.7	

Total mass Fe accounted for = (Fe in residues) + (Fe in solution)
= 426.056
Total mass iron in feed = 453.000

Error = 5.9 %

Total mass SiO2 accounted for = 18.0
Total mass SiO2 in feed = 17.5

Error = -2.7 %

APPENDIX B

Unreacted solid residue analyses and mass balance calculations for the continuous reactor tests.

In the following table the complete residue and solution analyses obtained for the continuous reactor study, are presented. Included are the calculations for the fractions leached. In addition, the mass balance calculations are shown.

The procedure for calculating the fractions leached is similar to taht described in APPENDIX A and will not be repeated here. In addition to calculating the fractions leached using SiO_2 as an inert tracer, a direct comparison of the mass of Sulphide and Iron in the feed and the leached residue was used, to obtain the fraction leached for these two components. Also shown in the following tables, is a back calculated retention time for the solids in the reactor, using the rate at which SiO_2 appeared in the leach product and comparing it to the rate at which it was fed to the reactor.

Table B1.1 Analyses for the unreacted solid residues.
Size Fraction : +53 -75um

	RESIDUE ANALYSES					Au			
Ret. Time (days)	SiO2 (%)	Fe (%)	S2- (%)	S(TOTAL (%)	As (%)	Cyanide leached (g/t)	Residue mass (g)	Sample Vol. (l)	Total Soluble Fe (g/l)
FEED	3.24	45.10	48.20	50.40	0.18	2.39	228.0	2.280	-
4.43	3.47	43.60	46.40	49.80	0.13		201.5	2.150	7.10
4.43	3.48	43.60	46.50	48.95	0.15		198.5	1.980	7.20
4.43	3.44	43.60	46.75	49.50	0.12		205.4	1.945	7.10
4.43	3.49	43.70	46.60	49.20	0.12		203.5	1.990	6.90
AVERAGE	3.47	43.63	46.56	49.36	0.13	1.75	202.2	2.016	7.08
FEED	3.24	45.10	50.40	51.50	0.18	2.39	131.9	1.319	-
7.66	4.63	42.40	47.70	49.60	0.08		89.3	1.180	15.80
7.66	4.71	43.30	49.65	50.55	0.08		85.8	0.940	16.00
7.66	4.75	42.70	46.70	51.80	0.07		92.4	1.380	15.90
7.66	4.72	43.40	47.80	51.90	0.08		86.6	1.110	16.20
AVERAGE	4.70	42.95	47.96	50.96	0.08	1.12	88.5	1.153	15.98
FEED	3.24	45.10	50.40	51.40	0.18	2.39	100.6	1.006	-
10.04	5.37	41.20	44.85	48.70	0.05		59.7	0.865	27.70
10.04	5.39	41.70	44.80	48.90	0.06		57.9	0.780	26.08
10.04	5.40	41.60	46.10	49.20	0.06		59.4	0.710	28.37
10.04	5.38	41.80	46.40	48.70	0.05		58.0	0.770	27.40
AVERAGE	5.39	41.58	45.54	48.88	0.06	0.51	58.8	0.781	27.39
FEED	3.24	45.10	49.90	50.95	0.18	2.39	66.6	0.666	-
15.16	7.02	39.70	46.40	59.60	0.04		31.1	0.570	32.00
15.16	7.05	39.40	46.30	48.50	0.04		33.1	0.490	31.40
15.16	6.98	39.80	45.10	49.10	0.05		32.3	0.570	30.63
15.16	6.98	39.90	45.20	49.80	0.05		34.6	0.550	31.77
AVERAGE	7.01	39.70	45.75	51.75	0.05	0.32	32.8	0.545	31.45

Table B1.2 Fractions leached and mass balance calculations.
Size Fraction : +53 -75um.

	FRACTION IRON LEACHED CALCULATED			SULPHIDE OXIDT CALCULATED		FRACTION		Ret. Calc. From	Solids Conc.	Mass	MASS BALANCE CALC.			TOTAL
Ret. Time (days)	Tracer SiO2	Res Assay	Soltn Assay	Tracer SiO2	Res. Assay	As Leached	Au Extrn	Tracer SiO2	(w/v) (%)	Loss (%)	Mass SiO2 (g/day)	Mass Fe(Res) (g/day)	Mass Fe(sol) (g/day)	Mass Fe Acc. (g/day)
	0.000	0.000	0.000	0.000	0.000	0.000			10.0		7.4			102.8
4.43	0.097	0.146	0.146	0.101	0.149	0.326		4.68	9.4	11.6	7.0	87.8	15.3	103.1
	0.100	0.158	0.136	0.102	0.160	0.224		4.74	10.0	12.9	6.9	86.5	14.3	100.8
	0.089	0.129	0.131	0.086	0.126	0.372		4.63	10.6	9.9	7.1	89.6	13.8	103.4
	0.100	0.135	0.131	0.102	0.137	0.381		4.61	10.2	10.8	7.1	88.9	13.7	102.6
AVERAGE	0.118	0.142	0.136	0.098	0.143	0.326	0.316	4.66	10.0	11.3	7.0			102.5
	-	-	-	-	-				10.0		4.27			59.5
7.66	0.342	0.363	0.309	0.338	0.359	0.689		7.91	7.6	32.3	4.1	37.9	18.6	56.5
	0.340	0.375	0.248	0.322	0.359	0.694		8.09	9.1	34.9	4.0	37.2	15.0	52.2
	0.354	0.337	0.364	0.368	0.351	0.735		7.46	6.7	30.0	4.4	39.4	21.9	61.4
	0.339	0.368	0.298	0.349	0.377	0.695		8.00	7.8	34.3	4.1	37.6	18.0	55.6
AVERAGE	0.344	0.361	0.305	0.344	0.361	0.703	0.677	7.87	7.8	32.9	4.2			56.4
	-	-	-	-	-				10.0		3.26			45.4
10.04	0.449	0.458	0.521	0.463	0.472	0.832		10.21	6.9	40.6	3.2	24.6	24.0	48.6
	0.444	0.468	0.442	0.466	0.488	0.800		10.48	7.4	42.4	3.1	24.1	20.3	44.5
	0.447	0.455	0.436	0.451	0.460	0.800		10.20	8.4	40.9	3.2	24.7	20.1	44.9
	0.442	0.466	0.458	0.446	0.469	0.833		10.49	7.5	42.3	3.1	24.2	21.1	45.3
AVERAGE	0.445	0.462	0.464	0.456	0.472	0.816	0.872	10.34	7.6	41.6	3.2			45.8
FEED	-	-	-	-	-						2.16	30.0		
15.16	0.594	0.589	0.600	0.571	0.566	0.897		14.99	5.5	53.3	2.2	12.3	18.2	30.6
	0.599	0.566	0.505	0.574	0.539	0.898		14.02	6.8	50.3	2.3	13.0	15.4	28.4
	0.590	0.573	0.574	0.580	0.562	0.871		14.54	5.7	51.6	2.3	12.8	17.5	30.3
	0.589	0.541	0.574	0.580	0.530	0.871		13.55	6.3	48.1	2.4	13.8	17.5	31.3
AVERAGE	0.593	0.567	0.563	0.576	0.549	0.884	0.938	14.27	6.0	50.8	2.3			30.1

Table 82.1 Analyses for the unreacted solid residues.
Size Fraction : +38 -53um

	RESIDUE ANALYSES					Au			Total
Ret. Time (days)	SiO2 (%)	Fe (%)	S2- (%)	S(TOTAL (%)	As (%)	Cyanide leached (g/t)	Residue mass (g)	Sample Vol. (l)	Soluble Fe (g/l)
FEED	2.74	45.20	50.40	52.00	0.20	1.71	240.5	2.405	-
4.20	3.00	43.20	48.10	50.60	0.10		218.3	2.165	8.20
4.20	2.97	43.30	48.40	50.40	0.11		217.4	2.108	7.65
4.20	2.95	43.10	47.80	49.80	0.08		216.4	2.140	8.10
4.20	2.93	43.00	48.80	50.50	0.11		218.5	2.180	6.80
AVERAGE	2.96	43.15	48.28	50.33	0.10	0.65	217.7	2.148	7.69
FEED	1.75	44.90	50.40	51.80	0.20	1.71	148.1	1.481	-
6.82	2.88	43.60	47.45	50.10	0.08		92.9	1.305	19.41
6.82	2.87	43.80	48.00	50.80	0.08		89.7	1.190	18.30
6.82	2.76	44.00	48.40	51.60	0.07		92.5	1.240	20.30
6.82	2.72	43.90	48.00	51.20	0.06		91.8	1.355	19.10
AVERAGE	2.81	43.83	47.96	50.93	0.07	0.40	91.7	1.273	19.28
FEED	1.60	45.00	50.40	51.40	0.20	1.71	99.7	0.997	-
10.13	3.12	43.50	47.60	49.80	0.06		54.6	0.750	28.90
10.13	3.05	43.00	45.90	50.00	0.05		53.1	0.805	27.75
10.13	3.07	43.30	46.20	50.10	0.05		55.1	0.820	27.20
10.13	2.95	42.80	46.30	50.50	0.06		53.0	0.780	28.30
AVERAGE	3.05	43.15	46.50	50.10	0.06	0.22	53.9	0.789	28.04
FEED	1.51	44.90	50.40	51.20	0.20	1.71	74.6	746.489	-
13.53	3.28	43.50	47.80	50.40	0.05		31.2	0.635	33.50
13.53	3.44	43.40	46.10	50.90	0.04		32.3	0.615	33.10
13.53	3.38	43.20	44.50	50.90	0.04		31.9	0.610	33.70
13.53	3.32	43.50	45.60	50.60	0.04		32.1	0.645	32.80
AVERAGE	3.36	43.40	46.00	50.70	0.04	0.15	31.9	0.626	33.28

Table B2.2 Fractions leached and mass balance calculations.
Size Fraction : +38 -53um

Ret. Time (days)	FRACTION IRON LEACHED CALCULATED Tracer SiO2	Res Assay	Soltn Assay	SULPHIDE OXIDT CALCULATED Tracer SiO2	Res. Assay	FRACTION As Leached	Au Extrn	Ret. Calc. From Tracer SiO2	Solids Conc. (w/v) (%)	Mass Loss (%)	MASS BALANCE CALC. Mass SiO2 (g/day)	Mass Fe(Res) (g/day)	Mass Fe(sol) (g/day)	TOTAL Mass Fe Acc. (g/day)
FEED	-	-	-	-	-				10.0		6.59			108.7
4.20	0.127	0.132	0.160	0.128	0.134	0.543		4.23	10.1	4.3	6.5	94.3	17.8	112.1
	0.116	0.134	0.145	0.114	0.132	0.493		4.29	10.3	4.6	6.5	94.1	16.1	110.3
	0.114	0.142	0.156	0.119	0.147	0.628		4.34	10.1	5.1	6.4	93.3	17.3	110.6
	0.110	0.136	0.134	0.095	0.120	0.486		4.32	10.0	4.2	6.4	94.0	14.8	108.8
AVERAGE	0.148	0.136	0.149	0.114	0.133	0.538	0.648	4.29	10.1	4.5	6.4			110.4
FEED	0.000	0.000	0.000	0.000	0.000				10.0		2.59			66.5
6.82	0.410	0.391	0.375	0.428	0.409	0.619		6.61	7.1	29.5	2.7	40.5	25.3	65.8
	0.405	0.409	0.322	0.419	0.423	0.618		6.87	7.5	32.0	2.6	39.3	21.8	61.1
	0.379	0.388	0.373	0.391	0.401	0.653		6.93	7.5	29.9	2.6	40.7	25.2	65.9
	0.371	0.394	0.384	0.387	0.410	0.698		7.08	6.8	30.4	2.5	40.3	25.9	66.2
AVERAGE	0.391	0.396	0.364	0.406	0.411	0.647	0.772	6.87	7.2	30.4	2.6			64.7
FEED	-	-	-	-	-				10.0		1.60			44.9
10.13	0.504	0.471	0.476	0.516	0.483	0.737		9.49	7.3	45.7	1.7	23.8	21.7	45.4
	0.499	0.491	0.491	0.522	0.515	0.775		9.98	6.6	47.2	1.6	22.8	22.3	45.2
	0.499	0.469	0.490	0.522	0.494	0.777		9.56	6.7	45.3	1.7	23.8	22.3	46.1
	0.484	0.494	0.485	0.502	0.512	0.721		10.33	6.8	47.3	1.6	22.7	22.1	44.8
AVERAGE	0.496	0.481	0.486	0.515	0.501	0.753	0.884	9.84	6.8	46.4	1.6			45.4
FEED	-	-	-	-	-				10.0		1.13	33.5		
13.53	0.554	0.595	0.628	0.563	0.604	0.791		14.90	4.9	53.2	1.0	13.6	21.3	34.8
	0.576	0.582	0.601	0.598	0.604	0.841		13.73	5.3	51.5	1.1	14.0	20.4	34.4
	0.570	0.589	0.607	0.606	0.623	0.838		14.14	5.2	52.1	1.1	13.8	20.6	34.3
	0.559	0.583	0.625	0.588	0.611	0.835		14.31	5.0	51.8	1.1	14.0	21.2	35.1
AVERAGE	0.565	0.587	0.615	0.589	0.610	0.826	0.928	14.27	5.1	52.2	1.1			34.7

Table B3.1 Analyses for the unreacted solid residues.
Size Fraction : -38um

Ret. Time (days)	RESIDUE ANALYSES SiO2 (%)	Fe (%)	S2- (%)	S(TOTAL (%)	As (%)	Au Cyanide leached (g/t)	Residue mass (g)	Sample Vol. (l)	Total Soluble Fe (g/l)
FEED	3.24	44.90	50.40	51.20	0.24	1.20	225.4	2.254	-
4.48	4.35	42.50	47.50	50.10	0.11		160.0	1.990	14.10
4.48	4.41	42.30	49.20	50.50	0.12		179.3	2.120	13.90
4.48	4.30	42.60	46.75	49.00	0.10		168.4	1.975	14.00
4.48	4.30	42.70	49.80	51.10	0.09		160.8	2.040	14.79
AVERAGE	4.34	42.53	48.31	50.18	0.11	0.49	167.1	2.031	14.20
FEED	2.79	45.20	50.65	51.50	0.24	1.20	134.0	1.340	-
7.54	4.95	41.90	45.80	47.10	0.07		81.5	1.140	24.90
7.54	4.99	41.90	45.70	49.00	0.06		79.6	1.180	24.60
7.54	5.02	41.70	44.90	48.40	0.07		78.5	1.135	23.50
7.54	5.00	41.65	44.80	48.50	0.08		79.0	1.200	23.80
AVERAGE	4.99	41.79	45.30	48.25	0.07	0.30	79.7	1.164	24.20
FEED	2.79	45.00	50.64	51.40	0.24	1.20	93.5	0.935	-
10.80	6.11	40.80	44.90	48.80	0.04		40.6	0.775	30.00
10.80	6.10	40.90	47.10	48.30	0.05		41.9	0.805	31.00
10.80	6.20	41.10	45.60	48.50	0.06		42.4	0.780	29.80
10.80	6.15	41.00	46.00	48.80	0.05		40.3	0.790	30.50
AVERAGE	6.14	40.95	45.90	48.60	0.05	0.19	41.3	0.788	30.33
FEED	2.79	44.90	50.50	52.10	1.20	0.24	73.1	0.731	-
13.81	6.88	40.60	45.10	47.10	0.04		30.5	0.580	35.80
13.81	7.13	40.80	46.10	47.95	0.05		29.8	0.530	36.00
13.81	7.04	40.70	45.30	47.80	0.05		29.1	0.510	36.30
13.81	7.06	40.75	44.90	47.35	0.04		27.8	0.560	35.70
AVERAGE	7.03	40.71	45.35	47.55	0.05	0.12	29.3	0.545	35.95

Table B3.2 Fractions leached and mass balance calculations.
Size Fraction : -38um

Ret. Time (days)	FRACTION IRON LEACHED CALCULATED Tracer SiO2	Res Assay	Soltn Assay	SULPHIDE OXIDT CALCULATED Tracer SiO2	Res. Assay	FRACTION As Leached	Au Extrn	Ret. Calc. From Tracer SiO2	Solids Conc. (w/v) (%)	Mass Loss (%)	MASS BALANCE CALC. Mass SiO2 (g/day)	Mass Fe(Res) (g/day)	Mass Fe(sol) (g/day)	TOTAL Mass Fe Acc. (g/day)
FEED	-	-	-	-	-				10.0		7.30	101.2		
4.48	0.295	0.328	0.273	0.298	0.331	0.659		4.70	8.0	29.8	7.0	68.0	28.1	96.0
	0.308	0.251	0.286	0.283	0.224	0.633		4.14	8.5	21.4	7.9	75.8	29.5	105.3
	0.285	0.291	0.268	0.301	0.307	0.686		4.52	8.5	26.2	7.2	71.7	27.7	99.4
	0.283	0.322	0.293	0.255	0.295	0.717		4.73	7.9	29.5	6.9	68.7	30.2	98.8
AVERAGE	0.265	0.298	0.280	0.284	0.289	0.674	0.695	4.52	8.2	26.7	7.3			99.9
FEED	-	-	-	-	-				10.0		3.74	60.5		
7.54	0.478	0.436	0.462	0.490	0.450	0.809		6.98	7.1	38.2	4.0	34.1	28.4	62.5
	0.482	0.449	0.473	0.496	0.464	0.838		7.09	6.7	39.6	4.0	33.4	29.0	62.4
	0.487	0.459	0.434	0.507	0.480	0.812		7.15	6.9	40.5	3.9	32.7	26.7	59.4
	0.486	0.457	0.465	0.506	0.478	0.784		7.13	6.6	40.1	4.0	32.9	28.6	61.5
AVERAGE	0.483	0.450	0.459	0.500	0.468	0.811	0.838	7.09	6.8	39.6	4.0			61.4
FEED	-	-	-	-	-				10.0		2.61	42.1		
10.80	0.586	0.606	0.547	0.595	0.615	0.912		11.36	5.2	59.6	2.5	16.6	23.3	39.8
	0.584	0.593	0.587	0.575	0.583	0.889		11.03	5.2	58.4	2.6	17.1	25.0	42.1
	0.589	0.586	0.546	0.595	0.591	0.869		10.71	5.4	57.8	2.6	17.4	23.2	40.7
	0.587	0.608	0.567	0.588	0.609	0.890		11.38	5.1	60.0	2.5	16.5	24.1	40.6
AVERAGE	0.586	0.598	0.562	0.588	0.600	0.890	0.916	11.12	5.2	58.9	2.5			40.8
FEED	-	-	-	-	-				10.0		2.04	32.8		
13.81	0.633	0.623	0.626	0.638	0.628	0.922		13.43	5.3	54.2	2.1	12.4	20.8	33.1
	0.644	0.630	0.574	0.643	0.628	0.905		13.26	5.6	55.3	2.1	12.2	19.1	31.2
	0.641	0.639	0.557	0.645	0.643	0.904		13.75	5.7	56.3	2.0	11.8	18.5	30.4
	0.641	0.655	0.603	0.649	0.662	0.924		14.36	5.0	58.3	2.0	11.3	20.0	31.3
AVERAGE	0.640	0.637	0.590	0.643	0.640	0.914	0.954	13.70	5.4	56.0	2.1			31.5

APPENDIX C

B.E.T. Specific Surface Area Determinations

Table C1 Specific surface areas for the leach residues of the batch tests obtained with the B.E.T. method.

+53 -75		+38 -53		+38 -53		-38	
Leach Time (days)	area (m2/kg)	Leach Time (days)	Control area (m2/kg)	Leach Time (days)	area (m2/kg)	Leach Time (days)	area (m2/kg)
0	240	0	200	0	200	0	560
4	200	6	160	6	220	4	580
9	520	8	210	8	230	6	620
12	240	12	210	12	310	10	720
16	270	17	200	17	290	15	620
22	250	30	220	30	320	30	650
30	280						

Table C2 Specific surface areas for the leach residues of continuous tests obtained with the B.E.T. method.

+53 -75		+38 -53		-38	
Retention Time (days)	area (m2/kg)	Retention Time (days)	area (m2/kg)	Retention Time (days)	area (m2/kg)
0.00	240	0.00	200	0.00	560
4.43	260	4.20	210	4.48	540
7.66	450	6.82	690	7.54	1150
10.04	390	10.13	220	10.80	710
15.16	1020	13.53	270	13.81	880

APPENDIX D

Batch and Continuous Reactor Parameters : Redox Potentials and Dissolved Oxygen

Table D1. Batch Reactor Redox Potential Profiles (mV).

TIME (days)	SIZE FRACTION +53 -75um	+38 -53um	-38um	CONTROL +38 -53um
0	340	328	340	342
1	358	346	404	336
2	366	362	463	335
3	418	415	483	334
4	476	485	519	337
5	537	530	550	339
6	566	540	553	340
7	562	550	565	351
8	575	567	557	344
9	565	558	562	348
10	557	558	564	351
11	553	569	558	355
12	555	556	555	356
13	540	568	578	350
14	550	570	586	353
15	551	554	585	349
16	544	558	589	357
17	535	566	578	365
18	540	560	588	368
19	541	563	599	371
20	544	565	589	373
21	552	569	580	374
22	559	558	585	368
23	562	548	580	369
24	559	565	591	376
25	562	569	590	378
26	545	558	578	381
27	560	548	581	388
28	563	555	588	389
29	567	560	576	393
30	561	570	591	401

Table D2. Continuous Reator Steady Sate Redox Potentials (mV).

SIZE FRACTION : +53 -75um

Retention Time (Days)	Redox Potential (mV)
4.43	520
7.66	527
10.04	542
15.16	528

SIZE FRACTION : +38 -53um

Retention Time (Days)	Redox Potential (mV)
4.20	524
6.82	544
10.13	549
13.53	540

SIZE FRACTION : -38um

Retention Time (Days)	Redox Potential (mV)
4.48	560
7.54	555
10.80	557
13.81	533

Table D3 Batch Reactor Dissolved Oxygen Levels.
(in parts per million)

TIME (days)	SIZE FRACTION +53 -75um	+38 -53um	-38um	CONTROL +38 -53um
0	6.4	6.4	6.4	6.5
1	6.1	5.8	5.4	6.4
2	5.7	5.5	4.5	6.4
3	5.3	4.8	4.4	6.4
4	5.2	4.9	3.4	6.3
5	5.2	4.3	2.0	6.3
6	4.3	3.4	1.5	6.4
7	3.7	2.8	1.4	6.4
8	3.1	2.3	1.3	6.4
9	2.6	1.5	1.4	6.3
10	1.8	1.5	1.4	6.3
11	1.5	1.4	1.5	6.3
12	1.4	1.6	1.7	6.3
13	1.5	1.4	1.4	6.4
14	1.4	1.4	1.7	6.4
15	1.5	1.5	1.8	6.3
16	1.7	1.5	2.2	6.3
17	1.8	1.8	2.5	6.3
18	2.3	2.4	3.1	6.3
19	2.6	2.5	3.8	6.4
20	2.8	2.9	4.2	6.3
21	3.1	3.5	4.6	6.5
22	3.4	3.7	5.0	6.4
23	4.3	4.4	5.7	6.4
24	4.6	4.8	5.8	6.3
25	5.0	5.2	5.9	6.2
26	5.3	5.7	5.9	6.2
27	5.4	5.6	6.1	6.1
28	5.7	5.8	6.1	6.2
29	5.6	5.9	6.1	6.3
30	5.7	5.7	6.1	6.2

Table D4. Continuous Reator Steady Sate Dissolved Oxygen Levels.

SIZE FRACTION : +53 -75um

Retention Time (Days)	Dissolved Oxygen (ppm)
4.43	1.4
7.66	1.0
10.04	1.0
15.16	1.1

SIZE FRACTION : +38 -53um

Retention Time (Days)	Dissolved Oxygen (ppm)
4.20	1.4
6.82	1.0
10.13	0.9
13.53	0.9

SIZE FRACTION : -38um

Retention Time (Days)	Dissolved Oxygen (ppm)
4.48	0.7
7.54	0.7
10.80	0.8
13.81	0.9

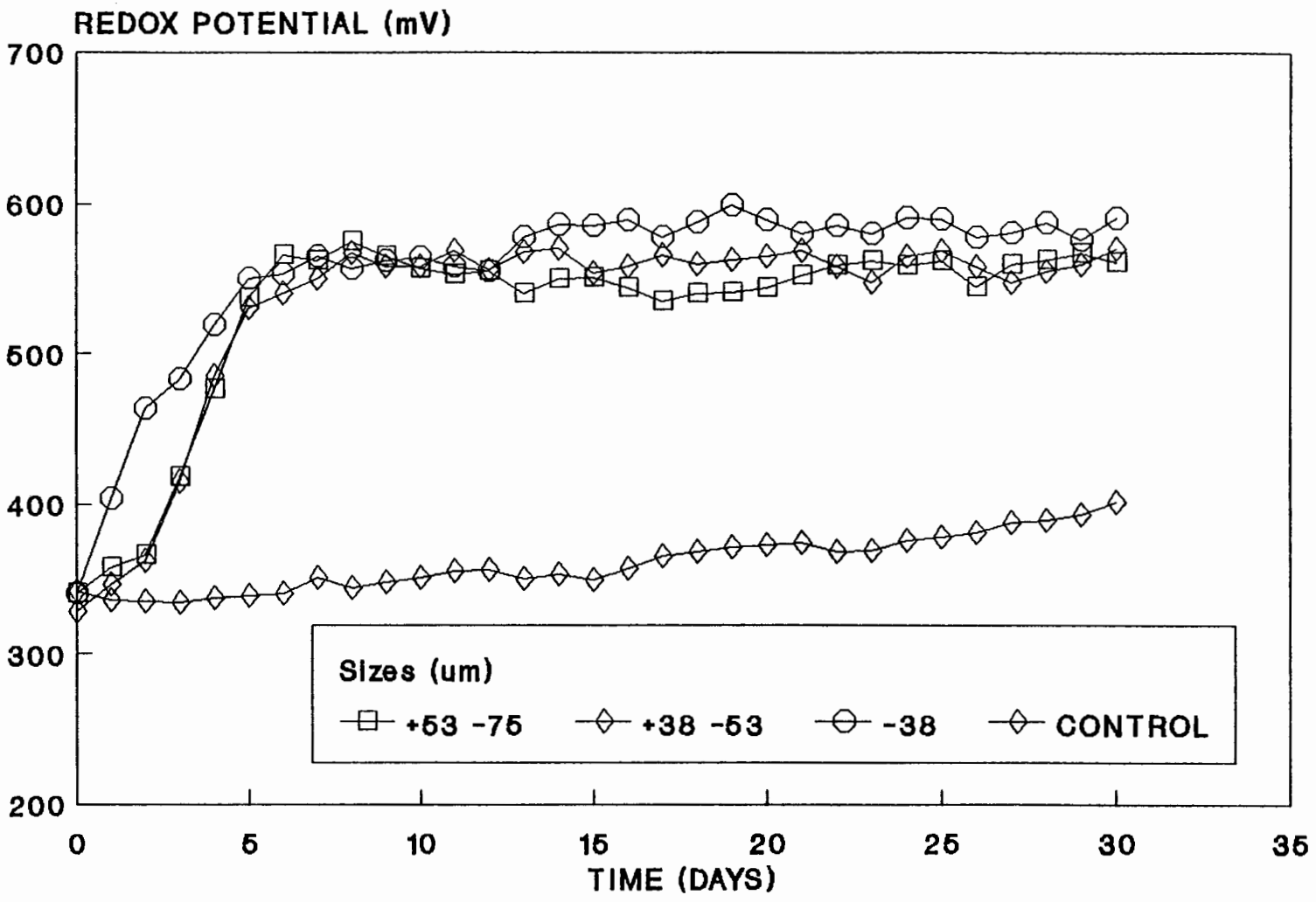

Figure D1. Redox potential profiles recorded for the duration of the batch runs.

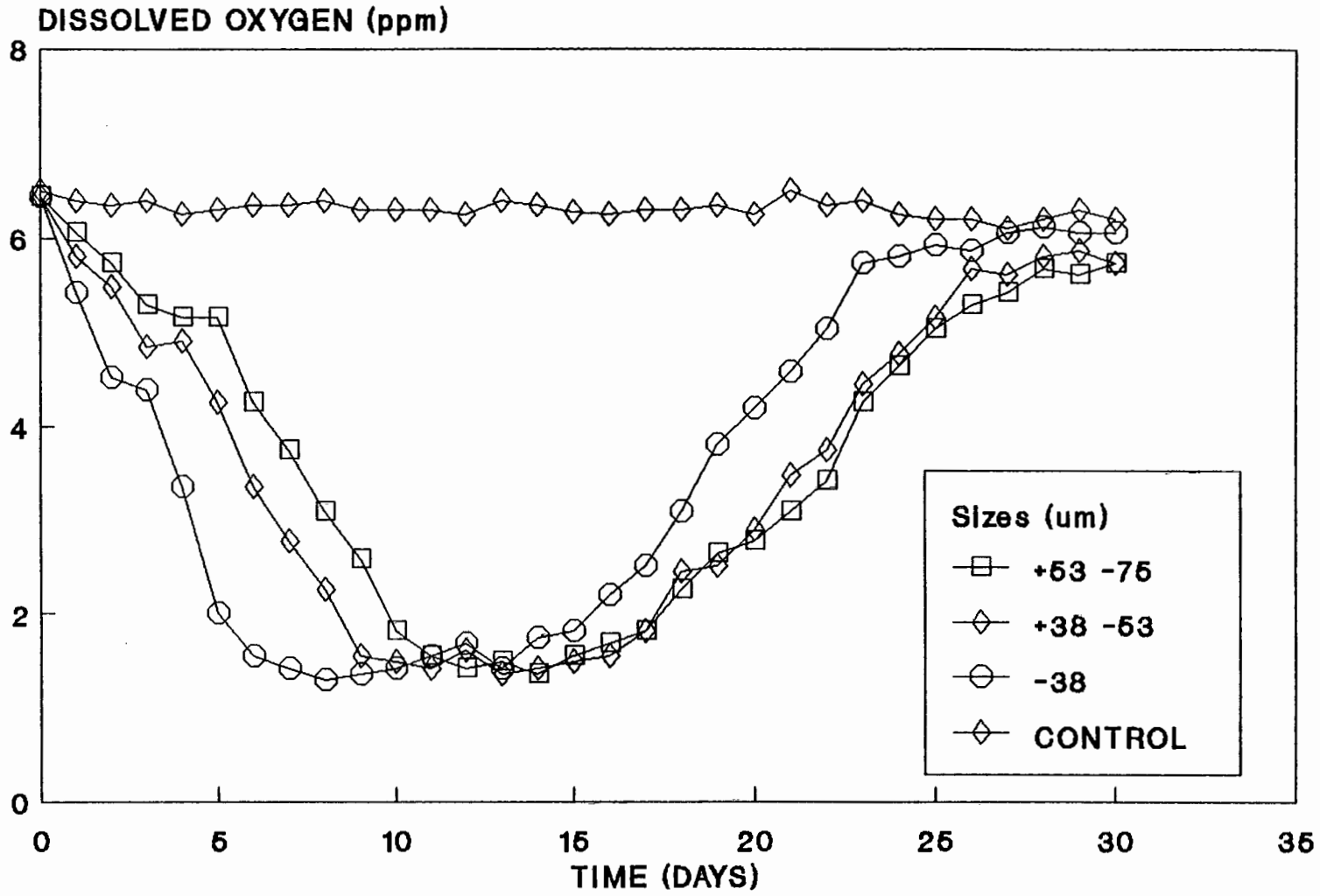

Figure D2. Dissolved oxygen concentrations recorded for the duration of batch runs.

Table A1.1 Analyses of unreacted solid residues and calculated fractions leached.
Size fraction : +53 -75um

		BACTERIAL LEACH RESIDUE ANALYSES						FRACTIONS LEACHED			
	Leach Time (days)	SiO2 (%)	Fe (%)	S2- (%)	S(TOTAL) (%)	As (%)	Au cyanide leached (g/t)	S2-	Fe	Au	As
FEED	0	2.78	44.90	48.90	49.10	0.18	2.39	0.000	0.000	0.000	0.000
	3	2.89	44.90	48.80	52.60	0.13	1.83	0.040	0.038	0.263	0.305
	6	2.95	44.80	49.40	51.40	0.09	1.24	0.048	0.060	0.511	0.529
	10	3.35	44.30	49.20	51.60	0.08	0.94	0.165	0.181	0.674	0.631
	15	4.24	42.90	48.90	51.50	0.07	0.71	0.344	0.374	0.805	0.745
	21	5.25	43.00	48.50	50.00	0.06	0.51	0.475	0.493	0.887	0.823
	30	6.26	39.80	45.80	47.40	0.06	0.36	0.584	0.606	0.933	0.852

Table A1.2 Mass balance calculations for iron and SiO2.
Size fraction : +53 -75um

Leach Time (days)	Residue Mass (g)	Mass SiO2 (g)	Mass Fe (g)	Liquid Sample Volume (l)	Total Fe conc. (g/l)	Mass Fe in Liquid (g)	Solids conc. (%)
0	1407.0	39.1	631.7	10.000			
3	115.0	3.3	51.6	0.875	1.85	1.6	13.1
6	101.5	3.0	45.5	0.895	3.90	3.5	11.3
10	85.5	2.9	37.9	0.820	10.10	8.3	10.4
15	70.2	3.0	30.1	0.790	18.60	14.7	8.9
21	83.6	4.4	35.9	1.090	28.80	31.4	7.7
30	330.0	20.7	131.3	5.830	35.10	204.6	5.7
TOTAL		37.2	332.3	10.300		264.1	

Total mass Fe accounted for = (Fe in residues) + (Fe in solution)
= 596.442
Total mass iron in feed = 631.743

Error = 5.6 %

Total mass SiO2 accounted for = 37.20
Total mass SiO2 in feed = 39.11

Error = 4.9 %